



UNIVERSITÀ  
DEGLI STUDI  
DI PADOVA

UNIVERSITA' DEGLI STUDI DI PADOVA

**Dipartimento di Ingegneria Industriale DII**

Laurea Magistrale in Ingegneria Aerospaziale

Development of a preliminary design tool for microsatellites  
structure in a concurrent engineering facility

Relatore: Zaccariotto Mirco

Correlatore: Franchini Sebastián

Candidato: Palumbo Davide

mat. 1039514

Anno Accademico 2014/2015



# Contents

<b>1</b>	<b>Introduction</b>	<b>3</b>
1.1	Objectives . . . . .	4
1.2	Introduction to satellite structure design . . . . .	6
1.3	Work environment: the Concurrent Design Facility . . . . .	10
<b>2</b>	<b>Concurrent Design Facility</b>	<b>21</b>
2.1	Introduction to the software structure of Concurrent Design Facility (CDF) . . . . .	21
2.2	The Student Concurrent Design Tool (SCDT) in <i>Matlab</i> © . . . . .	26
<b>3</b>	<b>Improvements to the SCDT module: the advanced analysis</b>	<b>41</b>
3.1	Dynamic analysis tool for single degree of freedom system . . . . .	41
3.2	Static and dynamic analysis tools for multiple degrees of freedom systems . . . . .	49
<b>4</b>	<b>Study cases examples</b>	<b>81</b>
4.1	Advanced static analyses results comparison. . . . .	82
4.1.1	Monocoque spacecraft configuration . . . . .	83
4.1.2	Semi-monocoque spacecraft configuration . . . . .	88
4.2	Advanced dynamic analysis results example . . . . .	94
4.2.1	Preconditions to the dynamic analyses results . . . . .	94
4.2.2	Random analysis and normal modes . . . . .	95
<b>5</b>	<b>Conclusions</b>	<b>99</b>
<b>A</b>	<b>Matlab additional scripts</b>	<b>101</b>
<b>B</b>	<b>Acronyms</b>	<b>103</b>
	<b>Bibliography</b>	<b>105</b>
	<b>Acknowledgments</b>	<b>107</b>



# List of Figures

1.1	The CDF of the Ignacio Da Riva department in Montegancedo, Madrid . . . . .	3
1.2	Load factors example table during transport operations, [11] Larson Wiley J., Wertz James R. <i>Space Mission Analysis and Design</i> , book, Space Technology Library . . . . .	7
1.3	A possible spacecraft loads classification, [10] Malcolm Macdonald, Viorel Badescu <i>The International Handbook of Space Technology</i> , book, Springer. . . . .	8
1.4	Loads frequency based classification, [4] A. Calvi <i>Spacecraft Loads Analysis</i> , presentation, ESA. . . . .	10
1.5	Space mission design process first steps, [11] Larson Wiley J., Wertz James R. <i>Space Mission Analysis and Design</i> , book, Space Technology Library. . . . .	11
1.6	Mission concept exploration. Every mission concept leads to many mission architectures, Francesconi A. <i>Impianti e sistemi aerospaziali</i> , lessons and presentations, Padova. . . . .	13
1.7	Schematic representation of the design process in a space mission.	14
1.8	Concurrent design vs concept design process. . . . .	16
1.9	An European Space Agency (ESA) team working in the CDF. This is an example and a demonstration of a typical CDF. . . .	17
2.1	General structure tool block diagram. . . . .	23
2.2	Main GUI structure tool window. . . . .	27
2.3	The Student Concurrent Design Tool (SCDT) window. Practical use example. . . . .	29
2.4	Axial buckling load coefficient (picture from [8] Larson Wiley J., Wertz James R. <i>Space Mission Analysis and Design</i> , book, Space Technology Library). . . . .	36
3.1	Single degree of freedom dynamic analysis window. . . . .	43
3.2	Forcing function load <i>Simulink</i> © file used in GUI. . . . .	47
3.3	Base drive single degree of freedom <i>Simulink</i> © files used in GUI.	48
3.4	Block diagram for advanced analysis. . . . .	50

3.5	Structure and coordinate frame reference figure. . . . .	51
3.6	Explanation figure for the advanced geometry compiling. . . . .	52
3.7	Detail of the applied forces and moments in the reference frame for the advanced static analysis. . . . .	61
3.8	Satellites geometry cross reference sections with reinforcements.	62
3.9	Structure idealization ([13] Megson T.H.G <i>Aircraft Structures for engineering students</i> ,book, Butterworth-Heinemann). . . . .	63
3.10	Reference picture for general shear flow calculations ([13] Megson T.H.G <i>Aircraft Structures for engineering students</i> , Butterworth- Heinemann. . . . .	65
3.11	Satellites geometry cross reference sections without reinforcements.	66
3.12	Geometric moment integral interpretation. . . . .	68
3.13	Detail of the internal forces calculation in a <i>Simulink</i> © file. . . . .	75
3.14	Single degree of freedom system diagram block; modal solving ( <i>Simulink</i> © file <i>FF_q_adv1_disp</i> ). . . . .	77
3.15	Difference in the block diagram respect to the one in figure 3.14 ( <i>Simulink</i> © file <i>FF_q_adv1_acc</i> ). . . . .	78
3.16	multiple degrees of freedom (MDOF) reference system for ran- dom base drive analysis, [20] Wijker Jaap <i>Random Vibrations in Spacecraft Structures Design</i> ,book, 2009 Springer. . . . .	79
4.1	finite element method (FEM) models for static and dynamic analysis: semi-monocoque structures. . . . .	83
4.2	Bending moment loaded monococque structures; Left fringe $[-4.04 \cdot 10^5; 4.04 \cdot 10^5]$ Pa, right fringe $[-1.06 \cdot 10^6; 1.06 \cdot 10^6]$ Pa . . . . .	84
4.3	Shear force loaded monococque structures; Left fringe $[-9.11 \cdot 10^5]$ Pa, right fringe $[-1.09 \cdot 10^6; 1.09 \cdot 10^6]$ Pa . . . . .	85
4.4	$\tau_{xy}$ stress component distribution in the skin along the perimeter due to shear force. . . . .	86
4.5	Torque moment loaded monococque structures; Left fringe $[-1.27 \cdot 10^6; 0]$ , right fringe $[-2.81 \cdot 10^6; -2.55 \cdot 10^6]$ Pa . . . . .	86
4.6	Axial (compressive) force loaded monococque structures; Left fringe $[-3.58 \cdot 10^5; 0]$ , right fringe $[-5.74 \cdot 10^5; -3.36 \cdot 10^5]$ Pa . . . . .	87
4.7	Bending moment loaded semi-monococque structures; Left fringe $[-1.45 \cdot 10^6; 1.45 \cdot 10^6]$ Pa, right fringe $[-1.32 \cdot 10^6; 1.32 \cdot 10^6]$ Pa . . . . .	89
4.8	Shear force loaded semi-monococque structures; Left fringe $[-9.04 \cdot 10^6; 9.04 \cdot 10^6]$ Pa, right fringe $[-1.04 \cdot 10^6; 1.04 \cdot 10^6]$ Pa . . . . .	90
4.9	$\tau_{xy}$ stress component distribution in the reinforcements along the perimeter of the cylinder structure due to shear load. . . . .	91
4.10	$\tau_{xy}$ distribution given by the tool (shear load, prism structure). . . . .	92
4.11	Torque moment loaded semi-monococque structures; Left fringe $[1.17 \cdot 10^6; 1.28 \cdot 10^6]$ Pa, right fringe $[2.30 \cdot 10^6; 2.77 \cdot 10^6]$ Pa . . . . .	92

4.12 Axial (compressive) force loaded semi-monocoque structures; Left fringe $[-2.77 \cdot 10^5; -2.19 \cdot 10^5]$ Pa, right fringe $[-2.93 \cdot 10^5; -2.40 \cdot 10^5]$ Pa . . . . .	93
4.13 Power Spectral Density function used in the random analysis example. . . . .	95

## Abstract

This thesis deals with the work done in a Concurrent Design Facility (CDF) environment in order to develop a new *Matlab*© calculus tool for the structure subsystem of microsatellites. This tool has been created during the *Erasmus* exchange program in the Polytechnic University of Madrid. It is based on another simple *Excel* document, providing calculus in order to obtain a preliminary design of the main structure of a satellite. This tool has been improved in term of versatility and quality, type and number of results. Its capabilities have been compared with some FEM models created in *Patran/Nastran*.



# Chapter 1

## Introduction

This project has been developed in the Concurrent Design Facility (CDF) environment at the Universidad Politecnica de Madrid (UPM) (figure 1.1) during the 2013/1014 Erasmus exchange program. The CDF installation has been created in July 2011 as a result of a deal between the ESA and the UPM, which permitted the employment by UPM of the student version software for the spacecraft and space mission preliminary design within the CDF, an ESA development. This software is made by some main parts, which are the software for the managing of the shared database (see section 1.3, page 10) and the series of calculation tools for proper preliminary design of all the spacecraft subsystems and all the moments of the space mission.



Figure 1.1: The CDF of the Ignacio Da Riva department in Montegancedo, Madrid

The further idea conceived in the Ignacio De Riva (IDR) department of UPM was to improve all the characteristics and potentialities of this installation, in order to develop an own more efficient, versatile and powerful set of tools. Some PhD students created the software capable of managing the

database, then the creation of calculation tools has followed, each one having its own interface. This latter part has been entrusted to five students of aerospace engineering who performed these works as their own university final projects. The subsystems tools that have been developed are:

- cost analysis;
- attitude determination and control;
- thermal;
- electric and power;
- structural.

## 1.1 Objectives

This work deals with the process of developing the structural subsystem calculation tool and with the presentation of its working environment. The work has been based on an existing calculating tool, programmed using Microsoft *Excel* and called SCDT, which can import the parameters from the database, use them to perform all the structural calculations by setting other option directly from the worksheet and then upload the results to the database in order to share them with the other subsystems. From the very beginning the work process has been organized using some objectives as follows:

- analysis of the logic *Excel* worksheets structure;
- creation of a simple Graphical User Interface (GUI) interface using *Matlab*©; this first tool is able to do the same calculus as SCDT;
- development of a more complex tool and the relative interface; this second tool contains all the potentialities of the simpler one, but has been improved by these competences:
  - to calculate more parameters, more accurately;
  - to use more complex models to perform analyses that were already performed;
  - to perform new kind of analyses which lead to a deeper and more complete knowledge of the system;
  - to make the design process easier and maybe useful for a further level design.

- to connect the calculus core of the tool and the CDF database (import/-export parameters), even though it must allow the user (an engineer) to freely perform calculus without affecting the database integrity and, if necessary, to modify the parameter within within the program itself. The former aspect is essential to guarantee the proper functions of the entire CDF, thanks to its characteristic of being an "almost real time" way to design, but it can not exist without the latter aspect because of the presence of the man in the loop (see section 1.3 at page 10).

## 1.2 Introduction to satellite structure design

The design process of a spacecraft is necessarily characterised by clear and defined criteria for the peculiarity of being most of the times a single one-off time product. The many objectives of a space mission are translated in specific requirements for the flight and ground segment that indicate the level of capability of the system to reach those objectives. More specifically, there is a defined set of ranges for the many quantities, that represent the behaviour of the system in all its aspects. The main requirements classes for the structure subsystem concern:

- i) functioning with regard the primary tasks: structure must permit all the functionalities of the instruments and when necessary facilitate them (mechanisms or adequate secondary structures);
- ii) mechanical loads: the structure must be able to handle all the possible loads during the life of the satellite;
- iii) material properties;
- iv) mass and balance: the structure must be as lighter as possible, and its mass distribution has to be known, together with the rest of satellite because it may be necessary to other subsystems (e.g. Attitude Determination and Control Subsystem (ADCS));
- v) reliability and lifetime: the satellite must provide its functioning through all the projected life and at least at a minimum level;
- vi) safety: the subsystem probability of failure must be minimised;
- vii) maintenance and repairs.

The design specifications are basic for the modelling of the satellite which is further analysed and tested, to verify its feasibility or the necessity to proceed with its elaboration and modification. The first step is to simulate analytically and numerically the behaviour of the single subsystem (or of sets of subsystems if strictly correlated) by building and virtually testing a simple but realistic model. Afterwards some physical models to perform real tests are built.

The simulations imply the prevision of all the possible loads to which a structure can be exposed, but the safety and reliability requirements establish a higher limit that has to be reached: the subsystem can not be able to handle the nominal charges, but must be dimensioned to resist to grater ones. Seldom norms refer to the capacity to resist to some loads with a certain probability. In general, some factors are applied to the nominal load in order to increment it, only then the simulations are computed. Operating this way confers higher

safety and reliability to the structure. The first factor considered is the *design factor* that is applied to the limit load (highest levels of possible loads) to get the design limit load in order to avoid failures during the design and testing. The *ultimate* and *yield* safety factors (or Factor of Safety (FS)) can be applied to the design limit load: the former product establishes the ultimate load that is the most critical load for the design since at this level the failure can be catastrophic, while the latter product sets the limit of elasticity of the structure above which the deformations are permanent<sup>1</sup>.

Medium/Mode	Longitudinal load factors	Lateral load factors	Vertical load factors
<b>Water</b>	±0.5	±2.5	±2.5
<b>Air</b>	±3.0	±1.5	±3.0
<b>Ground</b>			
• Truck	±3,5	±2.0	±6.0
• Rail (humping shocks)	±6.0 to ±30.0	±2.0 to ±5.0	±4.0 to ±15.0
• Rail (rolling)	±0.25 to ±3.0	±0.25 to ±0.75	±0.2 to ±3.0
• Slowly moving dolly	±3,1	±0.75	±2.0

Figure 1.2: Load factors example table during transport operations, [11] Larson Wiley J., Wertz James R. *Space Mission Analysis and Design*, book, Space Technology Library .

In general the level of safety is indicated by a parameter called Margin of Safety (MoS), which is the ratio between the allowable strength or stress and the actual stress multiplied by one of the safety factors minus one. The level of safety is as higher as the MoS is greater than zero:

$$MoS = \frac{allowable\_stress}{FS \cdot actual\_stress} - 1 \geq 0 \quad (1.1)$$

that means that the actual load (or stress), although increased, is still smaller than the allowable level one.

Some aspects of the procedure to size a satellite model and to test it have been shown, but that simulation step implies the knowledge of the types of loads that could charge the structure. A quick presentation of the main ones is made below. Note that this is the crucial point for the election of the simulation which have been developed in the calculating tool described in this work.

<sup>1</sup>Some typical values used by the European Space Agency (ESA) are 1.4, 1.5 for the design limit load, 1.1, 1.25 for the yield load and 1.25, 1.5 for ultimate load.

A possible classification is made respect to the mission phase to which the loads belong (figure 1.3).

- Handling and transportation loads are mainly considered including some load factors to the design limit loads. The factors vary depending on the means and mode of transportation and are different for every direction of the action;
- vibration tests for the qualification of the structure;
- launch loads and other orbit burns load; they are the hardest ones and include a wide variety: steady state accelerations, sinusoidal vibrations, random vibrations, acoustic and shock loads and pressure variations;
- re-entry loads;
- in orbit loads which can come from instrument deployment and debris impacts or can be heat flux and temperature gradients.

OPERATION			APPLIED ACCELERATIONS			REMARKS
			[g] (*)			
			X (+aft)	Y (+stbd)	Z (+up)	
Handling	Clean Room	Dolly	± 1.0	± 0.75	- 1 ± 0.5	Any S/C orientation
		In-door movements	± 0.2	± 0.2	- 1 ± 0.2	
		Vertical hoisting	± 0.2	± 0.2	- 1 ± 0.5	
		Launcher mate/demate	± 0.5	± 0.5	-2/0	
	Container	Hoisting	± 0.5	± 0.5	- 1 ± 0.5	
Road		Quasi-static	± 2	± 2	-3/ +1	40 km/h top speed
Air	Take-off		- 1.5	± 0.1	-2.5/ +1.5	
	Vertical manoeuv.(gusts)		0	± 1.5	-2.5	
	Lateral gusts		0	± 1.5	-1.0	
	Landing		± 1.5	± 1.5	-2.5	
Barge / Ship	Slamming		0.0	0.0	-1.8/ +0.2	
	Waves		± 0.3	± 0.5	-1.6/ +0.4	
Any Transportation Source		Continuous Vibration	± 0.1	± 0.1	± 0.1	Below 10 Hz, not including gravity effect
Transport Shock Load (S/C/SAR Panel)			± 2	± 2	± 3	

Figure 1.3: A possible spacecraft loads classification, [10] Malcolm Macdonald, Viorel Badescu *The International Handbook of Space Technology*, book, Springer.

Because the launch and the shock loads represent the highest level of stress for the structure subsystem the next classification can help to characterize them (refer also to figure 1.4).

- Steady state and static loads coming from the engine thrust, wind and manoeuvres: the main one is the longitudinal acceleration due to engine

propulsion caused by its constant increase due to the decrease of the mass while the thrust is almost constant, while the lateral loads are generally smaller. Because they are not subjected to quick variations in function of time and are in general "steady", they can be first modelled as constants, where the taken value is the most critical one. In these case a static analysis can be adequate to let the engineers speculate on the level of stress caused; obviously the load factors are applied for safety reason.

- Mechanical dynamic set of load is made of sinusoidal from low to high frequency vibrations, random vibrations and shock loads that come from the unsteady phenomena occurring during propulsion, from sound pressure loads, from the firing of pyro devices for the stages separation and from hyper-velocity debris and meteorites impacts. Except for the latter type that acts directly on the satellite once it is in orbit, the others are characterised by a load path passing through the interface that connects the satellite to the launcher. This fact makes the base enforced acceleration (and in general base displacement) analysis one of the most useful to understand the limits of the system. Using this type of simulation a lot of types of loads can be given in input:
  - time dependent enforced displacements, sinusoidal and in general periodic where the effective function can be set to have any frequency to simulate all the characteristic periodic loads;
  - time dependent enforced accelerations, with the same features of the displacements;
  - frequency dependent acceleration function; they usually simulate the probability function of the enforced acceleration level of random loads (Power Spectral Density (PSD)).
- Acoustic loads coming from the engines and the interaction with the atmosphere during lift off (reflection of waves on the ground) and of course during the transonic flight. They are loads that transmit vibration to the spacecraft through the base, but also through the portion of atmosphere present in the fairing of the launcher. Can be periodic with a wide range of characteristic frequencies (20 to 10000 Hz) or very high frequency random loads. This phase is characterised also by pressure changes that are spread loads acting on the surfaces of the satellite. For example if there is no possibility for the air to evacuate during the ascension the gradient of pressure straddle closed surfaces becomes critical.

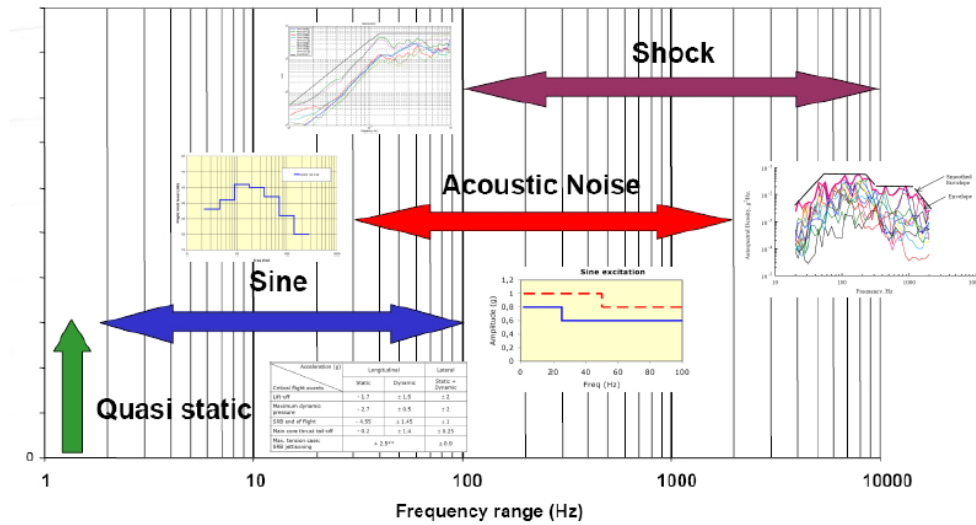


Figure 1.4: Loads frequency based classification, [4] A. Calvi *Spacecraft Loads Analysis*, presentation, ESA.

### 1.3 Work environment: the Concurrent Design Facility

Accreditation Board for Engineering and Technology (ABET)<sup>2</sup> defines engineering design as *the process of devising a system, component, or process to meet desired needs. It is a decision-making process (often iterative), in which the basic science, mathematics and engineering sciences are applied to convert resources optimally to meet a stated objective. Among the fundamental elements of the design process are the establishment of objectives and criteria, synthesis, analysis, construction, testing and evaluation. [...]* Moreover it is essential to include a variety of realistic constraints, such as economic factors, safety, reliability, aesthetics, ethics and social impact. One of the most important feature of the design is the iterative character of the decision making process, in fact, due to the complexity of the latter, it is almost impossible to follow a linear path. The whole process can be divided indicatively into some fundamental parts:

- research;
- conceptualization and feasibility assessment;
- establishing the design requirements;

<sup>2</sup>ABET, incorporated as the Accreditation Board for Engineering and Technology, Inc., (a non-governmental organization that accredits post-secondary education programs in "applied science, computing, engineering, and engineering technology").

- preliminary design;
- detailed design;
- production planning and tool design;
- production;

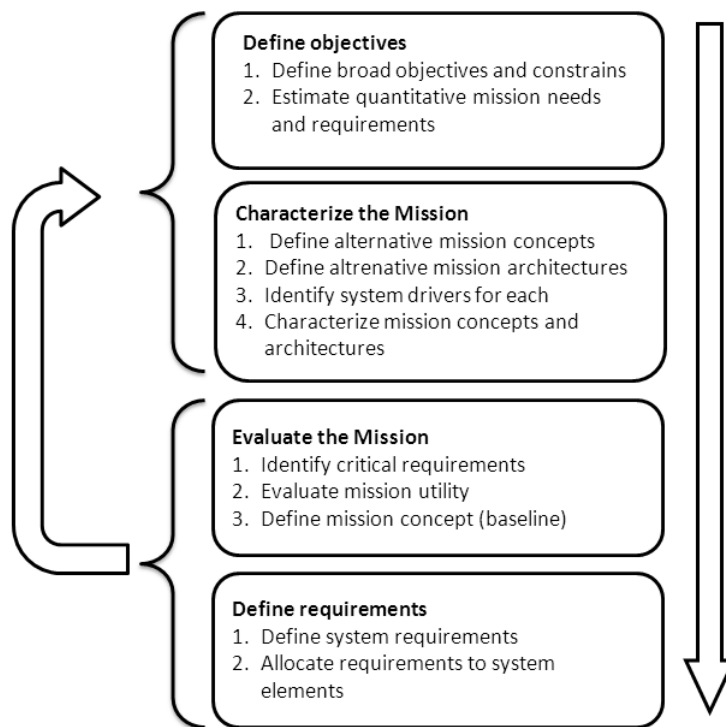


Figure 1.5: Space mission design process first steps, [11] Larson Wiley J., Wertz James R. *Space Mission Analysis and Design*, book, Space Technology Library.

It might be thought that the process simply consists in going through these few steps one by one and coming to the end, but usually in the first tasks it is necessary to interrupt the path, to review some previous concepts, to change them in order to reach a better compromise among all the aspect of the project. Therefore all the following decision plans will be affected by modifications, which could also be significant depending on the amount and relevance of the changes. Every part can consists of many sub-steps, therefore it can also be delineated by an iterative feature.

Figure 1.5 shows the first steps of the whole mission design process. The attention is focused on these early phases of the mission design in order to understand the strength of the new approach that is the concurrent engineering. The point list above can be easily specified through the following space mission life cycle, except for point *iv* that is a fundamental step of a space mission (footnote3);, but it may not be present (depends on the object of the design) in a generic design process. After the main mission objective has been established and the mission requirements have been derived, the mission is generally structured as follows:

- i) Concept exploration
- ii) Detailed development
- iii) Production and deployment
- iv) Operations and support

For simplicity all the design steps will be considered. The engineer teams classical approach to the preliminary and detailed design consists in dividing the problem in some specific tasks and assigning each of them to a different specialized engineer, also supported by a group, who works separately from the others. It follows that iterations can be performed only during some meetings among all the teams which take place at intervals of some weeks. Therefore the iterative process results quite slow, there are no prolific comparative relations among the different field specialists except during the meetings, on the other hand the manpower resources are used efficiently also because this is a well known and strongly based way to work.

The first two points have specific interests and suffer essential modifications by changing the design approach as it is happening within the space agencies and companies. Concept exploration refers to the initial phase of study, which results in a broad definition of the space mission and its components. The first stage is to define some mission concepts consisting of four basic elements:

- Data Delivery: how data are collected, stored, distributed and used;
- Communication architecture: how do the various part of the mission communicate;
- Tasking, scheduling and control: how the system decides what to do;
- Mission time-line: overall schedule for the rest of the mission, from design to dismissal.

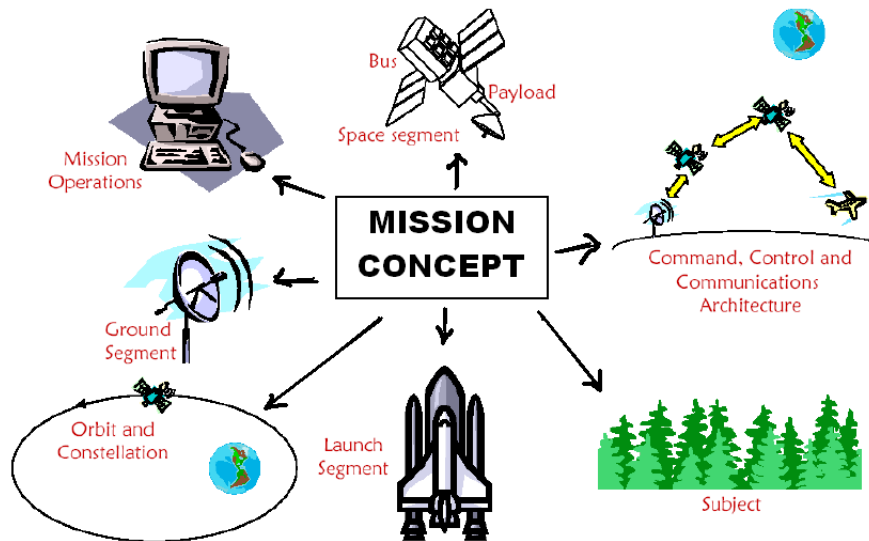


Figure 1.6: Mission concept exploration. Every mission concept leads to many mission architectures, Francesconi A. *Impianti e sistemi aerospaziali*, lessons and presentations, Padova.

The space system must satisfy all the requirements, so it is better defined by all the possible and alternative mission architectures. There can be many of them for each mission concept. Every architecture consists of its mission concept and the specification of every element that can be seen in figure 1.6. They represent the different ways to reach the objectives through the ideation of different paths, which is characterised by alternative approaches, therefore by alternative solutions, keeping in mind that some requirements are also constraints. All the requirements are allocated to the various mission elements. The goal is to define a certain number of candidate architectures, big enough to offer the majority of the advantages, but even small enough to allow a detailed definition, the overall management and finally to choose the best ones. To do so the team identifies the system drivers that are the principal mission parameters or characteristics which influence performance, cost, risk, or schedule and which the user or designer can control<sup>3</sup>.

Figure 1.7 briefly tries to show the design process. Attention must be paid on the strong iterative connotation that characterizes it. Given the study requirements and objectives (that are assumed constant from a certain time-step to the end), the design process involves the mission requirements, all the mission systems (now called *architecture*) and the intermediate results. In a way that can not be a straight line made of chronological subsequent and unidirectional steps. This would mean that the design perfection is reached in every single step through a reasonable amount of time, so it is possible to deal with

<sup>3</sup>Wiley J. Larson and James R. Wertz *Space Mission Analysis and Design*.

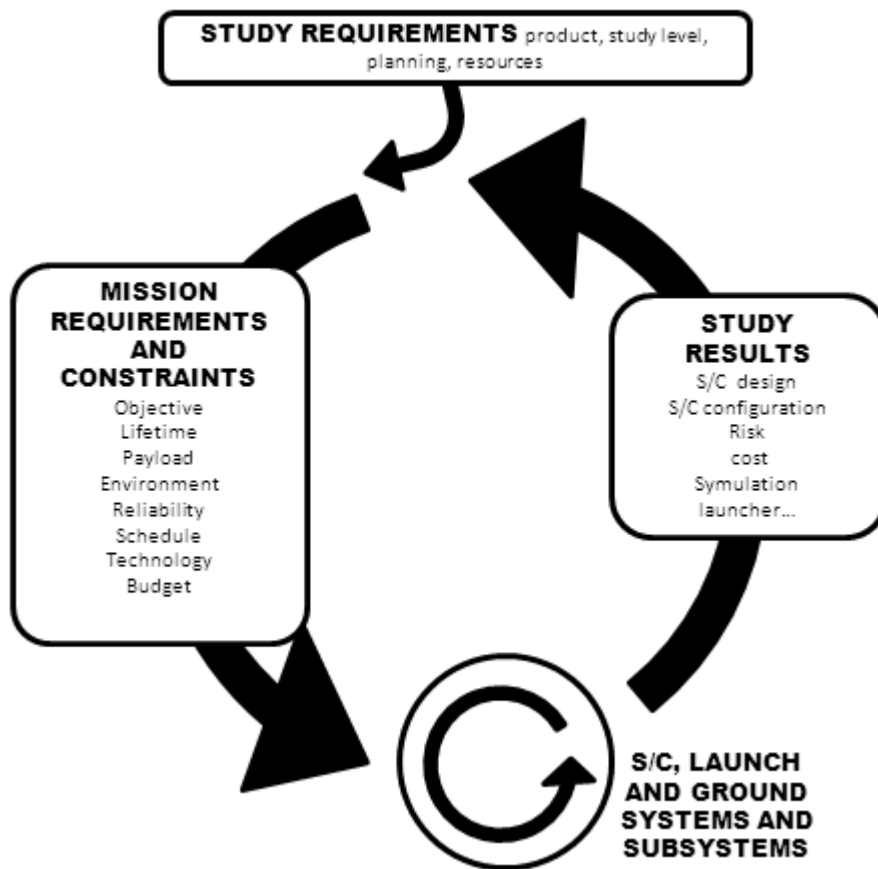


Figure 1.7: Schematic representation of the design process in a space mission.

the following step toward the end of the process. Clearly it can not be a realistic scenario. Indeed the design follows a circular path: after a first preliminary solution is reached, there is always the possibility of stepping back to levels that have to be modified and improved. The various part of the design are closely interconnected. The problem consists in the opposite features which characterize the industrial approach (top figure 1.8). In this case the need and its answer have clearly two opposite basic trends. In fact, the concept process had to adapt itself to the design iterative intrinsic peculiarity by continuously going back to previous point in order to review and modify the project. In a company where every system part is developed by a different team, it follows that the concept system has to go back and forth from an office to another and each of them would receive it with fewer degree of freedom, as the design proceeds to the end. Certainly it could be reviewed by a team, but with a lot of constraints and very little possibility to modify it, unless a spread review of all the following systems is accepted. This comes from the intrinsic subsystem interconnection that exists in the system engineering.

On the other hand an alternative approach to the design process has spread among many companies, universities and organizations during the '90s, especially in the aerospace sector. This is called concurrent engineering (CE), and ESA defines it as follow:

*is a systematic approach to integrated product development that emphasises the response to customer expectations. It embodies team values of cooperation, trust and sharing in such a manner that the decisions are made by consensus, involving all perspectives in parallel, from the beginning of the product life-cycle.*<sup>4</sup>.

This definition emphasizes the cooperative aspect of this approach. Another definition underlines the possibility to simplify the control of the entire project and consider from the very beginning all its possible aspects:

*CE is a systematic approach to the integrated, concurrent design of products and their related processes, including, manufacturing and support. This approach is intended to cause the developers from the very outset to consider all the elements of the product life cycle, from conception to disposal, including quality, cost, schedule, and users requirements.*<sup>5</sup>.

A short presentation of how the CE concept has been employed by ESA will follow, because this work has been developed within the Concurrent Design Facility (CDF) of Universidad Politecnica de Madrid (UPM), inherited from ESA itself. One of the first experiments on the effective use of this concept in the design of a space mission was accomplished in 1999 by ESA during the Common European Space Robot Controller (CESAR)<sup>6</sup> mission assessment. A list of five key elements was taken into account to form the first Concurrent Design Facility (CDF) in European Space Research and Technology Centre (ESTEC)<sup>7</sup>.

**Process** A general space system typically shows many reciprocal relations among the components, therefore the single component design affects all the other and causes changes in cascade. The CE approach aims to consider from the very beginning the impact of changes, in order to make easier the convergence to an optimized solution. The design process considers the presence of all the engineering specialists at the meetings, even those who would later participate to the design in order to avoid the development of mistaken trends. Also,

---

<sup>4</sup>M. Bandecchi, B. Melton, F. Ongaro *Concurrent Engineering Applied to Space Mission Assessment and Design*, 1999

<sup>5</sup>Bertrand Harold E., Pennell James P., Slusarczuk Marko M. G., Winner Robert I. *The Role of Concurrent Engineering in Weapons System Acquisition*, report R-338, Institute for Defense Analyses 1988

<sup>6</sup>Common European Space Robot Controller, ESA and *Agenzia Spaziale Italiana* (Italian Space Agency) (ASI) mission that constituted a reliable base subsystem of space robotics missions.

<sup>7</sup>European Space Research and Technology Centre, Noordwijk, Netherlands

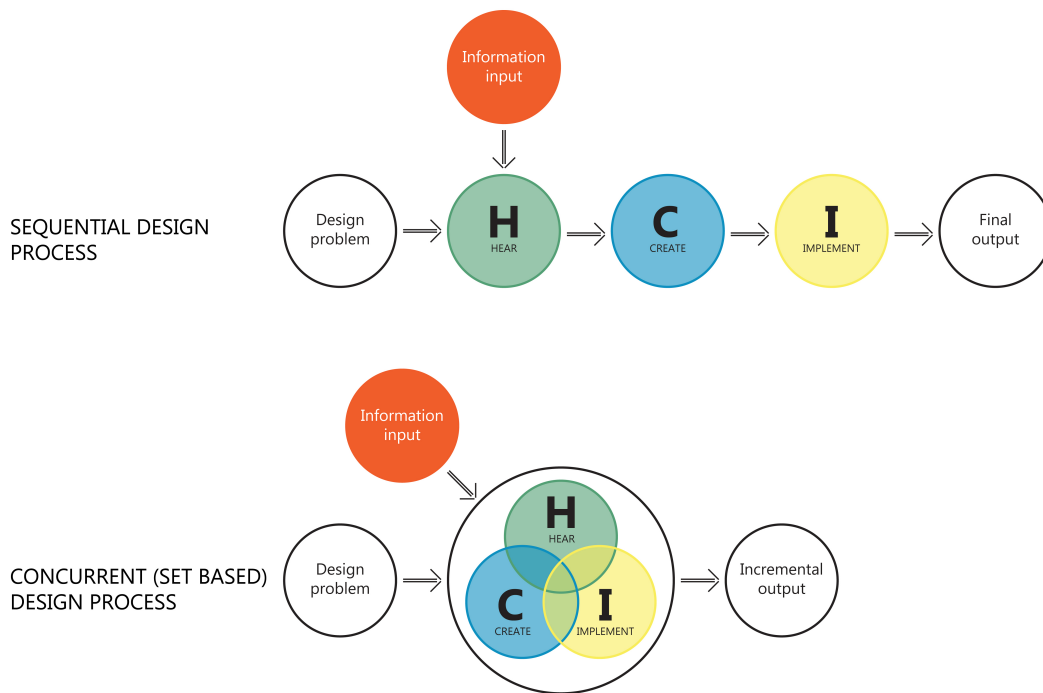


Figure 1.8: Concurrent design vs concept design process.

the customer is invited to the meeting session and he is not just a spectator, but contributes actively to the debate, discussing and working with the team to achieve a project design which could match his expectations, too.

**Multidisciplinary team** Is a group of engineering specialists brought together to work in the same sophisticated room. It must be an example of highly motivated and multidisciplinary team which accept to co-operate and provide answers in every moment. Every team member has to participate to all the meeting session bringing a computer based model of his own work (made in the facility) and being disposed to interact with the other specialists whenever they (the system engineer or the customer) pay him a question; or just may have influence on his domain while presenting the whole team work. Also he has to adapt his work to the needs and choices decided during the session, handling the records of all the design drivers, assumption and notes for the final project.

**Integrated design model** It is a parametric based model made up by all the informations collected from the various subsystem engineers (specialists). An essential feature of this model are parameters, for their characteristic of being general: many different architectures and scenarios can be simulated with the same software just changing parameters opportunely, a fast operation which

allows to perform a real-time process. For this reason also the iterations that lead to the optimum solution are faster and easier.

The subsystem models which compose the main one consist of input, output, calculation and results areas. The input and the output areas connect the model to the others through a database and a computer connection. All is managed by a software. The calculation area is the domain of the single specialist, where he can use equation, physical and scientific models to simulate his own part of the project. Finally the results area summarizes the products of the calculations in order to present them during the design process or at the end of it.

**Facility** The team works within the Concurrent Design Facility (CDF) which is composed by a design room and a meeting room. The design room is equipped with some computer workstation, one for each subsystem (including risk and cost analysis and system engineer) and some multimedia device like screens, projectors, charts, video conference devices, in order to facilitate the visualisation and sharing of the informations. Even though the subsystems with the higher probability to interact between each other are located closely, thereis the possibility to show the screen of each workstation on every visual device in the room.

**Software infrastructure** It allows the entire facility to work and it is an essential part of it. This infrastructure must comprehend all the tools to make it work correctly: software for the generation of the model, a mean to propagate data between models in real time, tools and software for domain specific calculations, a documentation support system and a storage capability.



Figure 1.9: An ESA team working in the CDF. This is an example and a demonstration of a typical CDF.

The use of the CE in the design process satisfied the ESA team expectations. It has been found out that the conceptual design required a shorter time and lower costs than the traditional approach and that the same principles could

be applied to the development of other entity than a whole system, for example individual instruments, subsystems or to other phases.

The Student Concurrent Design Tool (SCDT) is an educational software package based on a simplified CDF infrastructure and tools that has been developed by the European Space Agency Education Office to support the design process of a space mission in a concurrent method, specially conceived for education.

Since 2011, a deal between Universidad Politecnica de Madrid (UPM) and European Space Agency (ESA) has been allowing the use of the educational software in the Ignacio De Riva (IDR) department in *Montegancedo* campus in Madrid. Therefore it has been installed a facility counting on twelve computer workstations and audiovisual and on-line communication devices. All the computer are connected together and to a server to manage a shared database. It is also possible to provide every workstation some specific softwares for the model simulation in many scientific areas, which help the specialist in his work within the facility. UPM CDF operating principles, and the way a design session works are very similar to the ESA CDF ones; they will be explained below in order to have a clear idea about how does the facility work.

The work of the team alternates different phases: in some the engineers make researches, talk with colleagues and prepare the design of their own model; in some others the real design session occurs and the entire team meets to work together. A system engineer, or a team leader in general, usually leads the design session while a customer representative is attending. As previously mentioned, working this way all the decision can be made in real time, without waiting for the monthly meeting, and it allows a faster process due to the very short steps that characterize the iterations.

The Student Concurrent Design Tool (SCDT) is practically composed of three different type of Excel<sup>8</sup> workbooks:

1. Server type: divided into two different workbooks:
  - Parameters workbooks: stores all the parameters created and exchanged with the subsystems.
  - Data exchange workbook: allows to exchange the data stored in the parameters workbook with the input/output area of each subsystem workbook.
2. System type: summarizes all the most important parameters given by the various subsystems, therefore it provides a complex view of the mission and it should be managed by the system engineer, or by the team leader. The system workbook is made up of:

---

<sup>8</sup>A *Microsoft Office* software.

- the system workbook which properly summarizes the parameters, including costs;
  - the preliminary sizing workbook in which can be done a computation of the main parameters in order to start performing the whole space mission preliminary design.
3. Subsystem type<sup>9</sup>: it is made up of different worksheets, they allow each subsystem engineer to design their own particular model, performing calculation with database (server workbook) imported parameters and providing results and output parameters.

---

<sup>9</sup>Please remind that this project deals with the improvement of this tool through the programming of a Graphical User Interface (GUI) in a *Matlab*© environment, therefore this latter point, dealing with the subsystem SCDT, will be detailed in chapter 2 at page 21.



# Chapter 2

## Concurrent Design Facility

### 2.1 Introduction to the software structure of CDF

As it has been mentioned above, the software infrastructure of the Concurrent Design Facility (CDF) is essential for the good functioning of the entire facility. At the IDR department, it has been decided to develop a completely self-made version of this component, including all the various parts of the net connecting the server and the workstations and allow, after all, the entire concurrent engineering work process. These parts are basically a database, a platform for its management and the calculus tools. The software used for the database is *MySQL*<sup>1</sup>, which use has been simplified with the creation of a *Python* and *Qt* (PyQt)<sup>2</sup> based graphic interface and a bug tracker software called *Mantis*.

The subsystems tools dialogue with the database, importing and exporting sets of parameters from and to it. These sets are composed by some *inputs* and some *outputs*. These parameters are originally established during a concurrent engineering (CE) session where all the subsystems specialists and the group leader interact, in order to create the first primordial database for all their future work. All the parameters are classified by an *issue* and a *version* in order to avoid undesired overwriting of the same data. The issue identifies the entire set of data and changes every time a subsystem or a variable are created or when the team decides to *save* a configuration. The version can refer to a single variable and identify a change in its value, obviously when the calculating tool runs, even though the tool allows the specialist to decide when to update the version. This precaution is necessary to let the engineer design more independently, using the tool as many times as necessary, without creating hundreds of version of the same variable. Because the issue represents a specific

---

<sup>1</sup>Is (as of March 2014) the world second most widely used open-source relational database management system.

<sup>2</sup>is a Python binding of the cross-platform GUI tool kit Qt.

set of the variable, that is a configuration of the spacecraft, it is possible for any reason to go back to a precedent issue with a procedure managed by the system engineer. On the other hand just the last version of a variable can be used in every issue: it is not possible to access to previous versions of it.

The management of issues and versions creates a logic pattern easy to analyse and to access, moreover the way it is performed implies the almost-real time working of the facility; in fact, the subsystems specialists can realize their calculation at the same time using their own tools, which always share the same data issue. On the other hand, since each variable is editable just by the proper subsystem, by changing the value to the its variables every subsystem actually changes the version. Until the version is uploaded to the database, the subsystems continue to perform calculation with the old version of the variables. Whenever the engineers decide to upload the variables to the database, the new version become available for the use in the tools.

During the uploading of the variables, issue and version are compared with the last ones available in the database, in order to detect errors or incoherences. The set of data uploaded includes the values coming from the database and imported to perform calculations and the last values available in the database (those created by the last registered calculations). The comparison of these two sets of values could lead to the following events:

- Coherent calculation: values and versions are the same;
- Database error: the versions are the same, while the values are not;
- Infrequent event: the values are the same, while the versions are not;
- Incoherent calculations: neither values nor version are the same. Data may be decoupled among the calculation tools.

The original SCDT *Excel* program is composed of two main group of worksheets: the first allows to connect the tool and the database, importing and exporting the sets of parameters, the second is the core of the tool which is actually programmed with the necessary equation to perform calculations. The *Matlab*© tool described in this project has been developed starting from the mentioned *Excel* worksheets tool. Any student working on the development of a subsystem tool started from a pre-existing *Excel* document (except for cost and risk analyses). All these *Excel* tools share the spacecraft concept<sup>3</sup> that can be designed (for example the possible shapes of it) on which any student based his new tool, that had been changing and improving during the work, following a common direction and leading to a congruent set of tools, that can efficiently cooperate in the CDF environment.

---

<sup>3</sup>For the *spacecraft concept* meaning see section 1.3.

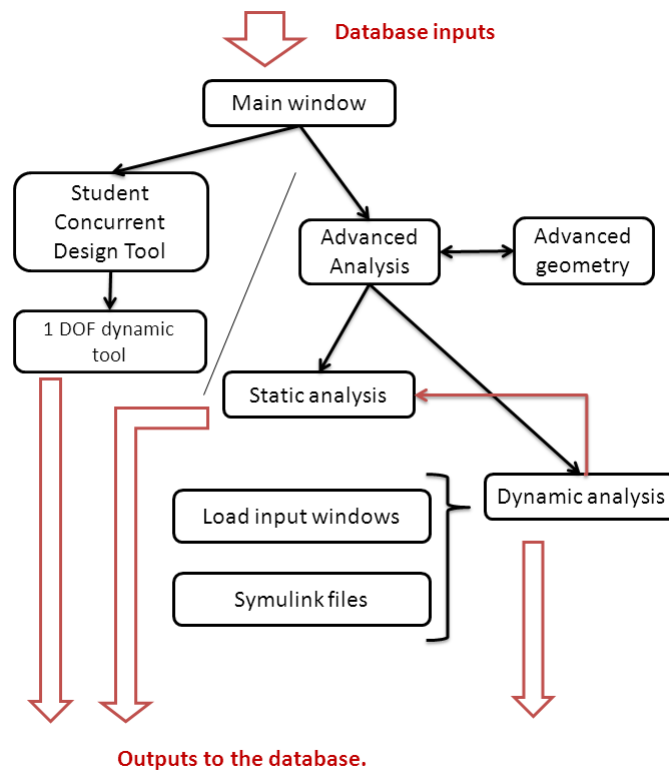


Figure 2.1: General structure tool block diagram.

One of the main objective that pulled this work has been to improve the existing worksheet. The leading idea consisted not only in merely add equations to the tool, but also to make the capabilities of the CDF a step towards a higher complexity. The aim was to place the new instrument in between the simplest imaginable tool concept and the complicate world of professional design softwares. Its position is just aside the former of tool, but there is quite large margin of improvement, that could bring to a mid-placed innovative and versatile and cheap instrument.

The new *Matlab*© based tool is actually composed of many different windows worksheets, which are interconnected among each others, in order to make it handy and structured in all its functionalities. A diagram is showed in figure 2.1 to make the reader understand the general structure of the tool.

Figure 2.1 shows the presence of a first discriminant window, from which two main and completely independent branches leave and articulate, representing different types of satellite structural analyses. This first window (called *structure*<sup>4</sup>) is also the one responsible for all the connection with the database in

<sup>4</sup>The different windows of the tool can work thanks to the presence of two different files running in the *Matlab*© environment. One is the figure file that shows the user interface itself, in which every kind of graphic instrument can be placed (i.e. buttons, lists, text,

both ways (i.e. importing and exporting sets of variables). The two branches of the logical structure gather together two sets composed by a lot of *.fig-m* couples of files<sup>5</sup> and some other *Simulink* files:

- Main window: *structure.m* and *structure.fig* files are responsible for the earlier mentioned functions. They are also connected to these files: *CDP\_module*, *circle*, *correspondence*, *Execute\_command*, *Exportar*, *Importar*, *set\_target*, *ImportDB*, *show\_input*, *GeneralSettings* which all work together to create the database connection. The majority of them have been written by a UPM PhD student and inherited for the purpose of this project.
- First set: reproduction of the Student Concurrent Design Tool (SCDT) potentialities and further improvements maintaining the single degree of freedom hypothesis.
  - i) *SCDT.m* and *SCDT.fig* files: use all the imported or set variables to perform basic static and dynamic calculations (basically the same as the *Excel* software did). Some *Matlab*© functions are seldom used in this part of program: *cilindro*, *circle*.
  - ii) *dynamic1GDL.m* and *dynamic1GDL.fig* files: work with the *BD\_TR\_a2*, *BD\_TR\_x2*, *FFx\_TR\_a2* *Simulink* files to perform some types of dynamic analyses on the single degree of freedom system. *define\_f* and *define\_PSD* are also part of this group of files.
- Second set: real improvement of the tool by changing the idealization of the system into a multiple degrees of freedom model, by improving the static analysis and preserving the main characteristics of the dynamic one, but allowing it to manage MDOF systems.
  - iii) *AdvGeom.m* and *AdvGeom.fig* files: allow the user to define a more complex geometry, maintaining the main shapes present in the SCDT module, but increasing the possibility to detail the inner structures and some appendage like solar panels.
  - iv) *AdvDynamic.m* and *AdvDynamic.fig* files: they are responsible for the dynamic analysis of the MDOF model cooperating with the *FF\_q\_adv1*, *FF\_q\_adv2*, *FF\_q\_adv3* *Simulink* group of files and some GUI windows, which define the system input forcing function: *defineAdv\_f*, *define\_PSD*.

---

etc...); it is generally named *namefile.fig*. The other is the script file which contains the proper code to make all the objects of the *.fig* file work and where all the variables, the calculations and the equations are defined; it is generally named *namefile.m*.

<sup>5</sup>The names of the files are important just because they are used to run the specific file during the tool functioning. It has been tried to find some intuitive names to make their identification easier. It is also true that the user will never look for them within the computers directories, except if some modification or code revision are needed.

- v) *AdvStatic.m* and *AdvStatic.fig* files take advantage of a more complex static analysis theory than the one used in the SCDT, which improves the quality and variety of calculations for the same spacecraft configurations, obviously using the advanced geometry settings.

In the section below (i.e. 2.2) the functionalities and the functioning of the structure interface are explained.

## 2.2 The Student Concurrent Design Tool (SCDT) in *Matlab*©

When the tool is run a first window appears and permits to perform the first preparing steps for the following analysis; as the reader can verify in figure 2.2, it displays a panel on the left, one on the right and two buttons in the centre. The user will always start its session using the former panel<sup>6</sup>

- i) by clicking on the *Connect to DB* button the software runs the file *CDP\_Module* that consists of a log in window where the user can insert his user-name, the name of the database which is willed to connect and a password<sup>7</sup>. The *ok* button creates the connection that identifies the engineer activity during the session.
- ii) Once the user has been connected to the database, it is necessary to import the set of parameters from the database and create an univocal correspondence with the variables used by the *Matlab*© GUI program. The click on the *Import variables and create correspondence* button runs the *ImportDB.m* file that is a function able to transfer the data from the database to the *Matlab*© workspace. The imported set of variables contains in a *Matlab*© structure<sup>8</sup> the input and the output variables (if they exist) and all the informations about issue, version, unit and a little description. All these informations are displayed in the first window under the left buttons, meanwhile a new window is opened: the *correspondence* window.
- iii) First of all it is necessary to upload the imported variables to this level. Note that only the variables that represent an input for the program will appear in the left list menu. By selecting one of the inputs a list of homogeneous (that have the same unit) variables will be displayed in the right list menu, allowing the user to select the desired one. Then the selected variables control can be done in the edit boxes below and the correspondence can be created through the specific button. From now on the coupled variables that will be used in the calculations assume the values of the database ones, even if it is still possible to assign them other values. At the end of the two static analyses, there is the possibility

---

<sup>6</sup>The way to operate with the tool and the calculation theories will be explained within this work. In order to understand the tool functionalities in detail, the reader is exhorted to see the program code, where every operation is further commented and explained.

<sup>7</sup>All these data are decided during the first meeting of the CDF group together with the creation of the database.

<sup>8</sup>A structure array is a data type that groups related data using containers called fields. Each field can contain any type of data.

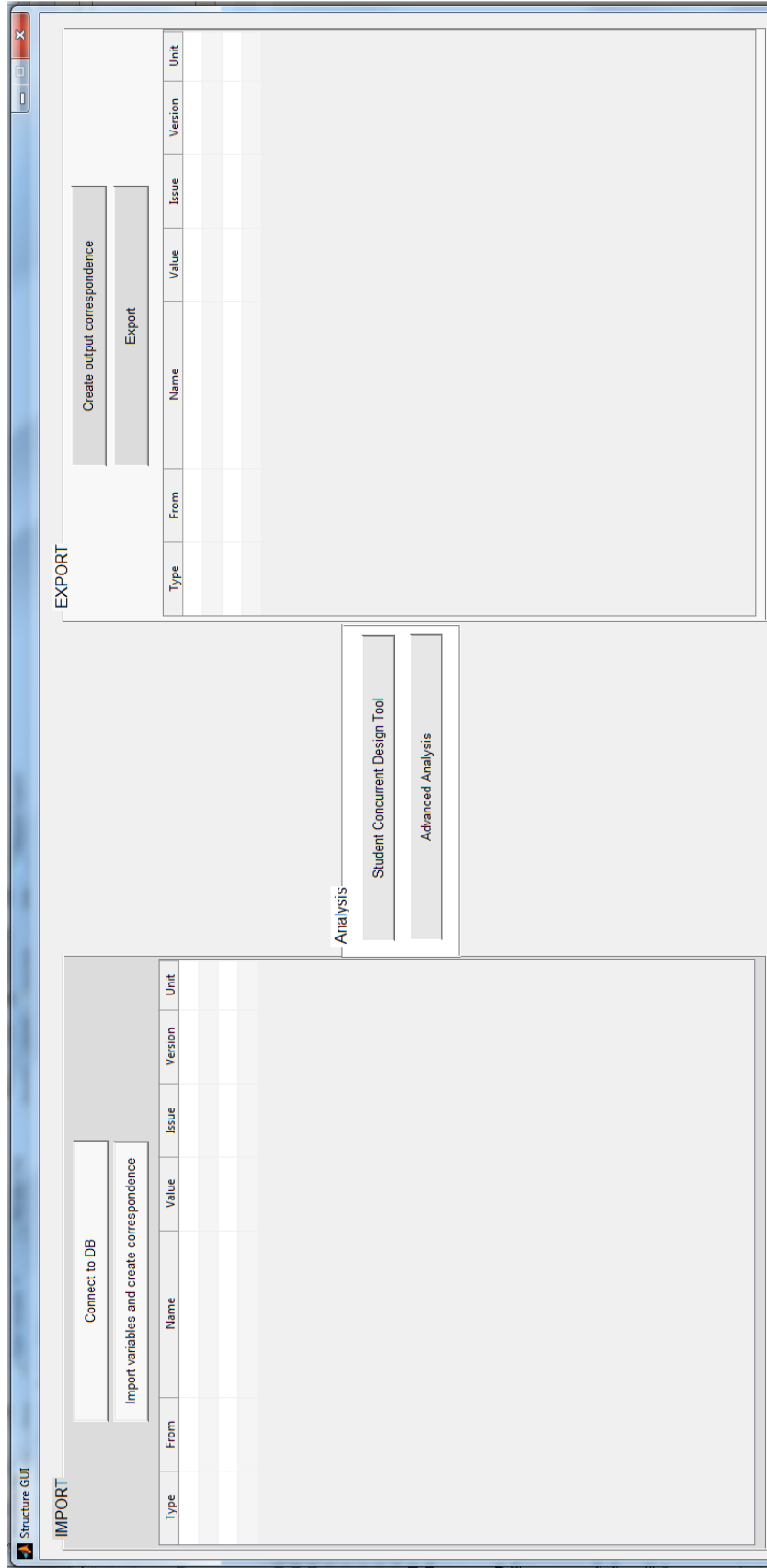


Figure 2.2: Main GUI structure tool window.

to upload the results to the database. To perform this action the user must have the will and the awareness that he is changing the data in the database; he also has to know that if he did not use the imported data to perform the calculation, then the results obviously mismatch and an eventual uploading to the database would create a lot of confusion. Moreover one of the error explained above would happen (i.e. list 2.1).

- iv) it is now possible to start the required analyses. In the central panel two buttons are accommodated, corresponding to the same quantity of available analysis levels of complexity: the SCDT button leads to the lower one. It reproduces the potentialities of the ESA *Excel* tool; the other button runs a set of files able to perform a more complex analysis (this part the new tool will be described in section ??).
- v) In the export panel two buttons and a table take place. The first button create a name and value correspondence between the set of outputs contained in the imported variables and the set of results just calculated. This action (if the hypotheses at point (iii) are satisfied) creates a cell array containing the last set of inputs used and the correspondent outputs. The array is exported to the database through the *Export* button which uses a script called *exportar* that compares the old outputs and the new ones updating the version if they result to be different. Before this final step the user can control the data by clicking anywhere in the table.

Figure 2.3 shows the new *Matlab*© Student Concurrent Design Tool (SCDT) aspect. It is possible to notice that despite its simple appearance, it contains and summarizes all the functionalities of the old *Excel* tool, which basically dealt with the static analysis of the satellite structure.

Many *text edit boxes* have been placed in the interface. They permit the type and insert all the data that the calculations need. It must be said that most of the data are inherited<sup>9</sup> from the initial window, coming directly from the database and that, if the user decides to left the boxes empty, the program automatically uses those data; in the other case the upper part of the window is dedicated to compiling these boxes. The International System of Units (SI) (or directly deduced units) is used for all the physical and geometric quantities, both in input-output parameters and from-toward the database. This choice

---

<sup>9</sup>The variable transfer between two different *Matlab*© interface windows is performed inserting and extracting them in and from the *Matlab* © *workspace* with the two command *assignin* and *evalin*, respectively. The *workspace* is the non physical place where *Matlab*© saves the variables that is using and those that it calculates. Normally they are automatically saved there, but using the Graphical User Interface (GUI) it is necessary to specify which of them must be shared among the windows. Moreover, within a single worksheet, the variables must be declared as *global* in order to be shared among all the functions that form the *m-file*.

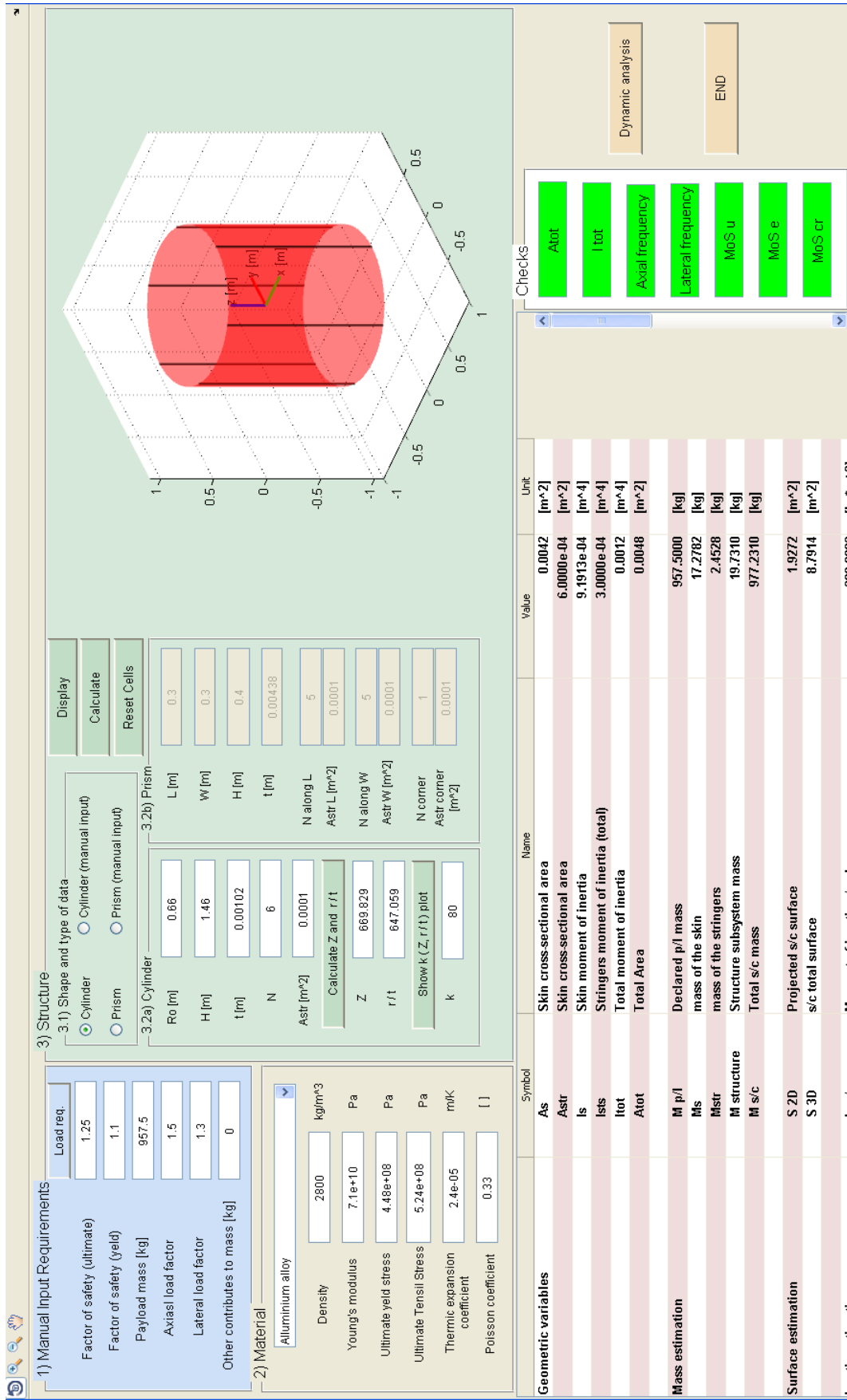


Figure 2.3: The Student Concurrent Design Tool (SCDT) window. Practical use example.

tries to conform all the possible uses of the tool and to avoid possible trivial errors in conversions.

The first list is composed of some general data that could be decided, calculated or given by the system or by some other subsystem engineer. These are:

- the axial  $a$  and lateral  $l$  load factors that are non dimensional quantity, even though they are expressed in multiples of the acceleration of gravity (g's). They represent the ratio between the load applied to the structure and its proper weight, allowing to quickly define a probable average level of the loads. They come from previous experiences or literature.
- the *payload mass* and an entry called *others contribute to mass*. In these two items all the non structural masses must be taken into account. The payload mass is the sum of all the subsystem of the spacecraft, it can be calculated or simply given by the system engineer; the other is an item that the engineer can use to adjust the analysis or to consider other mass contributes.
- the minimum *axial* and *lateral frequencies* are two requirements that in general descend from the launcher mission subsystem specifications. Because the launch loads are the strongest ones during the entire load history of the spacecraft, these frequencies will be part of the calculation for the stiffness sizing of the entire structure. In general the goal is to make the firsts natural frequencies be quite much higher than the typical launcher load frequency, in order to avoid resonance.
- the *Factor of Safety (FS)* for *ultimate* and *yield* stresses. These quantities are greater than one and are used to account for uncertainties that can not be fully analysed. They are generally applied to qualification loads<sup>10</sup> once they have been used as design loads. Each one of them is used to calculate the respective Margin of Safety (MoS) which is define as the ratio between the allowable strength or stresses and the actual stresses multiplied by a safety factor, minus one (in order to accomplish safety requirements, it must be greater than zero):

$$MoS = \frac{\sigma_r}{\sigma_a \cdot FS} - 1 \geq 0 \quad (2.1)$$

Where  $\sigma_r$  is the allowable stress and  $\sigma_s$  is the actual stress due to limit

---

<sup>10</sup>The qualification loads are those that are applied to the structure during the qualification tests, in order to have an higher level of confidence in trusting the design process.

load. For example the MoS yield load for a material is

$$MoS = \frac{\sigma_{yield}}{\sigma_{applied} \cdot FS} - 1 \quad (2.2)$$

Thanks to the following panel, the structure material properties can be chosen. The interface allows to choose among a list of materials and to type new properties of a new one. These characteristics are the density, the Young modulus, the ultimate and yield stresses, the thermal expansion coefficient and finally the Poisson modulus. In the SCDT tool the entire structure is made of just one material.

The next panel is the core of the Student Concurrent Design Tool (SCDT), in fact, it is responsible for the calculation of all the results parameters that the engineer can expect from this tool. In order to do that, it is first necessary to choose the configuration and the main dimensions of the structure: the first sub-panel let the user select the spacecraft configuration between an axial symmetric (cylindrical) shape and a rectangular based prism shape. Moreover, both the configuration have the double possibility to implement calculations on a monocoque or a semi-monocoque<sup>11</sup> structure: this selection is made directly by setting the number of longitudinal reinforcements (stringers) to zero or to  $N > 0$  in one of the edit boxes. As usual there is the possibility to use directly the imported dimensions or to set them manually. The dimension and parameters panel show the main quantities that must be set. The cylindrical shape is described by the radius (Ro [m]), the height (H [m]), the skin thickness (t [m]), the number of stringers (N [ ]) and the cross sectional area of each stringer (Astr<sup>12</sup> [m<sup>2</sup>]); instead the rectangular based prism shape is defined by more parameters, fact that permits to manage a wider set of cases in multiple configurations: the length (L [m]), the width (W [m]), the height ([m]), the skin thickness (t [m]), the number and the cross sectional area (CSA) of the reinforcements for each side along the length (N along L [ ], Astr L [m<sup>2</sup>]), the number and the CSA of the stringers for each side along width (N along W [ ], Astr W [m<sup>2</sup>]), the number and the CSA of the reinforcements placed along each edge corner of the structure<sup>13</sup> (N corner [ ], Astr corner [m<sup>2</sup>]).

Thanks to all the data that have been typed in the *edit text boxes* is now possible to start the calculations of all the geometrical and physical quantities, which provide a first description of the structure subsystem and of its theo-

---

<sup>11</sup>A monocoque structure is a simple thin walled shell (cone, prism, cylinder shaped); a semi-monocoque structure is a monocoque structure with some longitudinal or transverse reinforcements like stringers. From now on monocoque and semi-monocoque terms are going to be used as synonyms of shell and reinforced shell structures, respectively.

<sup>12</sup>STRinger Area

<sup>13</sup>If  $N_{corner}$  is set to be greater than one, in each corner will be placed  $N$  identical stringers. So the total corner stringer CSA is  $4 \cdot A_{str,corner} \cdot N$

retical limits. Because of the dissimilarities between the two main spacecraft configurations two separated dissertations follow below.

**Cylindrical shaped configuration** The calculations for this configuration need some more parameters to start with. These are the number  $Z$ , the  $r/t$  ratio and the buckling coefficient  $k$ . By clicking on the *Calculate  $Z$  and  $r/t$*  button in the cylindrical shape sub-panel, the former two parameters are obtained, then, when the  $k$  to  $Z$  graphic is showed, the  $k$  coefficient can be computed in function of the  $r/t$  ratio. The use and meaning of these latter quantities will be detailed during the explanation of the buckling theory<sup>14</sup>.

First of all, the geometrical quantities are obtained: the total cross sectional area and the total second moment of the section are calculated summing the contributions of the many element that participate to the definition of the structure. The cross sectional area of the skin ( $A_s$ ) is:

$$A_{skin} = \pi \cdot R_o^2 - \pi \cdot (R_o - t)^2 \quad (2.3)$$

the CSA of a single stringer is set as input, so the total area is simply

$$A_{str,tot} = N \cdot A_{str} \quad (2.4)$$

the respective second inertia moments of area are obtained by considering  $N$  concentrated areas placed all along the circumference:

$$I_{skin} = \pi/4 \cdot [R_o^4 - (R_o - t)^4] \quad (2.5)$$

$$I_{str,i} = (R_o \cdot \sin(\theta_i))^2 \cdot A_{str} \quad (2.6)$$

$$I_{str,tot} = \sum_{i=1}^N I_{str,i} \quad (2.7)$$

where  $\theta_i$  is the angle between de semi-axes passing through the centre of the circumference and the first stringers (which is set to be placed on the positive x semi-axis) and the radius connecting the  $i - th$  stringers and the centre. The sum of the areas gives the total one:  $A_{tot}$ . Since the moments of area are all calculated respect to the centre of the circumference, they can be summed together to obtain  $I_{tot}$ .

Some mass and inertia calculation follow logically:

$$M_{skin} = A_{skin} \cdot \rho \cdot H \quad (2.8)$$

---

<sup>14</sup>For all the sizing equations refer to chapter 11 of *Space Mission Analysis and Design*, edited by Wiley J. Larson (United States Air Force Academy) and James R. Wertz (Microcosm, Inc.), 1999.

is the mass of the skin and  $\rho$  is the material chosen density;

$$M_{str} = A_{str,tot} \cdot \rho \cdot H \quad (2.9)$$

is the mass of all the longitudinal reinforcement, while the total mass can be calculated with the following:

$$M_{structure} = M_{skin} + M_{str} + M_{other} \quad (2.10)$$

where  $M_{other}$  is the user manageable contribute to mass. Finally the spacecraft mass is

$$M_{s/c} = M_{p/l} + M_{structure} \quad (2.11)$$

where the p/l stays for payload and s/c means spacecraft. The mass moment of inertia are calculated thanks to the formulas for the homogeneous cylinder:

$$J_{xx,s/c} = \frac{M_{s/c}}{12} \cdot (3 \cdot R_o^2 + H^2) \quad (2.12)$$

$$J_{yy,s/c} = \frac{M_{s/c}}{12} \cdot (3 \cdot R_o^2 + H^2) \quad (2.13)$$

$$J_{zz,s/c} = \frac{M_{s/c}}{2} \cdot R_o^2 \quad (2.14)$$

The moments around x and y have the same expression and the other elements of the inertia tensor  $J_{ij}$  are equal to zero because of the symmetry of the structure. Some other preliminary calculation can be useful for other subsystems and actually the following parameters are necessary to the ADCS to calculate the drag force and to the thermal subsystem (TC) to the irradiation. They deal with the surface of the satellite:

$$S_{projected} = 2 \cdot R_o \cdot H \quad (2.15)$$

is the greatest cross section of the satellite which represents the worst case for drag phenomenon, as the resistance force in a fluid is proportional to it.

$$S_{tot} = 2 \cdot (R_o^2 \cdot \pi + R_o \cdot \pi \cdot H) \quad (2.16)$$

which is the total surface that potentially is subjected to irradiation.

The stiffness sizing starts now. First of all the software realises two main checks on the minimum cross sectional area and second area moment of inertia, that try to satisfy the axial and lateral frequency requirements given as inputs. The frequencies equation of the uniformly spread mass model is inverted in

order to calculate the minimum value of the parameters  $A_{min}$  and  $I_{min}$ :

$$f_{axial} = \frac{1}{4} \cdot \sqrt{\frac{A_{tot} \cdot E}{M_{s/c} \cdot H}} \quad (2.17)$$

$$f_{lateral} = 0.560 \cdot \sqrt{\frac{J_{tot} \cdot E}{M_{s/c} \cdot H^3}} \quad (2.18)$$

calculated for  $A_{tot,min}$ ,  $J_{tot,min}$ ,  $f_{ax,min}$  and  $f_{lat,min}$  become:

$$A_{tot,min} = (16 \cdot f_{ax,min})^2 \cdot \frac{M_{s/c} \cdot H}{E} \quad (2.19)$$

and

$$J_{min} = (f_{lat,min}/0.560)^2 \cdot \frac{M_{s/c} \cdot H^3}{E} \quad (2.20)$$

. These equations instantly procure some first important informations about the stiffness of the satellite, which is generally critical because it is important to avoid the coincidence (and even the similarity) between the natural frequencies of the spacecraft and the launcher proper frequency. For this reason, the *check* panel in the interface contains two *edit boxes* that become green or red if the requirements are fulfilled or not. Note that no importance has been given to the spacecraft orientation, due to its symmetry. This imply the constance of the physical and geometrical parameters in every horizontal direction. On the contrary, this will not happen to the prism configuration, where the two main directions of the reference frame will be taken into account. The stiffness analysis ends with an estimation of the axial and lateral displacements caused by the loads:

$$\delta_{ax} = \frac{M_{s/c} \cdot H}{2 \cdot A_{tot} \cdot E} \cdot a \cdot g \quad (2.21)$$

$$\delta_{lat} = \frac{0.125 \cdot M_{s/c} \cdot H^3}{J_{tot} \cdot E} \cdot l \cdot g \quad (2.22)$$

where  $g = 9.80665[m/s^2]$  is the gravity acceleration,  $l$  and  $a$  are the lateral and axial load factors.

The next calculations deal with the strength sizing of the s/c structure. Once more the load factors are used to define an axial force and a bending torque:

$$P_{axial} = M_{s/c} \cdot g \cdot a \quad (2.23)$$

$M_{s/c} \cdot g$  is the weight of the spacecraft, so, by the load factor definition,  $P_{axial}[N]$  is a force and it is taken as the maximum force acting on the structure axially. Similarly for the bending torque:

$$M_{bend} = M_{s/c} \cdot g \cdot l \cdot H/2 \quad (2.24)$$

the force is given by  $l$  times the weight and the moment is the result of the product between the force and the arm, that is equal to  $H/2$ . This is the distance between the base and the centre of gravity, assuming that the latter lies in the geometric centre of the structure thanks to the uniformity hypothesis. A combination of the two solicitations gives the equivalent force acting on the structure:

$$P_{eq} = P_{axial} \pm \frac{2 \cdot M_{bend}}{R_o} \quad (2.25)$$

which gives the maximum tension in the following cases: fibres of the beam are tensioned if  $P_{axial}$  results to be positive, while fibres are compressed if  $P_{axial}$  is negative. Applying the yield and ultimate load factor to the  $P_{eq}$  and remembering the equation 2.1, is possible to calculate the respective margins of safety. The *check* panel in the interface also shows the acceptability of the last two parameters, that is reached if they are greater than zero ( $MoS > 0$ ).

The last sizing for the cylinder shape allows to calculate the buckling critical compression force and the respective margin of safety, in both monocoque and semi-monocoque configurations. If there are no stringers the structure is represented just by the skin. In this case  $A_{tot} = A_{skin}$  and the elastic buckling stress is given by the following:

$$\sigma_{cr} = 0.6 \cdot \gamma \cdot E \cdot \frac{t}{R_o} \quad (2.26)$$

where  $\gamma = 1 - 0.901 \cdot [1 - e^{-\phi}]$  and  $\phi = 1/16 \cdot \sqrt{R_o/t}$ . The semi-monocoque configuration has a number of reinforcement greater than zero ( $N > 0$ ). When the structure loaded with an axial compressive load, it behaves like a set of panels jointed to the stringers along two parallel sides. This behaviour is different from the previous one and can be described by the following equations:

$$\sigma_{cr} = \frac{k \cdot \pi^2 \cdot E}{12 \cdot (1 - \nu^2)} \cdot (t/b)^2 \quad (2.27)$$

where  $b = \frac{2 \cdot \pi \cdot R_o}{N}$  is the width of the panels,  $k$  is called buckling coefficient that is derivable from the graph in figure 2.4. The graph shows the  $k$  values in function of the  $R_o/t$  ratio and  $Z = \frac{b^2}{rt} \sqrt{1 - \nu^2}$ .

However  $\sigma_{cr}$  has been found, the total critical load that causes buckling instability is easily calculated in both cases:

$$P_{cr} = \sigma_{cr} \cdot A_{tot}. \quad (2.28)$$

$$A_{tot} = A_{skin} + A_{str}$$

The margin of safety concept can now be used in an wider meaning in order to give informations about the outbreak of the buckling. For this reason the critical buckling margin of safety has been here define:

$$MoS_{cr} = \frac{P_{cr}}{P_u} - 1 \quad (2.29)$$

where  $P_u = P_{eq} \cdot FS_u$  is the ultimate load calculated through the respective safety factor. If the margin of safety is greater than zero means that the ultimate stress is reached before the buckling outbreaks and vice versa.

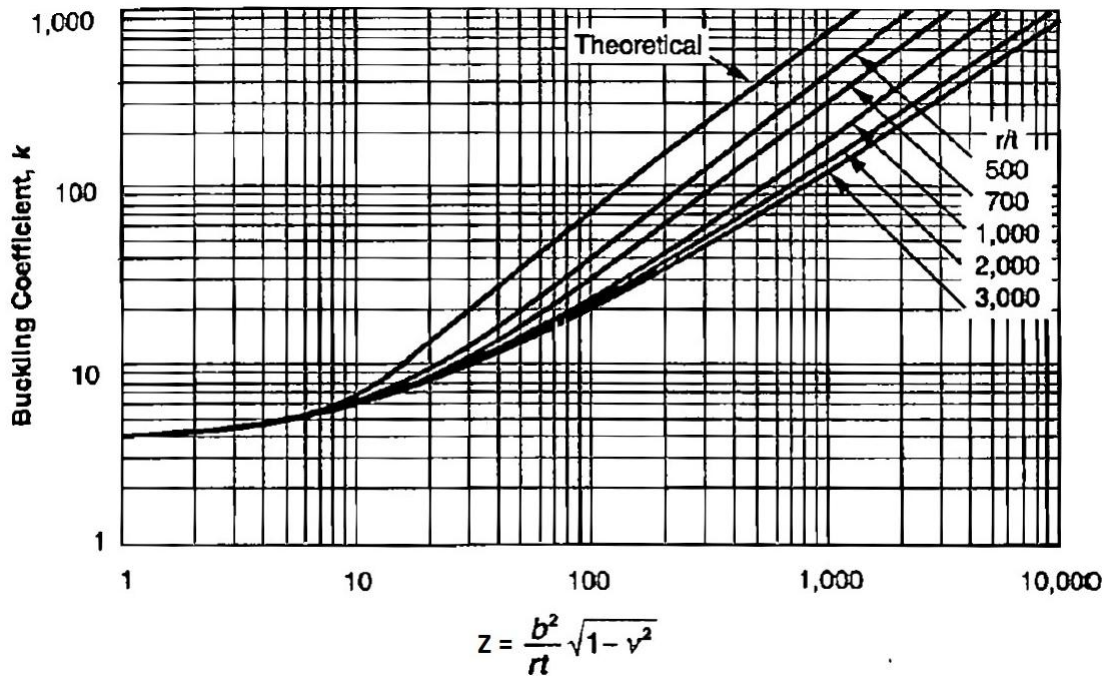


Figure 2.4: Axial buckling load coefficient (picture from [8] Larson Wiley J., Wertz James R. *Space Mission Analysis and Design*, book, Space Technology Library).

**Prism shaped configuration** This configuration has two plane of symmetry. This causes that during the dissertation some other considerations have to be made, but in general the reader shall find a resemblance with the cylinder shape spacecraft treatise. The first calculations deal with the skin and stringers cross sectional areas and the second moments of area:

$$A_{skin} = L \cdot W - (L - 2 \cdot t) \cdot (W - 2 \cdot t) \quad (2.30)$$

The second moments of area are different if calculated respect to two normal axis. The reference frame  $\{x,y,z\}$  is chosen in order to have the  $x$  axis parallel to the length ( $L$ ) of the prism section,  $y$  parallel to the width ( $W$ ) and  $z$  so that it complete the right-handed three axes frame; it follows that  $z$  is parallel to the height ( $H$ ) and that is oriented toward the free base of the satellite (the other base is wedged in the s/c-launcher interface).

$$I_{skin,x} = \frac{L \cdot W^3 - (L - t) \cdot (W - t)^3}{12} \quad (2.31)$$

$$I_{skin,y} = \frac{L^3 \cdot W - (L - t)^3 \cdot (W - t)}{12} \quad (2.32)$$

The stringers cross sectional area  $A_{str,i}$  is given as input, while the moment of the area for each reinforcement is given by the general equations:

$$I_{strX,i} = d_{x,i}^2 \cdot A_{str,i} \quad i = 1 : N_{tot} \quad (2.33)$$

and

$$I_{strY,i} = d_{y,i}^2 \cdot A_{str,i} \quad i = 1 : N_{tot} \quad (2.34)$$

where  $d_{x,i}$  and  $d_{y,i}$  are the distances between the  $i$ -th stringers and the  $x$  and  $y$  axes, respectively.  $N_L$  is the number of stringers along each side, that is parallel to the length;  $N_W$  is the analogous for the width side. Instead, note that  $N_c$  is the number of stringers for every corner of the prism structure. It means that every quantity related to it is automatically multiplied by four by the software, so  $N_{tot} = N_L + N_W + 4 \cdot N_c$ .

Finally the total area and total moment of area are the sum of the skin and stringers ones:

$$A_{tot} = A_{skin} + \sum_{i=1}^N A_{str,i} \quad (2.35)$$

$$I_{tot,x} = I_{skin,x} + \sum_{i=1}^N I_{strX,i} \quad (2.36)$$

$$I_{tot,y} = I_{skin,y} + \sum_{i=1}^N I_{strY,i} \quad (2.37)$$

The mass calculations are exactly the same as before, it is only changing the way to calculate the total area to get to the  $M_{s/c}$ . Once more the inertia quantities calculations are subjected to some changes: the moments around  $x$  and  $y$  axes are not equal any more, but the formulas for the three moments have the same structure, but changes the role of the quantities:

$$J_{x_i,s/c} = \frac{M_{s/c} \cdot [(L_{x_j})^2 + (L_{x_k})^2]}{12} \quad (2.38)$$

taking into account the three combinations of  $i, j$  and  $k$ , where the  $L_{x_{ijk}}$  are the dimension of the parallelepiped along the  $i, j, k$  axes, that are in order:  $x, y$  and  $z$ .

The surface calculation are also analogous to the former case. The total surface and the projected one have been calculated:

$$S_{projected} = max \left\{ \sqrt{(L_{Xi})^2 + (L_{Xj})^2} \cdot (L_{Xk}) \right\} \quad (2.39)$$

once more taking into account the three combinations of  $i, j$  and  $k$ . This quantity represents the greater projected surface of the spacecraft, which is obtained as a rectangular area by multiplying a dimension with the diagonal obtained from the others, as it is finally the area of the rectangular lying on a diagonal plane between two opposite corners of the parallelepiped. The total surface is

$$S_{tot} = 2 \cdot [(H \cdot L) + (H \cdot W) + (W \cdot L)] \quad (2.40)$$

The stiffness sizing for the cylinder structure continues to be valid also in the prism shaped satellite sizing: it is sufficient to use the same equations, taking care that, for safety reasons, the second moment of area to use is the minimum between the two ( $I_{tot,min} = min\{I_{tot,x}, I_{tot,y}\}$ ). Therefore the biggest value of stress that might be present in the structure is obtained. This strategy is necessary since the direction of the applied moment is theoretically unknown. For the same reason, also the lateral frequencies and displacements respect to both  $x$  and  $y$  axes are calculated using equations 2.18 and 2.22 and substituting the suitable values. The equations for axial natural frequency and displacement are exactly the same as the former s/c configuration.

In the stress sizing, the different section properties are considered, too. For the benefit of safety the minimum moment of area and the greatest arm are used in the equivalent load equation:

$$\sigma_{eq} = \frac{P_{axial}}{A_{tot}} + \frac{M_{bend} \cdot d_{max}}{I_{tot,min}} \quad (2.41)$$

where  $d_{max} = max\{L, W\}$ . The loads are obtained using the formulas 2.23 and 2.24, while the ultimate and yield stresses are deduced from the equivalent normal stress; finally, the respective margins of safety can be easily calculated using equation 2.1.

Also the prism buckling stability sizing follows the path of the cylinder one, including the two dissertations for the pure shell and stringers reinforced shell. The pure shell is the first being analysed as it is the simplest one. In fact, the Euler buckling critical load equations are applied to find the limits of the shell,

which is considered behaving as a simple compressed column:

$$P_{cr} = \frac{\pi^2 \cdot E \cdot \min\{I_{skin,x}, I_{skin,y}\}}{(2 \cdot H)^2} \quad (2.42)$$

where the total moment of area is made only by the skin because there are no stringers and it has been used the minimum one due to safety reasons. From the equation 2.42 follows that the critical stress and the MoS are

$$\sigma_{cr} = \frac{P_{cr}}{A_{skin}} \quad (2.43)$$

$$MoS_{cr} = \frac{\sigma_{cr}}{\sigma_u} - 1 \quad (2.44)$$

Once more, the sign of  $MoS_{cr}$  is the discriminant between the type of failure that can occur to the structure: if it is greater than zero the ultimate limit of the material is lower than the buckling limit of the structure; on the contrary if it is negative the Euler buckling could arise before.

As it had happened to the cylinder based structure, in the semi-monocoque case the behaviour under axial load changes. In fact, it is better described by the equations that consider the structure as a series of panels jointed to the stringers along two opposite parallel sides. As usual, for safety reasons the worst case scenario must be considered, so the buckling limit is occurring when the first panel collapses. This is likely going to happen to the widest panel, so the greater width dimension is calculated as follows:

$$b_{max} = \max\left\{\frac{L}{N_L + 1}, \frac{W}{N_W + 1}\right\} \quad (2.45)$$

For a rectangular planar panel jointed on two opposite sides the critical stress is given by the equation below:

$$\sigma_{cr} = \frac{4 \cdot \pi^2 \cdot E}{12 \cdot (1 - \nu)} \cdot (t/b_{max})^2 \quad (2.46)$$

and the MoS has the same expression and meaning as before.

Once all the requested parameters have been calculated the script is programmed to show all the results in the *table* placed in the bottom area of the SCDT window. These parameters are the same that were calculated by the *Excel* tool and basically are calculated in the same way. Next to the result table there is a *quick check panel* containing some *text edit boxes* which are not editable by the user, but show if the minimum requirements are achieved by changing its backgrounds color: if they becomes green it means that the cross sectional area, the area moment of inertia and the natural frequencies are greater than the minimum ones specified in the input by the other subsys-

tems or by the system engineer. Otherwise the non achieved requirement box become red, giving an instantaneous interpretation of the structure subsystem capabilities.

At the end of the Student Concurrent Design Tool (SCDT) is placed the *END* button that builds the *structure* file inserting the new variables to be uploaded<sup>15</sup> to the database and closes the tool. The user has returned to the main window, where the *Create output correspondence* button can be clicked. Follows the pop-up of the same *correspondence* window of the imported variables, but it has been adapted to manage the exporting parameters. It must be considered that the uploading to the database must be done only with the results obtained from the imported variables, otherwise the user creates a mismatch between output and input sets.

Finally, the user can find the so called *Dynamic analysis* button in the right bottom corner, which opens a new worksheet, that allows to make some more dynamic calculations on the last structure set for the static analysis. The capabilities of the new window are just the beginning of the improvements that this work has produced in the Student Concurrent Design Tool (SCDT); Other changes are described in chapter 3, within the second part of the program, that analyses the spacecraft modelled as a multiple degrees of freedom (MDOF) system.

---

<sup>15</sup>Since the database used to build the whole software is only an example to be sure that the tool can work, not all the results have been prepared to the uploading phase. Once a complete database is made up the user can chose all the desired results that must be typed in a *Matlab © structure* of data (i.e. *handles.toexport*) following the indications that can be found in the *END* button part of script (to reach it open the *structure.fig* file from the *Matlab © GUI* and click with the right button of the mouse on the *END* button and then on *view callbacks*). The same has to be made at the end of the advanced static analysis (see subsection 3.2)

# Chapter 3

## Improvements to the SCDT module: the advanced analysis

The improvements to the SCDT do not just consist of the new dynamic analyses of the system as it has been considered during the calculation in section 2.2, but consist also in more interacting worksheets that permit an enhanced set of analyses. These changes are based on a more complex initial geometry of the satellite, that allows lumped masses and internal shelves to be placed. It follows for instance that the dynamic analyses must take into account the mass distribution of the structure. Moreover, also the static analyses have been enhanced by the possibility to select multiple types of load (moments, shears, torques and axial loads) and to calculate the main stresses and deformation for each one of them.

### 3.1 Dynamic analysis tool for single degree of freedom system

First of all, the functioning of dynamic analyses of the SCDT is described below. The simplifying hypotheses for this dissertation are the same of the previous calculations, in fact, the mass will be considered uniformly spread and just the axial displacement are allowed. These two facts lead to the possibility to consider the mass like it was concentrated in the gravity centre of the structure (that is also the geometrical centre thanks to the symmetry) and develop a single degree of freedom model to describe the behaviour of the whole satellite. Note that the new *Matlab*© worksheet inherits all the parameters that needs from the previous one thanks to the button mentioned in the last lines of the section 2.2, while some other will be calculated.

The new *dynamic1GDL* window presents three main panels (see figure 3.1):

- i) the *Setup Parameters* panel is responsible for the calculation of the last

physical parameters needed and for the choice of the analysis type, selectable between *Forcing function* and *base drive*. The former is a time dependent load acting directly on the degree of freedom of the mass, considering that the base is an infinitely rigid frame so it can not move; the latter is a solicitation (a displacement or an acceleration) acting on the base.

The first step is to choose the nature of the load that is stressing the system; the correspondent physical scheme will appear in the reserved spot. It shows the parameters that are used during the calculation. The next step is to complete the *edit text* boxes for the s/c-launcher interface stiffness and the *quality factor* ( $Q$ ) that specifies the overall damping level of the structure. By pressing the *ok* button the table under the figure is filled with the corresponding parameters; later in this chapter, it is explained how they are obtained. The user has now the possibility to verify the values. Note that the software performs the calculation, but the man in the loop is still necessary. If no changes are needed the next button can be pressed obtaining the transfer functions<sup>1</sup> and the last parameters necessary to the analysis. Finally the bode diagrams of these function are plotted.

- ii) the *Nature of the force* panel contains the tools to select and define the load function with the possibility to chose a time dependent function or a PSD frequency dependent function, both definable. This panel even permits to evaluate and display the response of the system to the set load and deduce from it some useful parameters like stresses, strain and MoS.

The sequence of user action continues with the definition of the load: the time dependent load can always be selected as it can be applied both to the system and to the base; in the latter case there is the possibility to select if it is an acceleration or a displacement; on the other side, the PSD frequency dependent function can only be used in the base drive analysis, due to its typically random nature. The PSD simulates the load coming from the launcher<sup>2</sup>. If the *Forcing Function:  $f(t)$*  radiobutton is selected, then the user has to press on the *Define  $f(t)$*  button that opens a new window in which can be typed the duration of the analysis and the

---

<sup>1</sup>The transfer function (TF) is a mathematical relationship between an input and an output of a system. In this work only *bounded input-bounded output* linear systems are considered and all TF are frequency dependent.

<sup>2</sup>The response to a random load has few meaning from the point of view of time, can be significant instead to analyse the dependence with the frequency, also because of the existence of the resonance. Moreover, the properties of the resulting acceleration (the root mean square acceleration  $\ddot{x}_{rms}$ ) guarantee a relatively easy way to size the system in favour of safety, without knowing the exactly time response to the load (see the respective calculations).

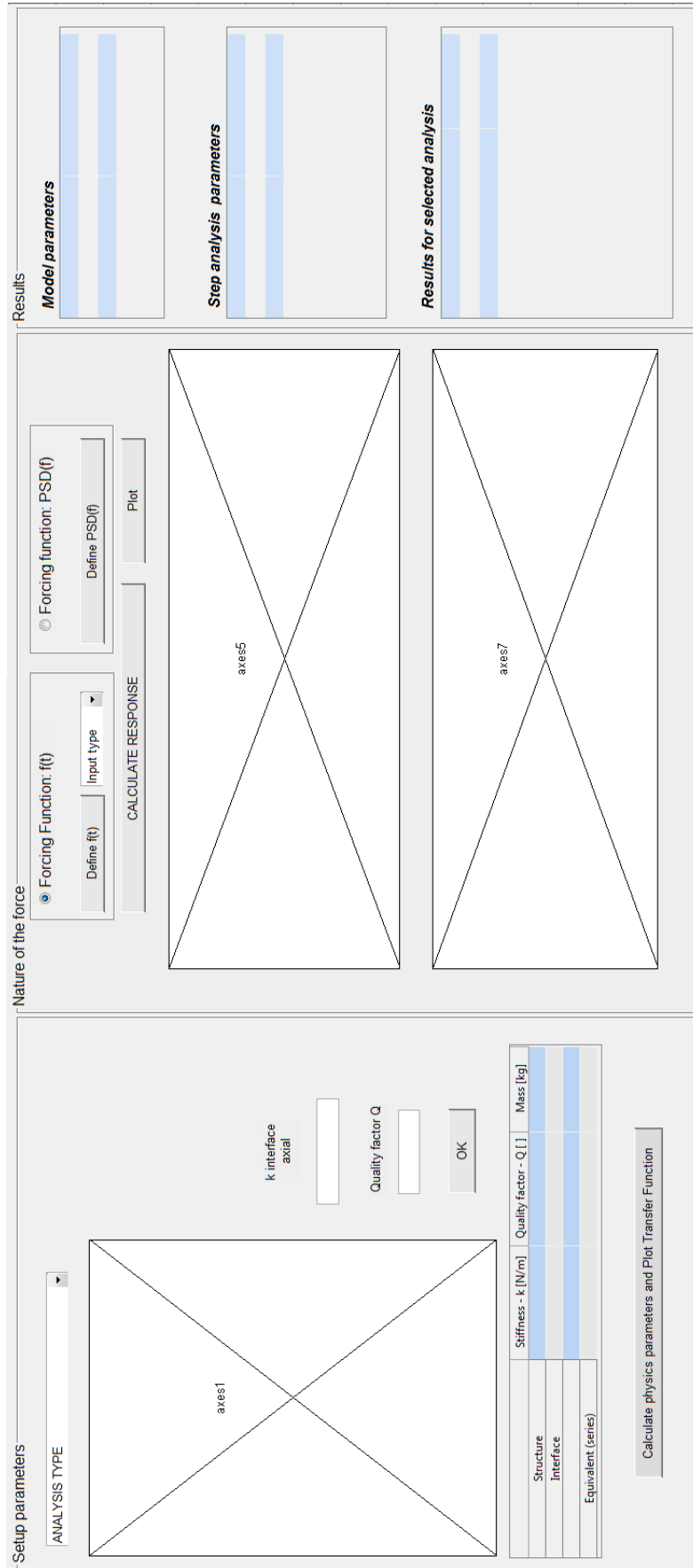


Figure 3.1: Single degree of freedom dynamic analysis window.

effective expression of the function<sup>3</sup>, that is automatically plotted; there is the possibility to select between the step and the impulse function using a menu on the right. If the PSD is needed during the base drive analysis, then the user will press the *Define PSD(f)* button and will be able to set its level in  $[g^2/Hz]$  unit for every frequency through an editable table, which data can be visualized with the bottom left button or can be saved by clicking on the bottom right one.

By clicking on the *OK* button, the selected force is saved in the *Matlab © workspace* and the window is closed, so the user can continue the operation in the main dynamic window pressing the *CALCULATE RESPONSE* button, which simply recall the right *Simulink©* file that performs the dynamic analysis. Every single analysis type is equipped with its file, that is ready to start the simulation. At the end of it, the user just has to close the *Simulink©* window knowing that the results (often are just arrays of data that represent the time response of the system physical quantities) have been saved in the *workspace* already. It is easy now to finish the analysis, clicking on the *Plot* button that displays the response of the degree of freedom of the system and the force that is generated in the mass-base connection. This is the s/c-launcher interface structure. The most interesting values are showed in the right tables.

- iii) the *Results* panel just shows the model parameters and the values of the main analyses results. To perform the uploading, it is necessary to close the windows with the *END* button and then use the initial window (see 2) to create the correspondence between the results and the name of the outputs imported from the database<sup>4</sup>.

All the calculation in the *dynamic1GDL* worksheet are performed by three buttons; they are the *OK*, the *Calculate physics parameters and Plot Transfer Function* and the *Plot* buttons, although the hardest calculations are done automatically by the *Simulink©* file.

**Obtaining the physical parameters** The quantities in the first table are necessary to define the transfer functions of the system. First of all the software takes the data from the *workspace* and from the *edit boxes* just filled and calculates the equivalent stiffness of the system: the structure and interface stiffness

---

<sup>3</sup>The function must be typed following the *Matlab©* rules for operation between arrays: +, -, \*, / symbols become +, -, .\*, ./, the exponential function is exp(...), the power is ^ and the square root is  $\sqrt{\dots}$ .

<sup>4</sup>Once a complete database is made up the user can chose all the desired results that must be typed in a *Matlab © structure* of data (i.e. *handles.toexport*) following the indications that can be found in the *END* button part of script

form a series of two springs, so we can substitute them with the equivalent one calculated as follows:

$$k_{eq} = [k_{structure}^{-1} + k_{interface}^{-1}]^{-1} \quad (3.1)$$

where  $k_{interface}$  has just been set and  $k_{structure} = A_{tot} \cdot E/H$  ( $[N/m]$ ) is the stiffness for a beam with cross sectional area equal to  $A_{tot}$  ( $[m^2]$ ), length  $H$  ( $[m]$ ) and made of a material whose Young modulus is equal to  $E$  ( $[Pa]$ ). Then the damping rate and the natural frequency of the system are obtained thanks to the quality factor and the equivalent stiffness:

$$\zeta = \frac{1}{2Q} \quad (3.2)$$

$$f_n = \frac{1}{4} \sqrt{\frac{k_{eq}}{M_{s/c}}} \quad (3.3)$$

and  $\omega_n = 2\pi f_{nat}$ .

On the basis of the analysis selected, the program builds the appropriate transfer functions. In the forcing function analysis case the necessary TF is:

$$H_1(s) = \frac{X(s)}{F(s)/k_{eq}} = \frac{1}{1 + \frac{2\zeta s}{\omega_n} + \frac{s^2}{\omega_n^2}} \quad (3.4)$$

where  $X(s)$  is the degree of freedom of the mass and  $s = i\omega$  is the complex variable of the Laplace transform<sup>5</sup>. An other TF is the so called *transmissibility* that is the ratio between the amplitude of the base reaction force ( $R(s)$  output) and the input force ( $F(s)$ ). The reaction can be expressed as:

$$R(s) = k_{eq} \left( 1 + \frac{2\zeta s}{\omega_n} \right) X(s) \quad (3.5)$$

so  $R(s)/F(s) = R(s)/X(s) \cdot X(s)/F(s)$ , therefore the *transmissibility* is

$$T(s) = \frac{R(s)}{F(s)} = \frac{1 + \frac{2\zeta s}{\omega_n}}{1 + \frac{2\zeta s}{\omega_n} + \frac{s^2}{\omega_n^2}} \quad (3.6)$$

Thanks to these TFs, the time response for the displacement and the reaction force can be calculated. On the other hand, if the base drive analysis is selected the TFs used are different. Now the degree of freedom of the mass is called  $x_1(t)$ , the base motion is  $x_2(t)$  and their Laplace transforms are respectively

---

<sup>5</sup>The Laplace transform is an integral transform perhaps second only to the Fourier transform in its utility in solving physical problems. The Laplace transform is particularly useful in solving linear ordinary differential equations such as those arising in the analysis of electronic circuits.

$X_1(s)$  and  $X_2(s)$ . The necessary TF are

$$H_2(s) = \frac{X_1(s)}{X_2(s)} = \frac{1 + \frac{2\zeta s}{\omega_n}}{1 + \frac{2\zeta s}{\omega_n} + \frac{s^2}{\omega_n^2}} \quad (3.7)$$

called *displacement transmissibility* and

$$H_3(s) = \frac{X(s)}{X_2(s)} = \frac{-\frac{s^2}{\omega_n^2}}{1 + \frac{2\zeta s}{\omega_n} + \frac{s^2}{\omega_n^2}} \quad (3.8)$$

In the latter equation  $X(s)$  is the Laplace transform of the relative displacement of the mass respect to the base  $x(t) = x_1(t) - x_2(t)$ . This quantity is very important because allows to calculate the reaction force:

$$R(t) = x(t)k_{eq} + \dot{x}(t)c \quad (3.9)$$

where  $c$  ( $[Ns/m]$ ) is the damping coefficient, so it is easily calculated once *Simulink*© has obtained  $x(t)$ . These transfer functions are needed when the base drive function is set to be the displacement of the base.

Instead, if the base acceleration is selected, the TF of interest are now

$$H_4(s) = \frac{X(s)}{A_2(s)} = \frac{-\frac{1}{\omega_n^2}}{1 + \frac{2\zeta s}{\omega_n} + \frac{s^2}{\omega_n^2}} \quad (3.10)$$

and

$$H_5(s) = \frac{R(s)}{A_2(s)} = \frac{-M_s/c(1 + \frac{2\zeta s}{\omega_n})}{1 + \frac{2\zeta s}{\omega_n} + \frac{s^2}{\omega_n^2}} \quad (3.11)$$

that is the product between  $R(s)/X(s)$  and  $H_5(s) = X(s)/A_2(s)$  which have been already calculated.

**Dynamic response calculations** If one between the impulse and step function is selected the response for every parameter of interest is calculated using the *Matlab* © functions *impulse*, *impzplot* and *step*, *stepplot*<sup>6</sup> that just need as inputs the transfer function and the total simulation time. The results are plotted in function of time and the characteristics values are reported in the right side tables. This happens also when a generic function is typed in the *define function* window, but the analysis is performed by the *Simulink*© files that now have all the required data available.

The *FF\_X\_TR Simulink*© file (see figure 3.2) is responsible for the forcing function analysis. It takes the  $F(t)$  array as input and processes it through the

---

<sup>6</sup>These are pre-existing function that simulate the two classic solicitations (with an impulse and a step) that often characterize some important aspect of a system. For example the step response describes the system stability after it has been exposed to a constant solicitation.

two TF  $H_1(s)$  and  $T(s)$  to obtain the  $x(t)$  and  $R(t)$  arrays. The *BD\_X\_TR\_x2 Simulink*© file (see figure 3.3) performs the base drive simulation when the input is the base displacement  $x_2(t)$ . It uses the  $H_2(s)$  and  $H_3(s)$  to give  $x_1(t)$  and  $x(t)$  as output. Finally the *BD\_X\_TR\_a2 Simulink*© file (see figure 3.3) takes the base acceleration  $a_2(t)$  as input and calculates  $x(t)$  and  $R(t)$  using the  $H_4(s)$  and  $H_5(s)$  transfer functions<sup>7</sup>.

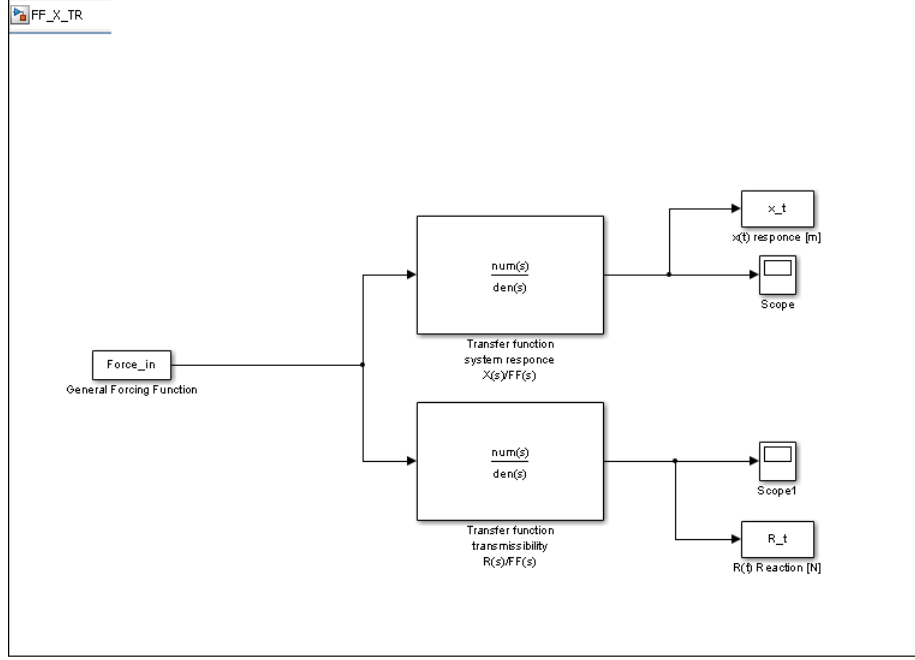


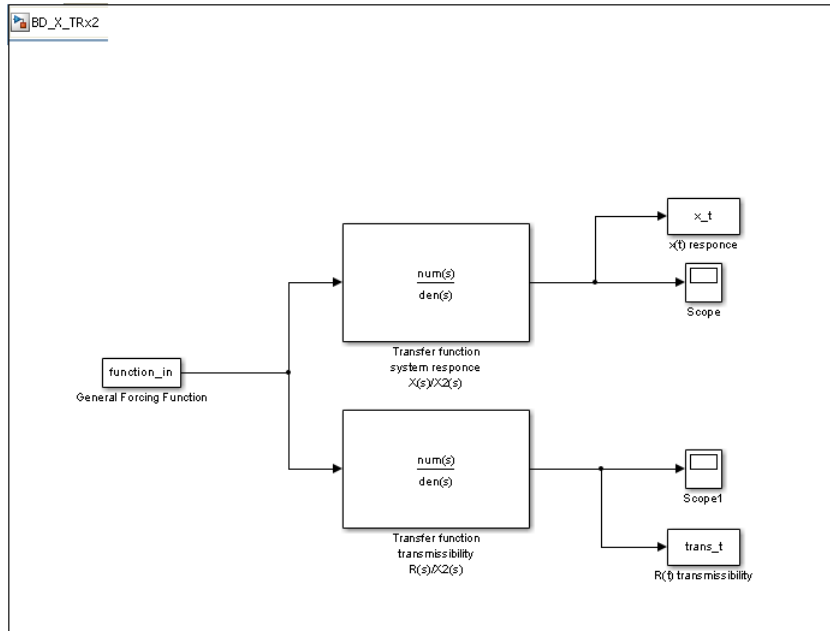
Figure 3.2: Forcing function load *Simulink*© file used in GUI.

Every time the reaction force at the base is obtained, the program calculates its maximum value and use it with the ultimate and yield load factors to calculate the margins of safety (eq 2.1). For every analysis the maximum value of the relative displacement between the basis and the mass is calculated and visualized with the level of stress and the MoS in the right side results table.

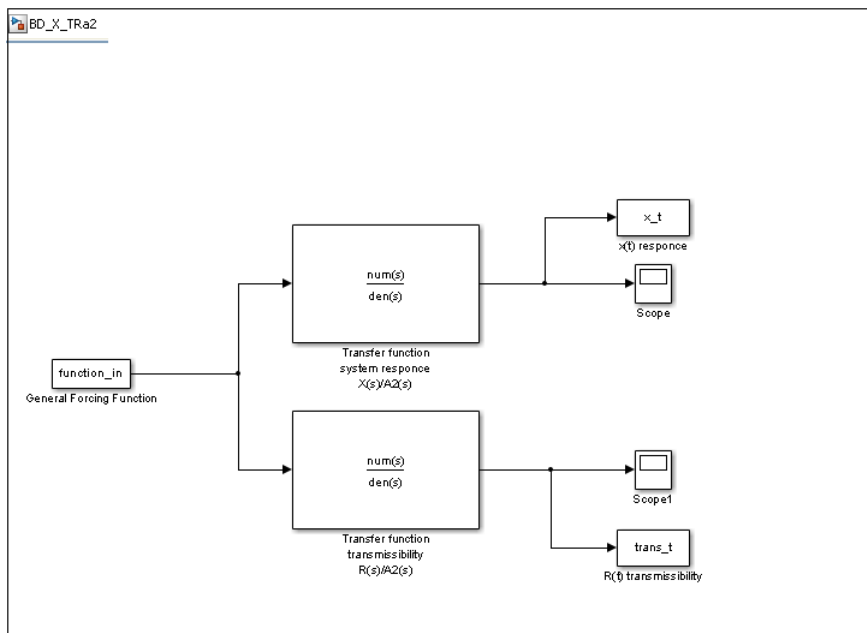
When the PSD base drive solicitation is selected the program calculates the root mean square acceleration ( $\ddot{x}_{rms}$ ) and the root mean square displacement ( $x_{rms}$ ) using the  $H_2(s)$  and  $H_3(s)$  transfer functions and the following equations

$$\ddot{x}_{rms} = \sqrt{\int_{f_1}^{f_2} gPSD(f) \|H_2(f)\| df} \quad (3.12)$$

<sup>7</sup>Once more pay attention to the little difference in the meaning of the variable  $x(t)$  in the forcing function and base drive analysis: in the first case it is the degree of freedom (absolute displacement)**and** the relative displacement respect to the base, in the second case it is only the relative displacement.



(a) Base drive load Simulink © file: displacement.



(b) Base drive load Simulink © file: acceleration.

Figure 3.3: Base drive single degree of freedom Simulink © files used in GUI.

$$x_{rms} = \frac{1}{(2\pi)^2} \sqrt{\int_{f_1}^{f_2} gPSD(f) \|H_3(f)\| df} \quad (3.13)$$

Thanks to the  $\ddot{x}_{rms}$  property to be equal to the standard deviation from the average value, it is easy to find the value of acceleration that is statistically the greatest in the 99.7% of the possible cases<sup>8</sup>:

$$\ddot{x}_{rms,3\sigma} = 3\ddot{x}_{rms} \quad (3.14)$$

its value is expressed as a multiple of the gravity acceleration  $g$ ; therefore the corresponding values of axial load are

$$N_{rms} = M_{s/c} \cdot \ddot{x}_{rms} \quad , \quad N_{rms,3\sigma} = M_{s/c} \cdot \ddot{x}_{rms,3\sigma} \quad (3.15)$$

The latter value is used to calculate the MoS for yield and ultimate stress, which as usual are obtained using the equation 2.1.

## 3.2 Static and dynamic analysis tools for multiple degrees of freedom systems

The advance analysis set of worksheets is accessible from the first window of the tool (named *structure* that allows to connect the database.): it is sufficient to press on the *Advanced dynamic* button and the first new worksheet for the definition of the geometry appears. The architecture of this part of the program is shown in figure 3.4. As usual, the related windows appearance and functioning are explained below. The explanation of all the calculation performed by the tool in this phase will follow.

The *AdvGeom* (i.e. advanced geometry) window is composed of two main areas: the left side is dedicated to the geometry definition and the right side to its display:

- i) The geometry definition starts with a button that leads to a window (*DefGenGeom*) completely analogue to the *geometry definition* panel of the SCDT worksheet, except for the fact that the non strictly geometrical fields have been removed. The data insertion is simple and no further explanation is needed. The possible geometries created are still the well

---

<sup>8</sup>The probability density curve of a random load describes the relative likelihood of acceleration being at a given value. From it the PSD function can be obtained: it is equal to the mean-square acceleration in a selected frequency band divided by the width, in Hz, of that band. The integral argument of the formula 3.12 is the mean square acceleration that passes to the system (thanks to the transfer function filter). The theory of PSD can demonstrate that the root mean square acceleration obtained from that distribution corresponds to the probability between the width of  $\pm 1$  standard deviations.

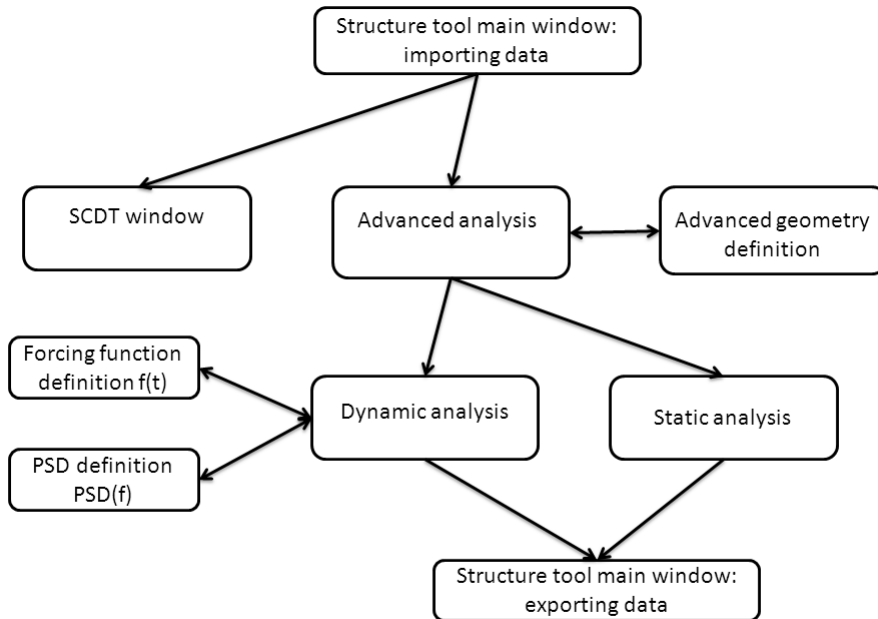


Figure 3.4: Block diagram for advanced analysis.

known cylinder and prism (with or without reinforcements) and the reference frame is set to have the origin in the geometrical centre of the structure. Once more, the  $x$  and  $y$  axes lie in the horizontal plane, and the  $z$  axis along the vertical direction (see figure 3.5). At the end of the typing the user clicks on the bottom right button and returns to the advanced geometry window aware that all the data have been saved in the *workspace*.

- ii) The second step is about the secondary structure definition. It has been thought to be composed of one, two or three internal shelves that support the whole payload. Thanks to two pop-up menus and some edit boxes, the user can chose the effective number of shelves, their thickness and material. Finally, the heights respect to the geometrical centre of the structure can be typed. Note that the heights must be entered in ascending order: if the number of shelves is set to be three, then the A-panel is the lowest and the C-panel is the highest. Remember also that the reference frame has been set to have its origin in the geometric centre of the structure (see figure 3.5).

- iii) The setting of the number and position of the lumped masses<sup>9</sup> tries to simulate the payload instruments and subsystems arrangement in the

---

<sup>9</sup>No information about the effective geometry of the subsystems or of the instruments is given, so the modelling has to be general.

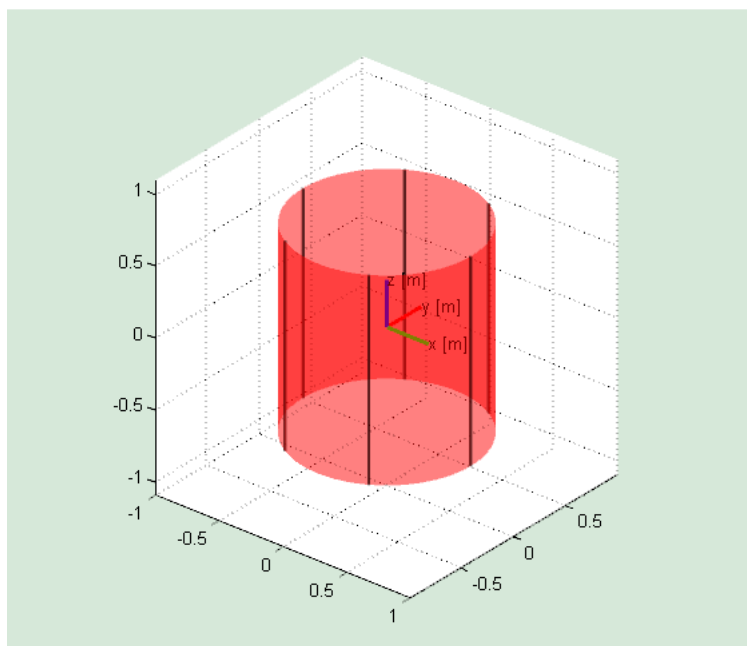


Figure 3.5: Structure and coordinate frame reference figure.

satellite, fact that is essential to calculate the centre of gravity and the moments of inertia more precisely. These data are requested for example by the Attitude Determination and Control Subsystem (ADCS) to perform its analyses, but are used also by the present tool during the MDOF dynamic analysis. It is important to note that the masses replace the role of the payload mass ( $M_{p/l}$ ), so they are meant to represent all the masses that are not specified in other parts of the advanced geometry worksheet. There have been put no limits to the boundary of the selectable area, so the user can simulate also the presence of off-board objects (obviously connected to the s/c, in order to contribute to its total mass).

Thanks to a pop-up menu the user selects the number of concentrated mass. By clicking on the *Place masses* button a new temporary window opens. It allows to directly chose the  $x$ - $y$  coordinates of every mass in the cross sectional plane without caring about its height: the  $z$  coordinate will be determined selecting the proper shelf from the summary table in the *Masses setting* sub-panel, where is still possible to modify the data and to finally insert the value of the masses. By clicking the *OK* button, all the data are saved and the resulting geometry is displayed in the area on the right part of the worksheet (to make the visualisation clearer no boom is plotted, even if their contingent presence is considered in all the calculations and aspects of the tool).

- iv) The *Solar arrays* sub-panel add the mass and inertia characteristics to the satellite model built until now. Two body mounted and the can-

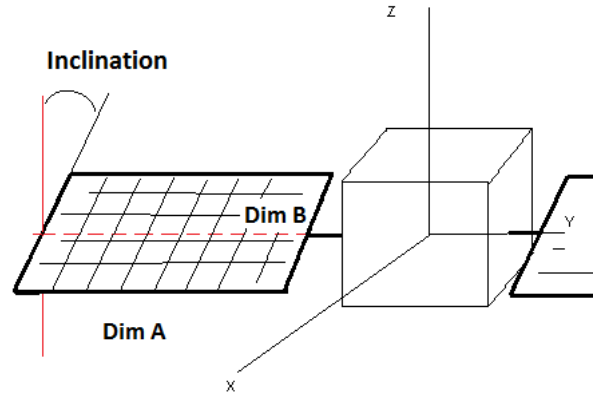


Figure 3.6: Explanation figure for the advanced geometry compiling.

tilted configurations are available for the prim shaped satellite, while just the former can be chosen for the cylindrical shell. This choice has been made due to the habit of use spin-stabilized satellite that are most often cylinders and the three axes stabilized ones that are mainly parallelepipeds.

After the type election the user can insert the principal dimensions (an explanation figure appears when the *Cantilevered* radio-button is chosen 3.6). For the cantilevered panels (two of them placed on the opposite faces which normal versor is parallel to  $y$  axis) length ( $[m]$ ), width ( $[m]$ ), inclination ( $[deg]$ ), thickness ( $[m]$ ) and area density ( $[kg/m^2]$ ) have to be specified, while for the body mounted ones just the last two parameters are needed, as they are supposed to cover the lateral curved spacecraft surface.

- v) By pressing on the *Inertia Tensor and Centre of Gravity* button starts the calculation of the inertia tensors of each single part of the satellite (skin, stringers, shelves, masses and solar arrays) and put them together thanks to the general Huygens Steiner theorem to obtain the total tensor of inertia. The knowledge of the mass distribution described also allows to calculate the position of the gravity centre. These two parameters are numerically visualized in the second column tables and the centre of gravity (CG) is also plotted in the figure on the right.
- vi) The user can now decide to perform a static or a dynamic analysis, clicking on the respective button. This action opens the correspondent worksheet and shares all the necessary data with it.

The first data needed to perform the calculations come from the general definition of the geometry (first button in the worksheet), they are:  $A_{skin}$ ,  $A_{str}$ ,

$A_{tot}$ ,  $I_{skin}$ ,  $I_{str}$  and  $I_{tot}$  (for the prism shape consider the quantities both respect to  $x$  and  $y$ ). The others have just been inserted.

This document proceeds now with a separated dissertation for each satellite configuration, due to their differences.

**Cylinder shape** The first calculation are about the mass of some parts of the structure and the surface parameters that are the same calculated in the SCDT part of the tool.

$$M_{skin} = A_{skin} \cdot \rho_{structure} \cdot H \quad , \quad M_{str,tot} = N_{str} \cdot A_{str} \cdot \rho_{structure} \cdot H \quad (3.16)$$

so the principal structure mass is

$$M_{structure} = M_{skin} + M_{str,tot} \quad (3.17)$$

The main useful surfaces are the total surface and the greatest projected surface of the solid figure:

$$S_{projected} = 2 \cdot R_o \cdot H \quad (3.18)$$

is the greatest cross section of the satellite which represents the worst case for drag phenomenon as it is force depends on and is proportional to it.

$$S_{tot} = 2 \cdot (R_o^2 \cdot \pi + R_o \cdot \pi \cdot H) \quad (3.19)$$

which is the total surface that potentially is subjected to irradiation.

The aim is now to calculate all the single inertia tensors and then sum them together to obtain the total one (the major part of the formulas is taken from [6] Dupac M., Marghitu D.B., *Advanced Dynamics: Analytical and Numerical Calculations with Matlab*, 2012, Springer Science and Business Media). The skin inertia tensor is the easiest to calculate because its symmetry it is sufficient to apply the formulas for the principals moments of inertia of a cylinder shell, aware that the secondary moments are equal to zero:

$$J_{skin,x} = J_{skin,y} = \frac{1}{12} \pi \rho H [3(r_2^4 - r_1^4) + H^2(r_2^2 - r_1^2)] \quad (3.20)$$

where  $r_1 = R_o - t/2$  and  $r_2 = R_o + t/2$ , while

$$J_{skin,z} = \frac{1}{2} \pi \rho H (r_2^4 - r_1^4) \quad (3.21)$$

So the inertia tensor for the cylinder skin is made of these moments put in the main diagonal. The moments of inertia for a single shelf are obtained with the

formulas for a homogeneous cylinder:

$$J_{x,shelf} = J_{y,shelf} = \frac{1}{12} M_{sh} (3R_o^2 + t_{sh}^2) \quad (3.22)$$

with  $M_{sh} = R_o^2 \cdot \pi \cdot t_{sh} \cdot \rho_{sh}$ , and

$$J_{z,sh} = \frac{1}{2} M_{sh} R_o^2 \quad (3.23)$$

The three shelf moment of inertia are calculated respect to a frame centred in the single shelf, so they have to be shift thanks to the Huygens Steiner theorem:

$$[J]_B = [J]_A + m[(\vec{r} \cdot \vec{r})[I_3] - \vec{r} \otimes \vec{r}] \quad (3.24)$$

that is general and can be applied to any rigid body. The  $[J]_A$  is the inertia tensor in the body centre of gravity,  $m$  is its mass,  $\vec{r} = \overline{AB}$  is the vector that express the displacement from the point  $A$  to the point  $B$ ,  $[I_3]$  is the identity  $3 \times 3$  matrix and  $\otimes$  stands for tensor product<sup>10</sup>. In this case A is the CG of a shelf, B is the final position of the shelf respect to the geometrical centre of the structure (which is the origin of the reference frame, too). For all the shelves the vector is vertical and its magnitude is equal to the norm of the height inserted in the apposite worksheet field. Once all the shelf tensors have been obtained, the program sums them to to have the total one.

The moments of inertia of a single stringer are obtained through the same equations of the shelves, with  $H$  instead of  $t_{sh}$  and the radius equal to  $r = \sqrt{A_{str}/\pi}$  and using the befitting mass. Once more, they are expressed in the body frame, so the shift follow now a set of radial vectors from the {x y z} origin to the circumference; no vertical shift is needed because the mid span of the the stringers remain at  $z = 0$ . The total stringer inertia tensor is the sum of all the ones obtained applying the Huygens Steiner theorem, using the vectors above mentioned.

For the calculation of the concentrated masses inertia tensor, its definition can be directly applied:

$$[J] = \sum_{k=1}^N m_k [(\vec{r}_k \cdot \vec{r}_k)[I_3] - \vec{r}_k \otimes \vec{r}_k] \quad (3.25)$$

with  $\vec{r}_k = x\hat{i} + y\hat{j} + z\hat{k}$  corresponds to the position vector of the k-th mass respect to the origin of the reference frame. The explicit expression for  $[J]_{mass}$

---

<sup>10</sup>The vector tensor product (or outer product) definition is:  $(\vec{u} \otimes \vec{v})_{ij} = (\vec{u}\vec{v}^T)_{ij} = u_i v_j$ .

is

$$[J]_{mass} = \sum_{k=1}^N m_k \begin{bmatrix} y_k^2 + z_k^2 & -x_k y_k & -x_k z_k \\ -y_k x_k & x_k^2 + z_k^2 & -y_k z_k \\ -z_k x_k & -z_k y_k & x_k^2 + y_k^2 \end{bmatrix} \quad (3.26)$$

which components are generally different from zero, because most of the times there is no symmetry in the arrangement of the masses. In this case, the  $x$  and  $y$  coordinates of the position vectors have been set when the user placed the masses in the structure and the  $z$  coordinate is equal to the corresponding shelf height.

At last the solar array inertia tensor is obtained. Because of just the body-mounted configuration can be chosen for the cylinder satellite, the solar array is considered to be a shell that covers the lateral satellite surface. The formulas for its moments of inertia are analogous to equations 3.20 and 3.21, where has been used the total mass instead of the density:

$$M_{panel} = 2 \cdot (R_o + t_{panel}/2) \cdot \pi \cdot H \cdot \rho_{panel}; \quad (3.27)$$

$$J_{panel,x} = J_{panel,y} = \frac{1}{12} M_{panel} \{3[R_o^2 + (R_o + t_{panel})^2] + H^2\} \quad (3.28)$$

$$J_{panel,z} = \frac{1}{2} M_{panel} [R_o^2 + (R_o + t_{panel})^2] \quad (3.29)$$

The diagonal outer terms are zero due to symmetry. Considering that all the results are expressed in the same reference frame and taking advantage of the superposition property, the total inertia tensor is:

$$[J]_{tot} = [J]_{skin} + [J]_{sh} + [J]_{str} + [J]_{mass} + [J]_{panel} \quad (3.30)$$

Some more calculations are necessary to find the gravity centre of the whole satellite. The major part of the following little dissertation will take advantage of the symmetry of the masses. Therefore in the numerator of the CG formula a lot of terms are not going to appear, but of course the correspondent mass will be counted in the denominator since it is the sum of the whole participating mass:

$$\overline{OG} = \frac{1}{M_{s/c}} \left[ \int_V \rho(\vec{r}) \vec{r} dV + \sum_{k=1}^N m_k \vec{r}_k \right] \quad (3.31)$$

where  $V$  is the volume of the homogeneous mass and  $N$  the number of lumped masses. considering that all the lumped masses and the homogeneous mass put together form the entire satellite. For all the axial symmetric struc-

tures the gravity centre is the origin of the reference frame  $\{xyz\}$ . Contributes to the shift of the CG are given by non symmetric masses: the shelves that are a source of non-symmetry in the z direction and the lumped masses that potentially can shift the CG in every direction. Considering these hypotheses and that the mass of the entire satellite is  $M_{s/c} = \sum_{k=1}^N m_k + n_{sh} \cdot M_{sh} + M_{structure} + M_{panel}$  the three coordinates e of the center of gravity expressed in the usual reference frame are:

$$x_G = \frac{\sum_{k=1}^N m_k x_k}{M_{s/c}} \quad y_G = \frac{\sum_{k=1}^N m_k y_k}{M_{s/c}} \quad z_G = \frac{\sum_{k=1}^N m_k z_k + \sum_{i=1}^n M_{sh} z_i}{M_{s/c}} \quad (3.32)$$

**Rectangular based prism shape** The mass parameters are the first calculated also for this architecture:

$$M_{skin} = A_{skin} H \rho \quad , \quad M_{str} = H \rho [N_W A_{str,W} + N_L A_{str,L} + N_c A_{str,c}] \quad (3.33)$$

$\rho$  is the volume density of the material selected for the structure. It follows that

$$M_{structure} = M_{skin} + M_{str} \quad (3.34)$$

The most interesting surface parameters are the total and the greatest projected surface, in the body-mounted configuration they are obtained through the following equation. Nothing changes respect to the single degree of freedom analysis:

$$S_{projected} = \max \{ \sqrt{L^2 + W^2} * H, \sqrt{L^2 + H^2} * W, \sqrt{H^2 + W^2} * L \} \quad (3.35)$$

is the greatest cross section of the satellite, while

$$S_{tot} = 2 \cdot (W \cdot H + W \cdot L + L \cdot H) \quad (3.36)$$

is the total surface that can be subjected to irradiation. If the solar panels are deployed in the cantilevered architecture both surfaces increase by the same term that represents the extreme scenario for irradiation and atmospheric drag:

$$S_{panels} = 2 \cdot L_{panel} \cdot W_{panel} \quad (3.37)$$

The calculation of the inertia tensor requires more passages, due to the

greater complexity in the geometry. The first contribute comes from the skin:

$$J_{skin,x} = 2 \cdot \left\{ \frac{1}{12} \left[ M_{LHpanel}(H^2 + L^2) + M_{WHpanel}(H^2 + t^2) \right] + \dots \right. \\ \left. \dots + M_{WHpanel}(L/2)^2 \right\} \quad (3.38)$$

$$J_{skin,y} = 2 \cdot \left\{ \frac{1}{12} \left[ M_{WHpanel}(H^2 + W^2) + M_{LHpanel}(H^2 + t^2) \right] + \dots \right. \\ \left. \dots + M_{LHpanel}(W/2)^2 \right\} \quad (3.39)$$

$$J_{skin,z} = 2 \cdot \left[ \frac{1}{12} M_{WHpanel}(W^2 + t^2) + M_{WHpanel}(L/2)^2 + \dots \right. \\ \left. \dots + \frac{1}{12} M_{LHpanel}(L^2 + t^2) + M_{LHpanel}(W/2)^2 \right] \quad (3.40)$$

where  $M_{WHpanel} = \rho WHt$  and  $M_{LHpanel} = \rho LHt$  are the masses of the lateral panel with sides  $W$ - $H$  and  $L$ - $H$  respectively. The formulas already take into account the Huygens Steiner theorem, so these are the moments of inertia for the lateral panels respect to the origin of the reference frame: the basic moment of inertia formula that has been used is:  $J = 1/12 Mass(length^2 + thickness^2)$  to whom has been added the shift contribute  $Mass(d_G)^2$ . For each axis, all the contributes related to half skin have been summed together and finally multiplied by two to get the moment of the whole structure. The symmetry guarantees that the outer diagonal terms of the tensor are equal to zero.

To get the tensor moment for the shelves, the calculation steps are very similar to the cylinder case. In fact, it just changes the shape of them, but the conceptual path is the same. The single shelf mass is now

$$M_{sh} = LWt\rho_{sh} \quad (3.41)$$

as the surface is a rectangle and the material can be set to be different from the primary structure one. The moments of inertia are those of a rectangular plate parallel to  $x$  and  $y$  axes plane and  $z$  axis passing through the centre:

$$J_{sh,x} = \frac{1}{12} M_{sh}(W^2 + t^2) \quad J_{sh,y} = \frac{1}{12} M_{sh}(L^2 + t^2) \quad J_{sh,z} = \frac{1}{12} M_{sh}(W^2 + L^2) \quad (3.42)$$

Like happened to circular shelves, also these ones have to be shifted along the vertical, so the  $z$  moment is already expressed in the reference frame, while the remaining are not: the program applies the Huygens Steiner formula using the position vectors  $\vec{r}$  that are vertical and have the heights of the shelves as magnitudes. The total inertia tensor for the shelves is the sum of the single

ones.

The calculation concept is similar even for the stringer moments of inertia: once they have been calculated for a stringer, the tensor must be shifted through the  $\vec{r}$  vector to its real position. Must be paid attention that there are three different stringers cross sectional area and that each type of stringer is associated to a different set of position. Then it is not difficult to apply the Huygens theorem. In the *Matlab*© script the most hard thing to do has been to find the position vector for every stringer automatically, but once this has been done the remain calculation just the mere application of a formula.

The calculations for the inertia tensor of the lumped masses are exactly the same, therefore they will not be reported again and the user can refer to equations 3.25 and 3.26.

In the prism shaped satellite the user can chose between the two solar array configurations: body-mounted or cantilevered. Obviously the inertia changes depending on the selected type. In the first case they cover the lateral surface of a parallelepiped, so the program uses the equations 3.38, 3.39 and 3.40 with  $t_{panel}$  instead of the thickness of the skin and with the masses calculated with the proper area density  $\rho_{panel}$ :

$$M_{panel,LH} = \rho_{panel}LH \quad , \quad M_{panel,WH} = \rho_{panel}WH \quad (3.43)$$

The distances from the reference frame origin used are the same as the ones used for the skin panels. Because the Huygens Steiner theorem has already been applied to each moment, the tensor is obtained placing them in the main diagonal of the matrix.

On the other hand the cantilevered solar array architecture needs a different approach. They are modelled as rectangular homogeneous plates to which can be assigned an orientation that implies a rotation of the body around the  $y$  axis, that must be taken into account. Because of these hypothesis, the inertia tensor of a plate and the rotation matrix around the second axis are first calculated

$$[J]_{plate} = \begin{bmatrix} \frac{M_{panel}}{12}L_{panel}^2 & 0 & 0 \\ 0 & \frac{M_{panel}}{12}W_{panel}^2 & 0 \\ 0 & 0 & \frac{M_{panel}}{12}(L_{panel}^2 + W_{panel}^2) \end{bmatrix} \quad (3.44)$$

$$[T] = \begin{bmatrix} \cos i & 0 & \sin i \\ 0 & 1 & 0 \\ -\sin i & 0 & \cos i \end{bmatrix} \quad (3.45)$$

where  $M_{panel} = L_{panel}W_{panel}\rho_{panel}$  and  $i$  is the inclination set as input in one of the *edit boxes* in the interface. Thanks to the properties of the tensors, the

new matrix for the rotated rigid body is obtained through the following

$$[J]^1 = [T][J][T]' \quad (3.46)$$

which has to be shifted twice: the first time along the position vectors  $\vec{r} = (-W/2 - L_{panel}/2)\hat{j}$  and the second time along  $\vec{r} = (W/2 + L_{panel}/2)\hat{j}$  because  $W/2 + L_{panel}/2$  is the distance between the CG of the panel and the origin of the axes. An inertia tensor has been obtained for each solar panel, so next step is to sum them and get the total one.

Once all the contributes have been collected, their sum gives the total spacecraft inertia tensor for the selected selection of solar panel and general shape (equation 3.30). Due to the symmetry of the deployed solar arrays they do not modify the position of the CG and of course neither the body mounted ones do, therefore once the panels mass is added to denominator of the CG vector components the calculation are not affected any more (equations 3.32).

The advanced analysis can continue by clicking on the *static analysis* button, action that opens a new worksheet. It perform the homonym satellite sizing. The window is made of two main panels for the input, a figure and some tables for the results:

- i) in the *General Requirements* panel some *edit text* boxes are placed. They allow to insert the factors of safety for ultimate and yield load and the axial and lateral load factor. The user can decide to use the latter two parameters and the mass of the s/c to define the bending moment and the axial load (in which case the fields are automatically filled with the correspondent value: equations 2.23 and 2.24), but it is not strictly necessary because the magnitudes of these load can be typed directly in the second panel. In the former case the user must pay attention to complete the *edit box* writing by transforming the real scalar in an array, because this is the accepted input format;

- ii) the second *Input* panel is dedicated to the election of the type of load and the specification of its magnitude and of the application point position vector, when necessary. The available loads are (figure 3.7)

- bending moment<sup>11</sup>  $\vec{M} = M_x\hat{i} + M_y\hat{j}$  [Nm] and its application point along the  $z$  axis  $P_M = z_M\hat{k}$  [m]. In the interface the input must be typed like a *Matlab*© vector:  $[M_x, M_y]$  and  $[z_M]$ . The third component of the moment is here considered separated because the torsion effect is treated in a different way;

---

<sup>11</sup>The reference frame has the  $x$ - $y$  plane parallel to the cross section of the structure and all moments are considered to be positive if they follow the right hand rule.

- shear force  $\vec{F} = F_x \hat{i} + F_y \hat{j}$  [N] and its application point  $\vec{P}_F = x_F \hat{i} + y_F \hat{j} + z_F \hat{k}$ ;
- torque moment  $\vec{T} = T_z \hat{k}$  [Nm];
- axial load  $\vec{P} = P_z \hat{k}$  [N].

Once the field have been filled the calculus can be started through the *Calculate* button;

- iii) the tool is programmed to display automatically all the results in one of the tables and in the figure. The table shows the most important stresses, the different kinds of deformations (displacement, rotations and twists) and the margins of safety for the ultimate and yield stresses. The stability to buckling analysis is always performed in the same way as the SCDT interface and the results are reported in one of the tables. The figure in general displays the cross section of the spacecraft with its booms (if they are present), so when obtained the stresses they are plotted or some indication is given in the figure, to help the results interpretation.

The core of the present worksheet is represented by the *calculation* button. It is responsible for the identification of the satellite configuration and for the application of the load. The calculations can be divided into for main blocks, one for each load type. Note that every time it is necessary to consider the stringers distribution in the cross section the user can refer to the following formulas and to figures 3.8. In the circular cross section the stringers are equally distributed along the circumference at constant  $\Delta\theta$

$$x_{str,i} = R \sin(\theta_i) \quad y_{str,i} = R \cos(\theta_i) \quad (3.47)$$

In the rectangular cross section instead they are equally spaced in every side in a symmetrical manner. Taking the number of stringers along the two directions  $N_{str,L}$  and  $N_{str,W}$  the calculations performed for every side are comparable to the following (paying attention to the indices) that refers to the right *W-side*

$$x_{str,i} = \frac{L}{2} \quad y_{str,i} = -\frac{W}{2} + i \frac{W}{N_{str,W} + 1} \quad i = 1 : N_{str,W} \quad (3.48)$$

By adding the four couples of coordinates representing the corner stringers among the four side stringers arrays, the entire reinforcements coordinates are set. Note that the stringers have been ordered starting from the positive  $x$  semi axis in the circular cross section and from the lower right corner in the rectangular one (fig 3.8).

**Bending Moment** The hypothesis in the case that a bending moment is applied to the structure are:

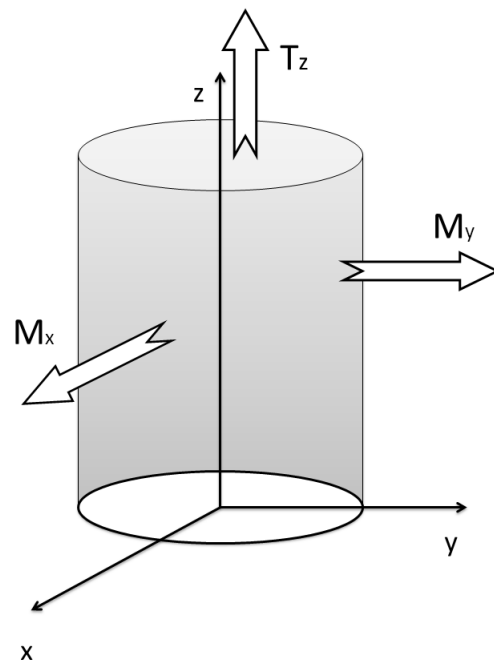
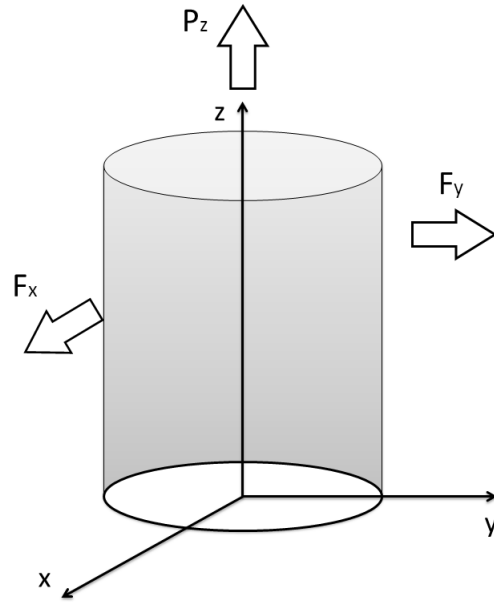


Figure 3.7: Detail of the applied forces and moments in the reference frame for the advanced static analysis.

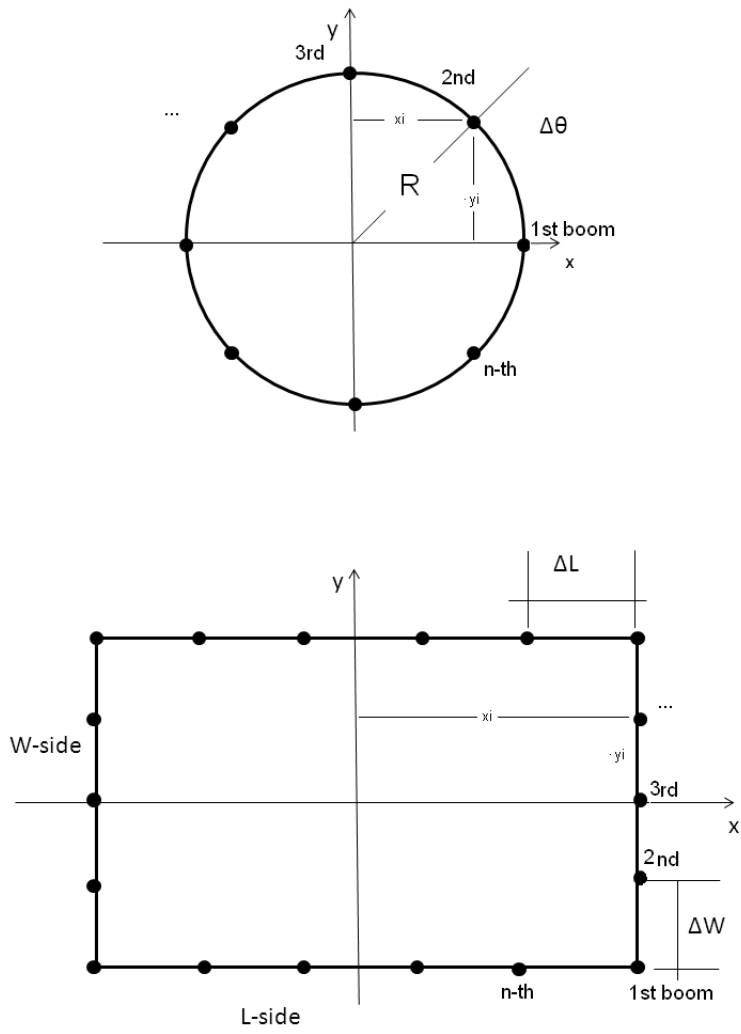


Figure 3.8: Satellites geometry cross reference sections with reinforcements.

- the structure is considered to be a thin walled beam if no stringer is present. In this case all the stress is absorbed by the skin, so the area moment of inertia is entirely the skin one. The formulas considered in this case are equation 2.5 for the cylindrical shape and equations 2.31 and 2.32 for the prism shape configuration;
- the structure is subjected to the idealization process if the user decides that some stringers are necessary to strength the whole structure (figure 3.9). In this case, the normal stress due to the bending moment is completely absorbed by the area moment of inertia of the booms and the skin does not contribute in any manner. This is an idealization that can be justified by the fact that the stringers purpose is to reinforce the skin and that actually their moment of area could be much greater than the skin one. The formulas considered in this case are equation 2.7 for the cylindrical shape and equations 2.33 and 2.34 (see [13]) for the prism shape configuration.

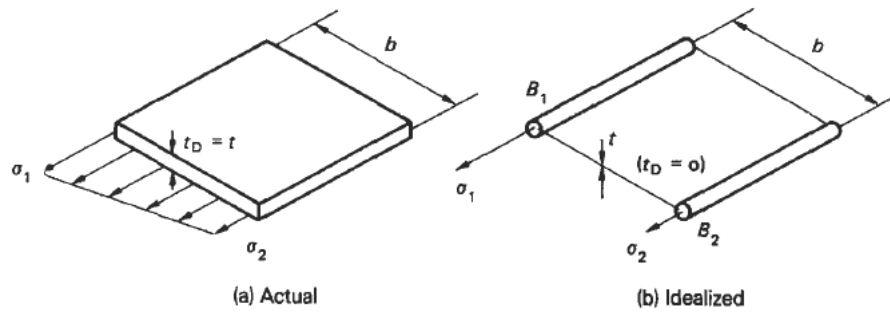


Figure 3.9: Structure idealization ([13] Megson T.H.G *Aircraft Structures for engineering students*,book, Butterworth-Heinemann).

In the cylindrical or prism shaped structure without booms the moment of area are equal to just the skin ones (3.11). Once they are known the program just apply the formula that correlates the normal stress and the bending moment <sup>12</sup>:

$$\sigma_z(x, y) = \frac{M_x}{I_{tot,x}}y - \frac{M_y}{I_{tot,y}}x \quad (3.49)$$

which is a function of the  $x$  and  $y$  coordinates, therefore the stress assumes the greatest value in the farthest point of the section from the neutral axis which inclination is also calculated, displayed among the results and plotted in the figure. If the number of stringers is greater than zero there are no conceptual

<sup>12</sup>Both bending moments around  $x$  and  $y$  axis are positive if they follow the right hand rule. Note that in [13] T.H.G. Megson *Aircraft Structures for Engineering Students* the moment around  $y$  axes is took positive in the other direction.

changes in the results theory: the formula continues to be valid, but it does not express a continuous function of the planar coordinates any more, instead it is defined punctually in any stringer in correspondence of its  $x$   $y$  coordinates:

$$\sigma_{x,i}(x_i, y_i) = \frac{M_x}{I_{tot,x}} y_i - \frac{M_y}{I_{tot,y}} x_i \quad , i = 1 : N_{str} \quad (3.50)$$

where the second moment of area are

$$I_{tot,x} = \sum_i^N A_{str,i} \cdot y_i^2 \quad , \quad I_{tot,y} = \sum_i^N A_{str,i} \cdot x_i^2 \quad (3.51)$$

As there is no shear, from the normal stress can be evaluated the margins of safety. This dissertation is valid for both the cylinder and the prism configuration. Independently from how the  $I_x$  and  $I_y$  have been calculated, the linear displacement ( $\delta$  [m]) of the satellite free base in the  $x$ - $y$  plane and the deflection angles ( $\theta$  [rad]) can be obtained through the following equations<sup>13</sup> (assuming small displacement and linear theory):

$$\delta_x = M_x \frac{(H-a)^2}{2EI_x} \quad , \quad \delta_y = M_y \frac{(H-a)^2}{2EI_y} \quad (3.52)$$

so the total deflection is  $\delta = \sqrt{\delta_x^2 + \delta_y^2}$ , and

$$\theta_x = M_x \frac{(H-a)}{2EI_x} \quad , \quad \theta_y = M_y \frac{(H-a)}{2EI_y} \quad (3.53)$$

where the parameter  $a$  is the distance from the free end and the application point, that is equal to  $H/2 - z_M$  being  $z_M$  the  $z$  coordinate of the application point. The normal stress  $\sigma_z$ , the margin of safety MoS, the deflections  $\delta$ ,  $\theta_x$  and  $\theta_y$  and finally the inclination of neutral axes  $\alpha = \arctan[(M_y I_x)/(M_x I_y)]180/\pi$  ([deg]) are all visualised in the results table.

**Shear force** First of all is reported the dissertation dealing with the effects of shear force applied to a shell structure, where the theory of thin walled closed section beams developing a shear flow has been used (see [13]):

$$q_s(s) = q_b + q_{s,0} = - \left( \frac{F_x I_x - F_y I_{xy}}{I_x I_y - I_{xy}^2} \right) \int_0^s t x ds - \left( \frac{F_y I_y - F_x I_{xy}}{I_x I_y - I_{xy}^2} \right) \int_0^s t y ds + q_{s,0} \quad (3.54)$$

$q_s(s)$  is the total shear flow defined as  $q_s(s) = \tau(s)t(s)$  that is the average value in the skin thickness. It is made of two contributes: the sum of the constant

---

<sup>13</sup> When  $z = H/2$ , note that the reference frame origin lies at half of the satellite length

multiplying the two integrals<sup>14</sup> is the shear flow calculated for the open section beam obtained by *cutting* the section in a point, while the  $q_{s,0}$  term is constant flow due to consider the contribute of the *cut* part (figure 3.10).

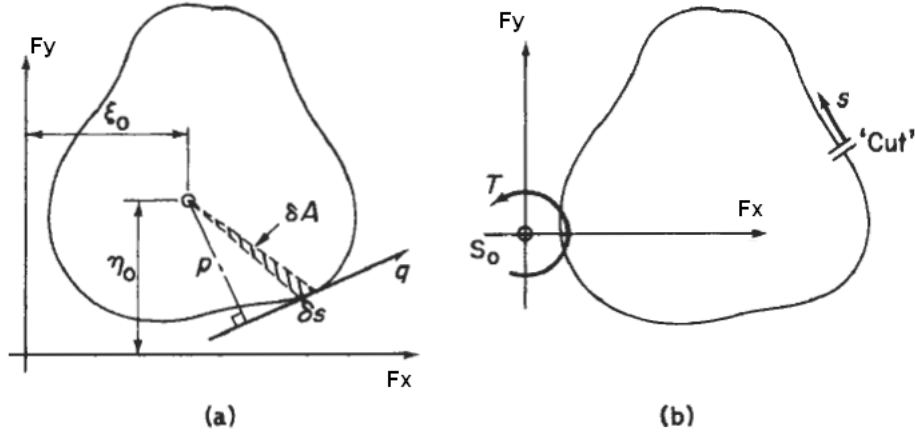


Figure 3.10: Reference picture for general shear flow calculations ([13] Megson T.H.G *Aircraft Structures for engineering students*, Butterworth-Heinemann).

This latter part can be found with the equivalence of the force moment between actions and reactions:

$$F_y \xi_0 - F_x \eta_0 = \oint p q_b ds + q_{s,0} \oint p ds \quad (3.55)$$

where the first member represents the sum of the actions that must be equivalent to the second member that is the sum (integral) of the reactions.  $\eta$  and  $\xi$  are the force arms respect to a point  $C$  and  $p$  is the arm of the shear flow from the same point. Once  $q_b$  has been calculated by equation 3.54, the only unknown variable is the constant shear flow  $q_{s,0}$ . The variable  $s$  is an (or more than one) auxiliary coordinate that follows the path of the thin walled cross section and that allows to find a single parametrisation of the quantities; usually it goes counter-clockwise. Since both the considered sections are symmetric and the smartest election for point  $C$  is  $O_{xyz}$  (because it is the geometric center and common point between the axes of symmetry) the area moment  $I_{xy}$  is null and the force arms are simply the first two coordinates of the application point  $P_F$ ; moreover the thickness of the skin is set to be constant, so the formulas become

$$q_s = q_b + q_{s,0} = -\left(\frac{F_x t}{I_y}\right) \int_0^s x ds - \left(\frac{F_y t}{I_x}\right) \int_0^s y ds + q_{s,0} \quad (3.56)$$

<sup>14</sup>All the integrals in the present dissertation have been performed through the well known trapezoidal rule.

and

$$F_y x_F - F_x y_F = \oint p q_b ds + q_{s,0} \oint p ds \quad (3.57)$$

The tool is programmed to apply these equation to a circumference using a single auxiliary coordinates  $s$  and a polar reference system  $\{R_o, \theta\}$ <sup>15</sup> during the calculations for the shear flow of the cylinder, while four different coordinates have been used for the rectangle (one for each side, see figure 3.11).

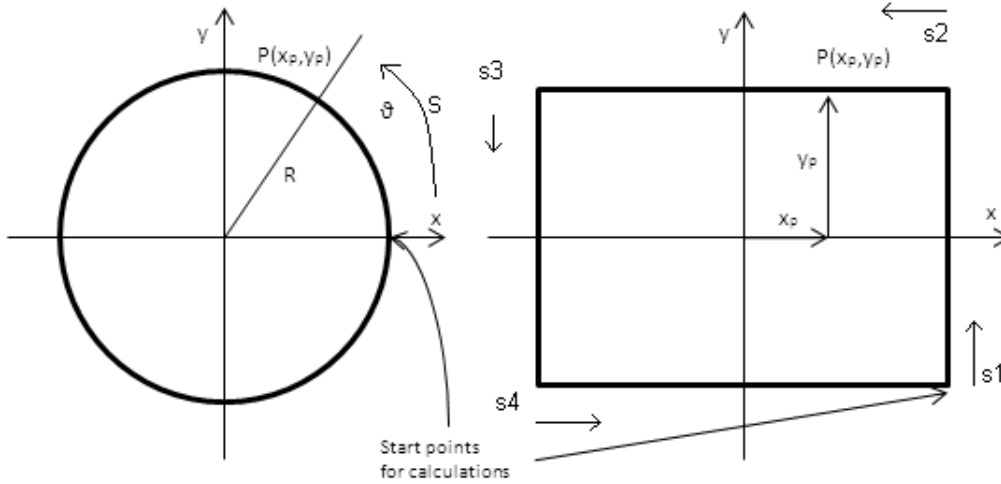


Figure 3.11: Satellites geometry cross reference sections without reinforcements.

The above shear flow equations for thin walled structure are now explained as they have been used in the script. One single angular equispaced vector  $s$  from 0 to  $2\pi$  rad has been created for the circular section, while they are four in the rectangular case, each of them going from a vertex to the subsequent one. The equation 3.56 gives the shear flow  $q_b$  in one and in four different arrays respectively for the two cross sections, then the 4 rectangular contributes have been joined in order to obtain the whole rectangular section shear flow. The first integral in the equation 3.57 is obtained integrating the two shear flow vectors with the arm  $p(x,y)$ , being simply  $R$  in the first case and  $L/2$  and  $W/2$  in the second (depending on the considered side, performing four different integrals, one for each  $s$  auxiliary coordinate vector). The second integral is simply two times the whole cross section area (see equation 3.60 and its explanation):  $2R_o^2\pi$  and  $2LW$ .  $q_{s,0}$  is obtained inverting the formula 3.57. Finally the  $q_s(x,y)$  is obtained summing the constant value  $q_{s,0}$  to the function  $q_b(x,y)$ .

When there are no booms the shear is a continuous function of the  $s$  coordinate, but if some boom is put into the structure some other considerations have

<sup>15</sup>Paying attention to insert the determinant of the Jacobian of the change reference matrix in the equations.

to be done. The theory for this kind of structure idealizes the reinforcements as concentrated areas (as it did in the case of bending moment, figure 3.9) making the hypothesis that they introduce discontinuities in the  $q_s(s)$  function. In this case the shear flow is still a function of  $s$ , but to simplify the analysis will be considered that the skin thickness tends to zero compared to the area of the stringers that become the main cause of the  $q_s$  variation. This imply that the shear flow is constant between every boom couple, while its variation is concentrated straddle every stringer. It follows that the constant value of the shear flow is the average value of its real profile in the same skin section. The equation used is:

$$q_s = q_b + q_{s,0} = -\left(\frac{F_x}{I_y}\right) \sum_{r=1}^n A_{str,r} x_r - \left(\frac{F_y}{I_x}\right) \sum_{r=1}^n A_{str,r} y_r + q_{s,0} \quad (3.58)$$

The sum is meant to be done numbering the stringers from the *cut* and proceeding in the counter-clockwise sense; this is the term of the equation that give the variation in the shear flow  $q_b$ . The *cut* is performed in the intersection between the section boundary and the positive  $x$  semi axis of the circular cross section and in the bottom right corner of the rectangular one. For simplicity in the script formulas the effects of the two component of the shear force  $\vec{F} = \vec{F}_x + \vec{F}_y$  have been obtained separately and then added thanks to the superposition principle, hich is valid for linear systems like the considered ones. The  $q_b$  moment is calculated considering that its value is constant between two subsequent stringers ( $i$  and  $i + 1$ ), so, because of considerations made on the geometry (figure 3.12) the integral becomes the product between the constant  $q_{b,i}$  and twice the area of the triangle made by connecting  $O(0,0)$  and the two booms, similarly to equation 3.60 (see [13]):

$$Mq_{i,rectangular} = q_{b,i}|x_i - x_{i+1}|W/2 \quad Mq_{i,circular} = q_{b,i}|y_i - y_{i+1}|L/2 \quad (3.59)$$

for the four rectangular sides; while for the circular section integral formula has been used again, thanks to its simplicity. The value of  $q_{s,0}$  is obtained through equation 3.57, taking care that since the flow is constant every section integral  $\oint pq_b ds$  can be replaced with this writing

$$M_q = \int_1^2 q_{12} p ds = 2Aq_{12} \quad (3.60)$$

where  $A$  is the area of the geometric figure that is delimited by the two position vector of point 1 and 2 and the skin:  $A = \pi R_o^2$  or  $A = LW$ .

Once  $q_s(s)$  has been obtained, the software calculates the principal shear stress  $\tau(s)$  and applies the Tresca criterion to obtain the equivalent stress for

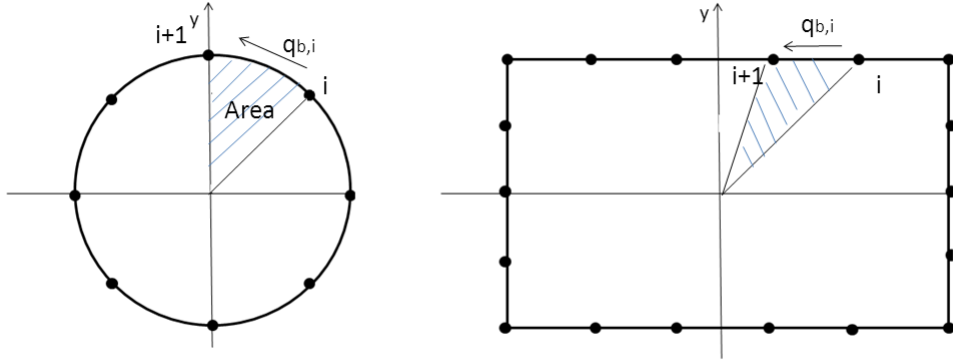


Figure 3.12: Geometric moment integral interpretation.

the uniaxial tensile testing:

$$\tau_{max} = max \left\{ \frac{|\sigma_1 - \sigma_2|}{2}, \frac{|\sigma_1 - \sigma_3|}{2}, \frac{|\sigma_2 - \sigma_3|}{2} \right\} \quad (3.61)$$

where 1, 2 and 3 stand for the three normal directions of the reference frame, but in the uniaxial testing only one of them is different from zero, so it reduces to  $\tau_{max} = \sigma_z/2$ , therefore the MoS for ultimate and yield stresses become

$$MoS_e = \frac{\sigma_e/2}{F_e \tau} - 1 \quad , \quad MoS_u = \frac{\sigma_u/2}{F_u \tau} - 1 \quad (3.62)$$

As usual,  $\tau$  is the maximum present value in the thin wall and the ultimate and yield stresses are characteristics of the structure material.

Finally, the deflections and the twist due to the eventually shift of the shear force application point respect to the centre (that is also the shear centre<sup>16</sup>) is given by the next equation

$$\frac{d\theta}{dz} = \frac{1}{2A} \oint \frac{q_s}{Gt} ds \quad (3.63)$$

where  $G = E/[2(1 + \nu)]$  is the shear modulus and  $A$  the area contained by the close section thin wall. When the load is not applied to the shear centre,  $q_s$  is not symmetric; in this case, the formula shows that the section twist will be present because the integral is not equal to zero. The consequent twist is simply obtained multiplying the rate of twist by the distance of the application point from the fixed base  $\theta_{twist} = \frac{d\theta}{dz} \cdot (H/2 + z_F)$ . The displacements at the

<sup>16</sup>Characteristic geometry dependent point of a cross section. A shear applied directly to it or on a straight line passing through it does not produce twist.

free end of the beam and the deflection angles are respectively:

$$\delta_x = \frac{F_x}{6EI_x}(2H^3 - 3H^2a + a^3) \quad , \quad \delta_y = \frac{F_y}{6EI_y}(2H^3 - 3H^2a + a^3) \quad (3.64)$$

so the total deflection is  $\delta = \sqrt{\delta_x^2 + \delta_y^2}$ , and

$$\theta_x = -F_x \frac{(H-a)^2}{2EI_x} \quad , \quad \theta_y = -F_y \frac{(H-a)^2}{2EI_y} \quad (3.65)$$

where  $a = H/2 - z_F$  is once more the distance of the application point from the free beam end (see footnote 13).

The shear stress results are visualised in the figure as a line that follows the path of the section: when it is out of it, the shear flow is counter-clockwise and vice versa. Note that the plot is out of scale and the maximum value is showed in the table together with the other parameters. Moreover, two plots for the punctual evaluation of the shear flow and of the shear stress are plotted in function of the  $s$  coordinate (or in function of the series of the  $s_i$  in the stringer presence cases).

**Torque moment** Since the booms are longitudinal reinforcements and there is no longitudinal action on them (differently from the shear load case) it is assumed that they do not absorb shear flow, the pure torque moment causes shear stress only in the skin. The dissertation depends basically on the geometry of the section:

$$q = \frac{T_z}{2A} = \text{constant} \quad (3.66)$$

where  $A = \pi R_o^2$  for the cylinder shape and  $A = LW$  for the prism. Since  $q = \tau t$  and the thickness is constant also the shear stress is constant along  $s$ . The torque moment rate of twist is

$$\frac{d\theta}{dz} = \frac{1}{2A} \frac{2\pi}{Gt} \quad (3.67)$$

with  $G$  the shear modulus. Applying the Tresca criterion and the definition of MoS the other parameters can be calculated (equations 3.61 and 3.62).

All the calculated parameters are reported in the tables with their units and the level of stress is plotted in the figure following the same rules of the shear load case.

**Axial load** The axial load analysis is performed the same way it was in the SCDT tool. The calculations are quickly reported, but no further explanation

is required.

$$\sigma_z = P_z/A_{tot} \quad , \quad \varepsilon\% = \frac{\sigma_z}{E} \cdot 100 \quad , \quad H_{new} = H(1 + \varepsilon) \quad (3.68)$$

$P_z$  is meant to be positive if tensile and vice versa. As usual, thanks to the normal stress and the factors of safety, the software calculates the margins of safety for yield and ultimate loads.

Finally, for the buckling stability analysis the reader can refer to the section 2.2 since no change has been done to it. The relative results are also reported in the tables and they are calculated independently from the analysis selected.

Another window opens if the dynamic analysis is selected from the advanced geometry worksheet. The present part of tool allows to perform a multiple degrees of freedom (MDOF) analysis of the structure, where the various dof are represented by the shelves and the masses on them. Like the single degree of freedom (SDOF) one it is made of three main panels:

- i) The *Setup parameters* panel is responsible for the selection and typing of the analysis type and of the remaining physical quantities. They will be used by the dynamic tool. They are the mechanical stiffness, damping rates and the equivalent masses for the degrees of freedom. With the first menu the user select to effectuate a forcing function, analysis where the loads are applied directly to the masses, or to perform a drive base one, in which the load can be either a displacement, an acceleration or a random load. Differently from the other dynamic tool in this case the direction of the force can be selected from a pop menu. The two options are *axial* or *lateral* that affect in different ways the parameters calculations. The following *edit text* boxes are necessary to insert the structure-launcher interface stiffness and to define the damping coefficients. A peculiar choice has been done for this quantity, the reasons will be explained below. Finally the minimum frequencies requirements can be specified. By clicking on the *OK* button the first calculation are computed. They deal with the many equivalent stiffness and the quality factors (that are more than one because of the choice made on the damping coefficients), the masses of the degree of freedom and the natural frequencies and pulsations. With these quantities the software can calculate the transfer functions of the system: there are now as many TF as the number of degrees of freedom through which the time or frequencies dependent loads determine the output of the system;
- ii) the *Type of load* panel permits the definition of the function that is going to stress the system: through the *radiobutton* menu can be chosen the time dependent forcing function or the PSD frequency dependent random

load. The former choice is active for both the type of analysis, while the latter is only available for the base drive one. By clicking on the *Define f(t)* button the *defineAdv\_f* window opens and the user is able to define the total simulation time and the the three functions that stress the three degree of freedom. If the base drive analysis is selected, only the first function is editable because in this case it represents the time dependent solicitation of the base, that can be both acceleration and displacement. With the *ok* button the data are saved in the workspace and the analysis can go on. In fact, the eventual next step is to select the effective type of load of the base drive simulation (acceleration or displacement) by the pop-up menu next to the last button used. Through the *define PSD* button the user defines the frequency dependent random acceleration using the same window of the SDOF analysis.

Now the software is ready to compute the dynamic simulations by running some *Simulink*© files<sup>17</sup>. They have been programmed with all the needed data already inserted, so it is sufficient to run the analysis and then close the window. In fact, the response has been saved in the workspace automatically. The description of this file can be found below during the explanation of the performed calculations. With the last pop-up menu the results are displayed: the degrees of freedom response is plotted in the figures in the second panel and the main numerical results are visualised in the tables of the third panel.

- ii) The *Results* panel reports the main data of the analysis; they are for both axial and lateral cases (if the load is time dependent): the maximum displacement of the masses and the correspondent time of the analysis, the deformations, the maximum forces and stresses and the correspondent simulation time and finally the margins of safety calculated with the maximum stress that occurs arises in the structure. For the frequency dependent load the results are the root mean square accelerations and the relative loads, stresses and margins of safety.

As already mentioned, the calculations done in the parameters preparations deal with the degrees of freedom masses, stiffness and damping. The detail of the passages is exposed below considering that the equivalent system is a series of  $N_{sh}$  masses connected with stiffness and a dampers where only the first mass is connected to the frame.

The mass of a single dof is made of all the masses that can be considered to be concentrated in it. For each of them it has been decided to sum the shelf

---

<sup>17</sup>The axial and lateral analyses for the system loaded with a set of  $N_{dof}$  forces are computed by the *FF-q-adv1*, *FF-q-adv2* and *FF-q-adv3* files depending on the number of dof; all the base drive analyses are performed by the three couples *FF-q-adv1-disp* and *FF-q-adv1-acc*, *FF-q-adv2-disp* and *FF-q-adv2-acc*, *FF-q-adv3-disp* and *FF-q-adv3-acc* files.

mass, all the lumped masses that are placed on the shelf and the part of main structure (skin and booms) that lies between the  $i$ -th and the  $(i - 1)$ th degrees of freedom:

$$M_i = M_{shelf,i} + \sum_{k=1}^m m_{k,i} + A_{tot}\rho(H_{dof,i} - H_{dof,i-1}) \quad i = 1 : N_{sh} \quad (3.69)$$

where  $A_{tot}$  is still the total cross sectional area of the structure and the last term is intended to be positive and if  $i = 1$  the second height is the coordinate of the frame. If the solar arrays are in the body mounted configuration the additional contribute  $S_{panel}\rho_{panel}$  is added. The dof stiffness is calculated in two different ways depending on if the load is in the axial or in the lateral direction, in the former case

$$k_i = \frac{EA_{tot}}{(H_{dof,i} - H_{dof,i-1})} \quad i = 1 : N_{sh} \quad (3.70)$$

and in the latter case

$$k_i = \frac{3EI_{tot}}{(H_{dof,i} - H_{dof,i-1})^3} \quad i = 1 : N_{sh} \quad (3.71)$$

but the interface stiffness must be considered so

$$k_{1,eq} = [k_1^{-1} + k_{interface}^{-1}]^{-1} \quad (3.72)$$

Finally the damping coefficients are set to be a linear combination of the  $i$ th mass and the stiffness with two coefficients  $\alpha$  and  $\beta$ . This choice has been made because it allows to diagonalise also the damping matrix (see below).

$$c_i = \alpha M_i + \beta k_i \quad i = 1 : N_{sh} \quad (3.73)$$

The differential system of equations that describes the dynamic of the system can be written in the matrix form using the data just calculated. The three degrees of freedom case is described:

$$\begin{aligned} \begin{bmatrix} M_1 & 0 & 0 \\ 0 & M_2 & 0 \\ 0 & 0 & M_3 \end{bmatrix} \begin{Bmatrix} \ddot{x} \end{Bmatrix} + \begin{bmatrix} c_1 + c_2 & -c_2 & 0 \\ -c_2 & c_2 + c_3 & -c_3 \\ 0 & -c_3 & c_3 \end{bmatrix} \begin{Bmatrix} \dot{x} \end{Bmatrix} + \\ + \begin{bmatrix} k_{1,eq} + k_2 & -k_2 & 0 \\ -k_2 & k_2 + k_3 & -k_3 \\ 0 & -k_3 & k_3 \end{bmatrix} \begin{Bmatrix} x \end{Bmatrix} = \begin{Bmatrix} F \end{Bmatrix} \end{aligned} \quad (3.74)$$

The system can be described by the following writing

$$[M]\ddot{\vec{x}}(t) + [C]\dot{\vec{x}}(t) + [K]\vec{x}(t) = \vec{F}(t) \quad (3.75)$$

that is general and can be applied to any  $N$  degrees of freedom systems.

The theory of the mechanic vibrations helps the dissertation by suggesting to describe the more complex system using the modal coordinates. Following this way and thanks to the hypotheses made on the damping matrix, the three matrix can be diagonalised by the eigenvector matrix. Once the eigenvalue problem<sup>18</sup> has been resolved, the system equations can be written using the following:

$$[\hat{M}]\ddot{\underline{q}}(t) + [\hat{C}]\dot{\underline{q}}(t) + [\hat{K}]\underline{q}(t) = \underline{\hat{F}}(t) \quad (3.76)$$

where the matrix are diagonal<sup>19</sup> and equal to

$$[\hat{M}] = [\Phi]^T[M][\Phi] \quad [\hat{C}] = [\Phi]^T[C][\Phi] \quad [\hat{K}] = [\Phi]^T[K][\Phi] \quad (3.77)$$

where  $\underline{\hat{F}}(t) = [\Phi]^T\vec{F}(t)$  because  $\vec{x}(t) = [\Phi]\underline{q}(t)$  and the entire equation has been pre-multiplied by  $[\Phi]^T$ ;  $[\Phi]$  is the eigenvectors matrix. The three equation are now independent and every line can be resolved separately to find the solution for the  $i - th$  modal coordinate; then by multiplying the vector  $\underline{\hat{q}}(t)$  by the eigenvector matrix the original coordinates can be found again:

$$\begin{bmatrix} \hat{M}_1 & 0 & 0 \\ 0 & \hat{M}_2 & 0 \\ 0 & 0 & \hat{M}_3 \end{bmatrix} \left\{ \ddot{\underline{q}} \right\} + \begin{bmatrix} \hat{c} & 0 & 0 \\ 0 & \hat{c}_2 & 0 \\ 0 & 0 & \hat{c}_3 \end{bmatrix} \left\{ \dot{\underline{q}} \right\} + \begin{bmatrix} \hat{k}_1 & 0 & 0 \\ 0 & \hat{k}_2 & 0 \\ 0 & 0 & \hat{k}_3 \end{bmatrix} \left\{ \underline{q} \right\} = \left\{ \underline{\hat{F}} \right\} \quad (3.78)$$

so the single equation is

$$\hat{m}_n\ddot{q}_n + \hat{c}_n\dot{q}_n + \hat{k}_nq_n = \hat{F}_n \quad n = 1 : N_{dof} \quad (3.79)$$

that is the equation for the single degree of freedom (SDOF) system loaded with a time dependent force, but pay attention to do not confuse the facts: this is valid for the modal coordinates because they are a privileged point of view to see the system, but they are not the degree of freedom at all. All this means that every modal coordinate has its own transfer function that obviously

---

<sup>18</sup>The eigenvalue problem applied to a mechanic system allows to find the natural pulsations (root square of the eigenvalues) and the modal vectors (eigenvectors) that describe the position of the degrees of freedom of the system for every characteristic vibration mode. In the present case it is equal to solve the  $\det([K] - \lambda_n[M]) = 0$ , therefore  $\omega_n = \sqrt{\lambda_n}$   $n = 1 : N_{dof}$  and the  $\vec{\phi}_n$  are those that satisfy the  $([K] - \lambda_n[M])\vec{\phi}_n = 0$ .

<sup>19</sup>The fact that the new matrix are diagonal comes from the theory of the modal coordinates, in fact, they have the following property respect to those matrix:  $\vec{\phi}_n[M]\vec{\phi}_m = \delta_{nm}m_n$ .

has the same writing of the equation 3.4:

$$H_n(s) = \frac{q_n(s)}{\hat{F}_n(s)/\hat{k}_n} = \frac{1}{1 + \frac{2\zeta_n s}{\omega_n} + \frac{s^2}{\omega_n^2}} \quad n = 1 : N_{dof} \quad (3.80)$$

These TFs will be utilised for both the forcing function analysis and the base drive one, the reason will be explained in a few lines. To end this part of calculations, the tool finds the frequencies and the quality factors for every dof:

$$Q_n = \frac{1}{2\zeta_n} \quad , \quad \zeta_n = \frac{1}{2\omega_n} + \frac{\omega_n}{2}\beta \quad (3.81)$$

from the definition of  $c_i$ , while  $\nu_n = \omega_n/(2\pi)$ .

Before continuing with the description of the *Simulink*© files for every different type of analysis, must be said that once the stiffness and the damping have been set there is no conceptual difference in the dissertation depending on the direction of the force, so the program uses the same files aware that the change in the  $[K]$  matrix calculation mode makes the difference. The first simulation analysed deals with the system subjected to a time dependent load  $\vec{F}(t)$ . Consider the three dof system since it is the maximum number of selectable shelves and in order to comprehend automatically the other two cases. The force vector has three components that are defined through the *defineAdv.f* window together with the total simulation time  $t_{sym}$ . Thanks to these data the software creates three matrix containing a line with the time increments from zero to  $t_{sym}$  and another containing the function values. They are passed to the *Simulink*© file *FF\_q\_adv3*<sup>20</sup> in which the vectors are multiplied by the  $[\Phi]^T$  matrix to obtain  $\hat{F}$ . This is divided in its components that are connected to a gain block containing the  $\hat{k}_i$  stiffness and to the TF blocks which outputs are already the normal mode time responses. These are collected together to be multiplied by the eigenvectors matrix to obtain  $\vec{x}(t)$ . This vector contains the three degrees of freedom responses that can be used to find also the internal forces of the system. In fact, in every moment the forces between two degrees of freedom are by definition

$$N_n(t) = k_n z_n(t) + c_n \dot{z}_n(t) \quad (3.82)$$

with  $z_n(t) = x_n(t) - x_{n-1}(t)$  for  $n = 2, 3$  and  $z_1(t) = x_1(t)$  because the frame has infinite rigidity. If the load is in the axial direction,  $N_n(t)$  is the internal constant (in the relative section of beam) axial reaction, while if it is in the lateral direction  $N_n(t)$  stands for constant shear force and takes the  $T_n(t)$  sym-

---

<sup>20</sup>The 1 and 2 dof file are respectively *FF\_q\_adv1* and *FF\_q\_adv2* which follow the same internal logic, but are adapted to each case.

bol. Therefore by taking opportunely the response components, performing the time derivative and using some gains containing the stiffness and damping coefficient the file can also give the internal forces as outputs (see figure 3.13).

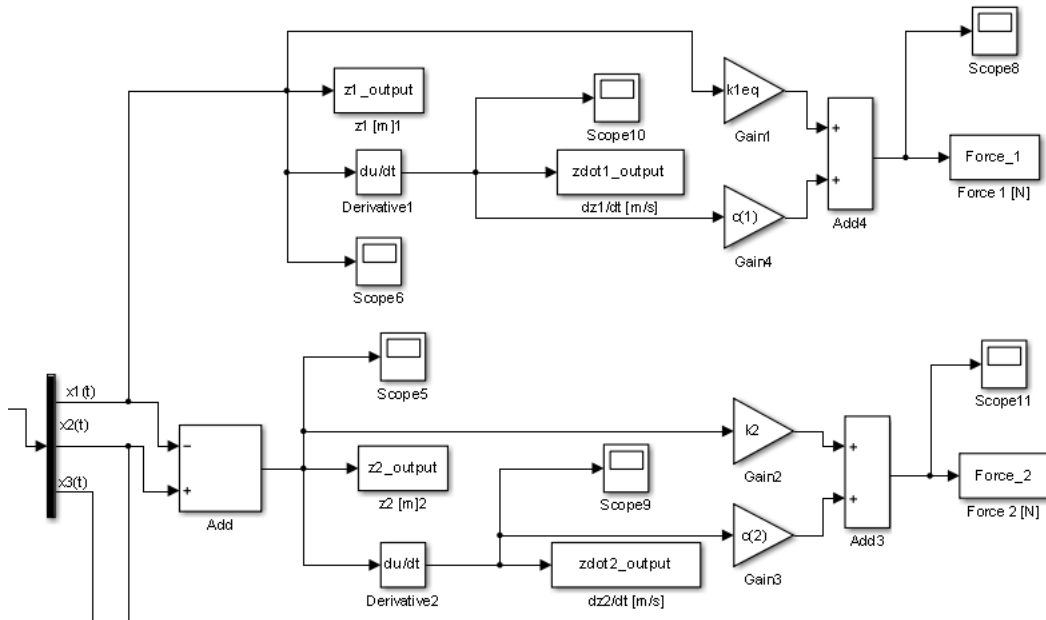


Figure 3.13: Detail of the internal forces calculation in a *Simulink*® file.

The forces and displacements arrays are passed automatically to the workspace at the end of the simulation. They are loaded in the structure tool and are used to extract its maximum values from which the normal stresses and the margins of safety are calculated in the case the action are axial, otherwise the maximum values of the internal shear forces are saved and displayed in order to let the user use them in the *AdvStatic* worksheet. The user just have to report the values in the input *edit text* boxes of the window taking care about two hypothesis:

- the circular section has no further problem, but if the analysis is done on the rectangular one the user must be aware that in the dynamic analysis has been considered the worst case for the possible occurring stresses, that is the one where the lateral loads are applied in the direction with the minimum second moment of area (for the rectangle it is the direction with the minor side);
- every degree of freedom is made of a beam segment and a mass and the internal shear force is caused mainly by the concentrated masses in the shelve (that should represent the greatest value of mass in the satellite); for these reason is like the shear was applied to the end of the length of the beam segment corresponding to the degree of freedom. Therefore the

user must take care to type the right values in the third component of the application point *edit text* box.

To not caring about this hypothesis leads to errors in the resulting lateral displacements and rotations, but does not cause any difference in the shear distribution because it is dependent on the property of the section and not on the  $z$  coordinate along which is constant.

In this way the results are more accurate and complete than the hurried calculations that could have been performed in the dynamic window. In the axial case the equation are simpler and the calculation can be done directly.

As it has been run over above, the time dependent base drive analysis uses the same transfer function (TF) of the simulation with the explicit forces as loads. The reason is simply because thanks to a stratagem, that the use of *Simulink*® allows to do, it has been translated the base movement into a force that affect only the first degree of freedom:

$$\vec{F}(t) = \begin{Bmatrix} F_1(t) \\ 0 \\ 0 \end{Bmatrix} = \begin{Bmatrix} (x_1(t) - x_o(t))k_{1,eq} + (\dot{x}_1(t) - \dot{x}_o(t))c_1 \\ 0 \\ 0 \end{Bmatrix} \quad (3.83)$$

The reader can note that this way to model the force needs the knowing of  $x_1(t)$  that is still unknown because is a result of the analysis, but the problem is solved through a feedback in the block diagram of the system. If the function specified is a displacement, it is passed to the file and by two gain blocks, a derivative one and the sum with the  $x_1(t)$  feedback the force is built. Then, the latter passes through the same passages as in the *FF\_q\_adv3* file with the only change dealing with the feedback line. If the defined function is an acceleration, the only difference in the path is a double integration at the very beginning (see figures 3.14 and 3.15).

Finally, next paragraph deals with the random analysis implementation for the MDOF system (figure 3.16) <sup>21</sup>. The explanation will be detailed for the three degree of freedom system in order to clarify the specific calculation performed. Considering the usual multiple degree of freedom system and the modal approach dissertation made previously is now possible to define some more equations that allow to estimate the root mean square accelerations for every mass due to the base random acceleration load of the base. The load (called  $W_{\ddot{u}\ddot{u}}(f)$ ) is a function of the frequency, that is the well known Power

---

<sup>21</sup>The present calculations are based on section 2.5.2 *MDOF System Loaded by Random Enforced Acceleration* of the textbook by Jaap Wijkker, *Random Vibrations in Spacecraft Structures Design*, Springer 2009.



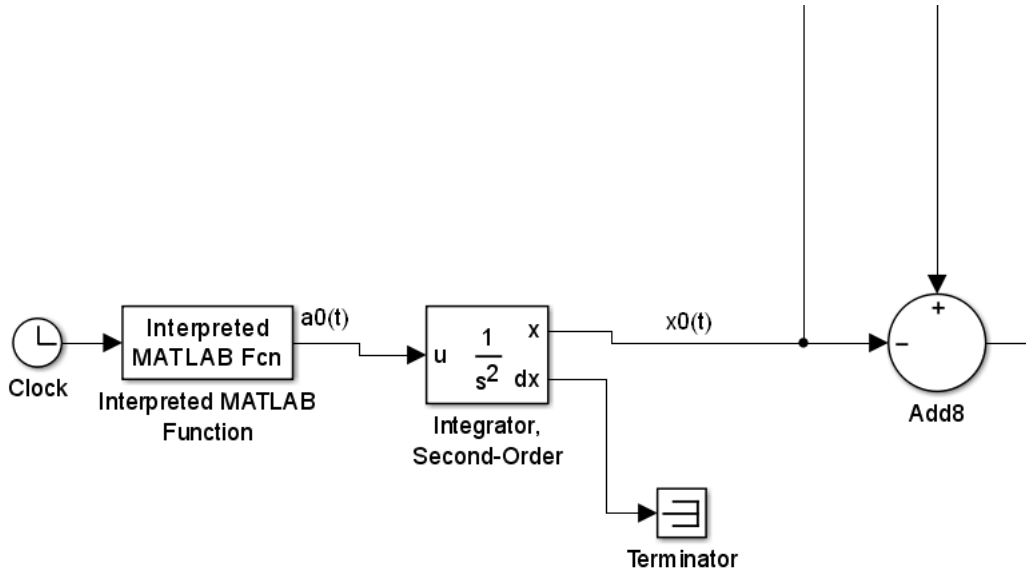


Figure 3.15: Difference in the block diagram respect to the one in figure 3.14 (*Simulink*© file *FF-q-adv1-acc*).

Spectral Density (PSD) which is defined through the same window used in the SDOF part of the program (section ??).

The equation of the undamped free system

$$[M]\ddot{\vec{x}}(t) + [K]\vec{x}(t) = \vec{0} \quad (3.84)$$

is modified by the rigid body vector  $T = (1, 1, 1)^T$  in the following

$$[M]\ddot{\vec{z}}(t) + [K]\vec{z}(t) = -[M]T\ddot{u}(t) \quad (3.85)$$

considering that  $\{z(t)\} = \{x(t)\} - \{T\}u(t)$  and that  $[K]\{T\}u(t) = \{0\}$  because  $\{T\}$  represents the rigid body mode in the direction of the enforced displacement  $u(t)$ .

The enforced root mean square accelerations are extracted by making the root of the principal diagonal of the following matrix

$$[E(\ddot{x}_i\ddot{x}_j)] = \int_0^\infty [W_{\ddot{x}_i\ddot{x}_j}(f)] df \quad (3.86)$$

where the argument is obtained by the following set of equations:

$$[H_{zu}(2\pi f)] = (2\pi f)^2 [\Phi] \left( \left[ \frac{H_i(2\pi f)}{m_i} \right] [\Phi]^T [M] \{T\} \right) \quad (3.87)$$

which is a column vector with the length equal to the dof number, where  $[M]$  is

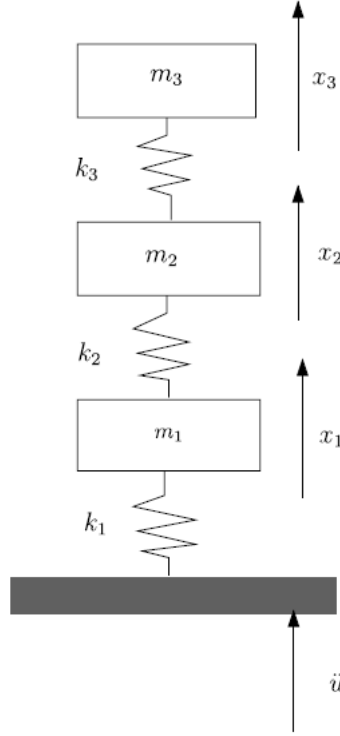


Figure 3.16: multiple degrees of freedom (MDOF) reference system for random base drive analysis, [20] Wijker Jaap *Random Vibrations in Spacecraft Structures Design*, book, 2009 Springer.

the original mass matrix,  $[\Phi]$  is the eigenvector matrix coming from the modal analysis and  $[\frac{H_i(2\pi f)}{m_i}]$  is the diagonal matrix made up by dividing the  $i$ -th transfer function (evaluated in the willed frequency  $f$  multiplied by  $2\pi$  in order to get the pulsation) by the masses of the matrix  $[\hat{M}]$ . The  $[H_{zu}(2\pi f)]$  term is used to calculate  $[H_{z\ddot{u}}(2\pi f)]$  by adding to it the  $\{T\}$  vector. Finally

$$[H_{z\ddot{u}}(2\pi f)] = [H_{zu}(2\pi f)] + \{T\} \quad (3.88)$$

$$[W_{\ddot{x}_i\ddot{x}_j}(f)] = ([H_{z\ddot{u}}(2\pi f)][H_{z\ddot{u}}^*(2\pi f)]^T)W_{\ddot{u}\ddot{u}}(f) \quad (3.89)$$

and

$$\{\ddot{x}_{rms}\} = \sqrt{E(\ddot{x}_i\ddot{x}_i)} \quad (3.90)$$

where  $[H_{z\ddot{u}}^*(2\pi f)]$  denotes the complex conjugate of the  $[H_{z\ddot{u}}(2\pi f)]$  term.



# Chapter 4

## Study cases examples

This chapter deals with the evaluation of the whole structure tool capabilities. During a mission design process the preliminary design is a very important step because it gives the opportunity to perform quick counts and produce very useful data that allow the mission team to make important choices. These are could be made in the selection of a system architecture or in the evaluation of a mission concept that maybe have to be discarded due to the same results, which briefly show the impossibility to reach the mission objectives. The preliminary design must not have any presumption of being perfectly effective or precise, but it is expected to be quick, intuitive, easily usable and to give a complete but rough idea of the considered system.

The present structure preliminary design tool has been thought using the guidelines above, in fact, the calculation theories have always been chosen considering a certain level of idealization and approximation. From the SCDT to the so called *advanced analyses* (static and dynamic) the system modelling always simplified the design process using analytical tools that, for obvious reasons, can be applied only under restrictive hypothesis. They basically put the system in a *controlled virtual reality* where the parameters are carefully controlled and most of the times the system characteristic are ideal, but also allow to obtain results in a valid and quick way. Nowadays a useful and spread tool for design and virtual testing of structure and mechanism subsystem is the *Finite Element Method*. The FEM software is certainly a powerful design tool, but it is not quick. The realistic model implementation needs lots of work and time. Obviously it could be also used with simplified model, but it is enormous potentiality would be ignored. Moreover the FEM software are usually licensed, and its use is not free. This can or can not be a problem, but is true that it could be enough to access a self made tool that produces *good* results and allows quick evaluations, so the point is to have had applied in an efficient way the theory and to have built a considerable calculus tool.

The worth of the structure preliminary design tool developed is evaluated

below, comparing the results of some fictitious analyses with some *Nastran*<sup>1</sup> outputs from some models made for the purpose.

## 4.1 Advanced static analyses results comparison.

As it has been explained in 2 the advanced static part of tool performs calculations to simulate various types of load in a relatively wide range of scenarios, rendered by the possibility to decide the application point:

- Bending moment:  $\vec{M} = 100\hat{i} + 100\hat{j}$  Nm at  $P(0, 0, 0.4)$ ;
- Shear force:  $\vec{S} = 1000\hat{i} + 1000\hat{j}$  N at  $P(0, 0, 0.4)$ ;
- Torque moment:  $\vec{T} = 1000\hat{k}$  Nm at  $P(0, 0, 0.4)$ ;
- Axial (compression or traction) force:  $\vec{P} = -1000\hat{k}$  N at  $P(0, 0, 0.4)$ ;

This section deals with the simulations results comparison of four models analysed by the tool and by a FEM software<sup>2</sup>. One of the most interesting result for a static analysis is the stress structure tensor. The main stress have been compared below. The four models are:

1. Cylinder monocoque micro-satellite:  $R_o = 0.25$  m,  $H_{cyl} = 0.5$  m,  $t_{skin} = 0.002$  m, two internal shelves and two lumped masses<sup>3</sup>;
2. Square based prism monocoque micro-stellite:  $L = 0.3$  m,  $W = 0.3$  m,  $H = 0.4$  m,  $t_{skin} = 0.002$  m, two internal shelves and two lumped masses;
3. Cylinder semi-monocoque micro-satellite:  $R_o = 0.25$  m,  $H_{cyl} = 0.5$  m,  $t_{skin} = 0.002$  m,  $N_{str} = 8$ ,  $A_{str} = 0.0001$  m<sup>2</sup>, two internal shelves and two lumped masses;
4. Square based prism semi-monocoque micro-satellite:  $L = 0.3$  m,  $W = 0.3$  m,  $H = 0.4$  m,  $t_{skin} = 0.002$  m,  $N_{str,L} = 3$ ,  $A_{str,L} = 0.0001$  m<sup>2</sup>,  $N_{str,W} = 3$ ,  $A_{str,W} = 0.0001$  m<sup>2</sup>,  $N_{str,corner} = 1$  (each corner),  $A_{str,corner} = 0.0001$  m<sup>2</sup>, two internal shelves and two lumped masses;.

---

<sup>1</sup>*MD Nastran* is a *MSC* finite element method (FEM) software and *Patran* is its preprocessor software owned by the same company.

<sup>2</sup>The models of the monocoque configurations are made of shell elements in which the reference frame first coordinate  $x$  is parallel to the third global axis  $z$ ; the ones representing the semi-monocoque satellites have the second axis of the shell element coordinate  $y$  frame parallel to the third global axis  $z$ . For simplicity the results refer to the local coordinate frame.

<sup>3</sup>The internal shelves and the masses do not affect the static simulation, but the models have been used also in the dynamic simulations.

Figure 4.1 shows the semi-monocoque structure models created in *Nastran*. Note the presence of the longitudinal reinforcements and the MPC rigid elements: the highest has been used to apply the loads to the structure, the others represent the shelves which support in the centre the lumped masses. The monocoque models are analogous, except for the absence of the stringers.

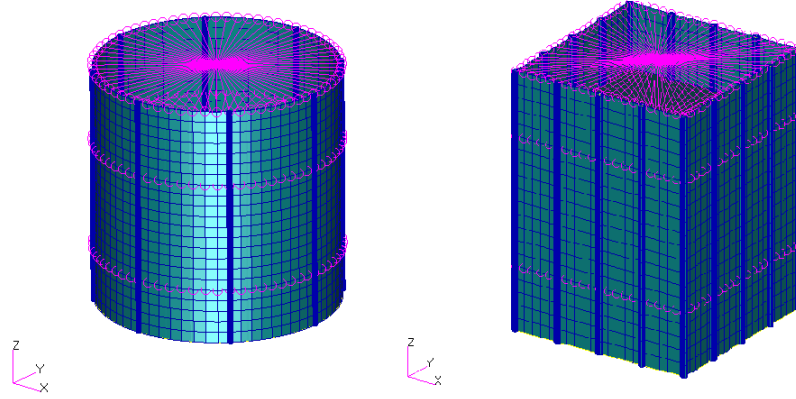


Figure 4.1: FEM models for static and dynamic analysis: semi-monocoque structures.

The tools simulate just a principal stress at the time, so it neglects the other tensor components. For this reason the results have to be considered incomplete, even if the output stress is the most representative and highest one (except for shear force, where shear and normal stress can have the same order of magnitude depending on the structure aspect ratio  $AR = \frac{A_{section}}{L_{beam}}$ ).

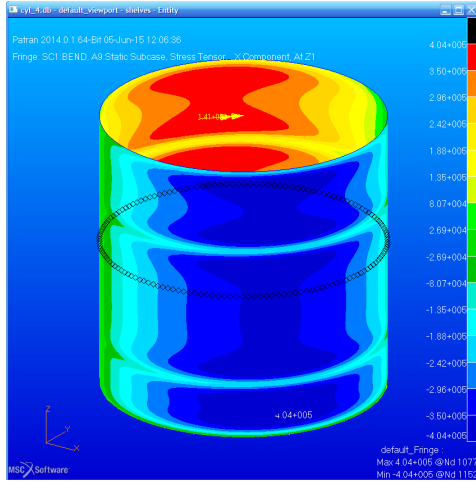
#### 4.1.1 Monocoque spacecraft configuration

**Monocoque micro-satellite: bending moment** The figure 4.2 shows the  $\sigma_x$  normal stress distribution in the cylindrical structure. From the right scale the stress is  $\sigma_{x,fem}max = 4.04 \cdot Pa$  and that the dark blue zone has a mean stress value equal to  $\sigma_{x,fem}mean = 3.77 \cdot 10^5 Pa^4$ . The tool result for the maximum stress is  $\sigma_{x,tool}max = 3.6447 \cdot 10^5 Pa$ . The FEM and tool models agree with the theory having the most critical stress in the furthest point from the neutral plane, that is for obvious reasons a vertical plane pointing to the 45 degree direction (aligned to the moment).

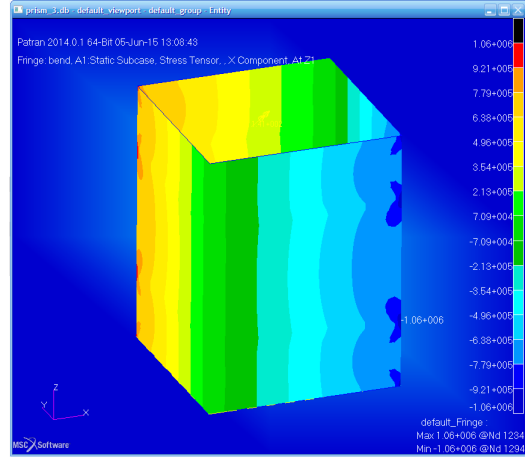
The complete FEM model result shows that the stress tensor highest value calculated through the *Von Mises* rule is  $\sigma_{VM,fem}max = 3.95 \cdot 10^5 Pa$ .

The square based prism satellite stress distribution is shown in figure 4.2. Once more can be noted that it does agree with the bend theory, having the most critical normal stresses in the furthest point of the structure (corners not

<sup>4</sup>Stress values units Pascal ( $Pa = \frac{N}{m^2}$ ) when missing.



(a)  $\sigma_x$  stress component fringe due to bending moment in cylinder satellite.



(b)  $\sigma_x$  stress component fringe due to bending moment in prism satellite.

Figure 4.2: Bending moment loaded monococque structures; Left fringe  $[-4.04 \cdot 10^5; 4.04 \cdot 10^5]$  Pa, right fringe  $[-1.06 \cdot 10^6; 1.06 \cdot 10^6]$  Pa

aligned to the moment vector direction) and showing an almost uniform value of stress along the beam axis.

The simulation results are

$$\sigma_{x,fem}max = 1.06 \cdot 10^6 \text{ Pa} \quad \sigma_{x,tool}max = 8.50 \cdot 10^5 \text{ Pa} \quad (4.1)$$

so the error is  $\epsilon\% = \frac{10.60-8.50}{10.600} \cdot 100 = 19.79\%$ , but comparing the medium value visible in the figure relative to the light blue area, the error decreases to  $\epsilon\% = \frac{8.0000-8.5019}{8.0000} \cdot 100 = -6.27\%$ . Also in this case the FEM stress distribution has peaks of value higher than the mean tool value. The rest of the distribution must respect the equilibrium, so its mean value is lower than the one calculated with the tool because the latter descend from the hypothesis of uniformity along the beam axis.

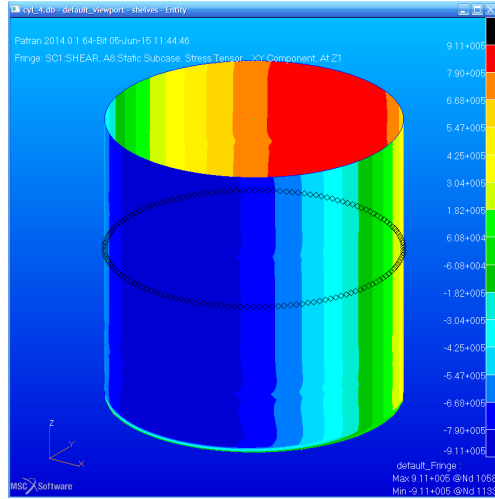
### Monocoque micro-satellite: shear force

$$\tau_{xy,fem}max = 9.11 \cdot 10^5 \text{ Pa} \quad \tau_{xy,tool}max = 9.06 \cdot 10^5 \text{ Pa} \quad (4.2)$$

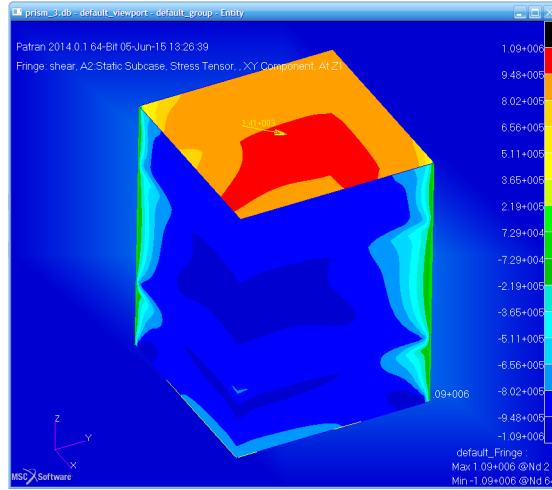
The relative error is  $\epsilon\% = \frac{9.11-9.06}{9.11} \cdot 100 = 0.57\%$

The two results do agree and the shear stress distribution in the tool (figure 4.4) is similar to the FEM one visible in the fringe. In this case the tool neglects the existence of the normal stress that is associated to the shear force application:  $\sigma_{x,fem}max = 1.89 \cdot 10^6 \text{ Pa}$

A cantilevered beam loaded with a concentrated shear force develops a linear bending moment, so a normal stress linearly distributed along the beam axis.



(a)  $\tau_{xy}$  stress component fringe due to shear force in cylinder satellite.



(b)  $\tau_{xy}$  stress component fringe due to shear force in prism satellite.

Figure 4.3: Shear force loaded monococque structures; Left fringe  $[-9.11 \cdot 10^5; 9.11 \cdot 10^5]$  Pa, right fringe  $[-1.09 \cdot 10^6; 1.09 \cdot 10^6]$  Pa

In the prism satellite the shear force is aligned to the square cross section diagonal and it induce a shear stress in the skin structure as the one in figure 4.3. The results value agree in the order of magnitude, but they are quite different in the modulus, being the relative error equal to  $\epsilon\% = \frac{1.09-1.28}{1.09} \cdot 100 = -17.00\%$ :

$$\tau_{xy,fem}max = 1.09 \cdot 10^6 \text{ Pa} \quad \tau_{xy,tool}max = 1.27 \cdot 10^6 \text{ Pa} \quad (4.3)$$

#### Monocoque micro-satellite: torque moment

$$\tau_{xy,fem} = 1.27 \cdot 10^6 \text{ Pa} \quad \tau_{xy,tool} = 1.27 \cdot 10^6 \text{ Pa} \quad (4.4)$$

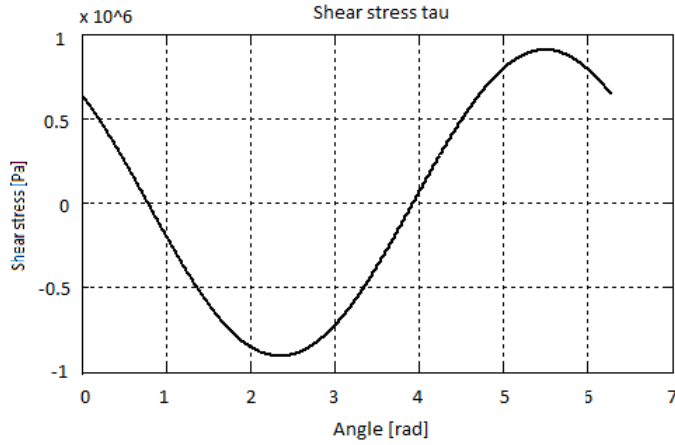
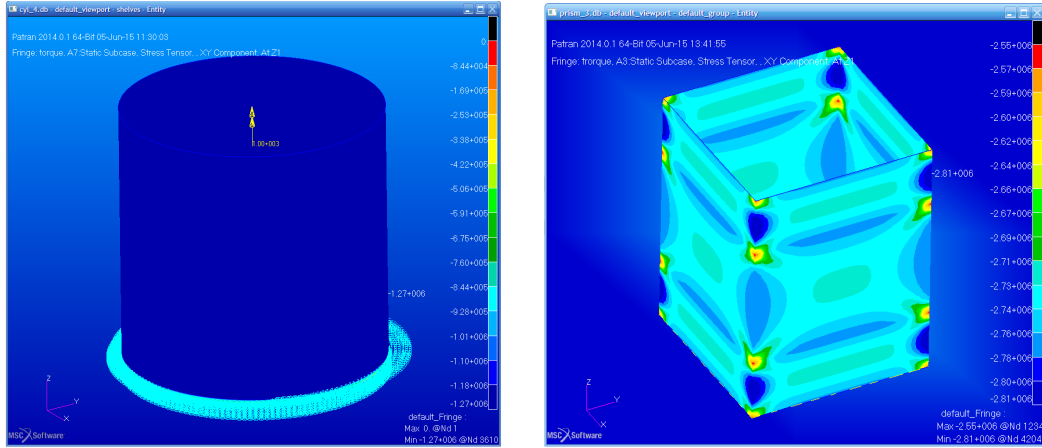


Figure 4.4:  $\tau_{xy}$  stress component distribution in the skin along the perimeter due to shear force.



(a)  $\tau_{xy}$  stress component fringe due to torque moment in cylinder satellite.

(b)  $\tau_{xy}$  stress component fringe due to torque moment in prism satellite.

Figure 4.5: Torque moment loaded monococque structures; Left fringe  $[-1.27 \cdot 10^6; 0]$ , right fringe  $[-2.81 \cdot 10^6; -2.55 \cdot 10^6]$  Pa

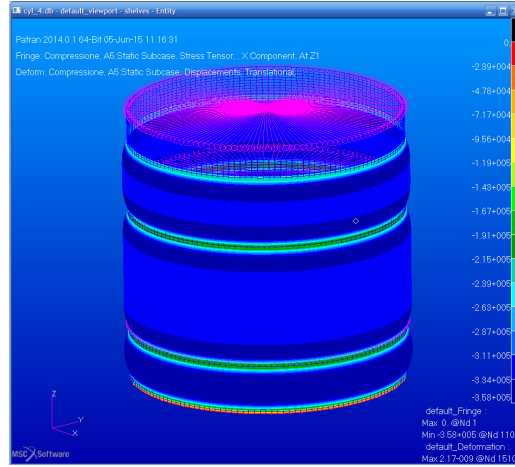
(see figure 4.5). There is no macroscopic error in the calculated value.

The values are practically equal, so there is full match in the shear stress prediction. Note that the existence of the internal shelves does not affect the  $xy$  shear stress component distribution, as a torque applied to the torque centre deforms the structure leaving the cross section parallel to itself.

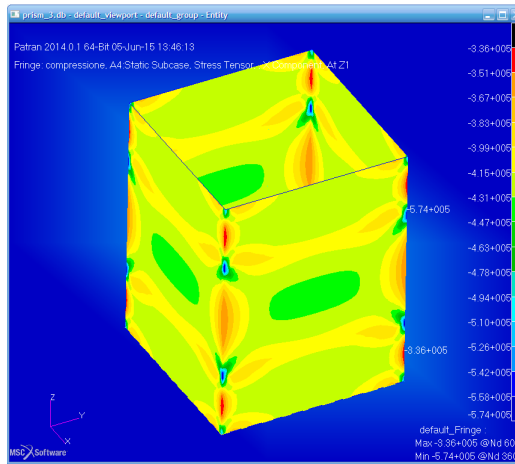
$$\tau_{xy,fem}mean = 2.74 \cdot 10^6 \text{ Pa} \quad \tau_{xy,tool} = 2.78 \cdot 10^6 \text{ Pa} \quad (4.5)$$

(see figure 4.5). The relative error is  $\epsilon\% = \frac{2.74-2.78}{2.74} \cdot 100 = -1.23\%$ . The  $\tau_{xy,fem}$  mean stress is derived from the average operation in the most spread values in the figure 4.5 fringe, which is more representative than the maximum one

$$(\tau_{xy,fem}max = 2.81 \cdot 10^6 \text{ Pa}).$$



(a)  $\sigma_x$  stress component fringe due to axial compressive force in cylinder satellite.



(b)  $\sigma_y$  stress component fringe due to axial compressive force in prism satellite.

Figure 4.6: Axial (compressive) force loaded monocoque structures; Left fringe  $[-3.58 \cdot 10^5; 0]$ , right fringe  $[-5.74 \cdot 10^5; -3.36 \cdot 10^5]$  Pa

**Monocoque micro-satellite: axial force (compression)** The cylinder configuration is subject to the following stresses:

$$\sigma_{x,fem}max = 3.58 \cdot 10^5 \text{ Pa} \quad \sigma_{x,tool}max = 3.19 \cdot 10^5 \text{ Pa} \quad (4.6)$$

The relative error is  $\epsilon\% = \frac{3.58-3.19}{3.58} \cdot 100 = 10.73\%$ , although the fringe shows that the real distribution has a mean value around  $\frac{3.11+3.34}{2} = 3.23$  Pa. This is the representative stress of the skin if there were not the internal shelves. They actually concentrate stress around their joints to the skin. The tool neglect their presence since it uses the simple uniform beam theory. So finally

it can be assumed that the mean stress  $\sigma_{x,fem}mean = 3.23 \cdot 10^5 \text{ Pa}$  (light blue in figure 4.6) is the result to be compared, giving the following error:  $\epsilon\% = \frac{3.23-3.19}{3.23} \cdot 100 = 1.06\%$  due basically to the load non-homogeneity in the fem model: the tip and base local lower stress values rise the central part stress in order to have equilibrium.

The two maximum normal stress values in prism shaped satellite due to axial compressive load are

$$\sigma_{x,fem}max = 5.74 \cdot 10^5 \text{ Pa} \quad \sigma_{x,tool}max = 4.19 \cdot 10^5 \text{ Pa} \quad (4.7)$$

so the error is  $\epsilon\% = \frac{5.74-4.19}{5.74} \cdot 100 = 26.92\%$  which is a non acceptable error even for preliminary design. Note instead that repeating the logic path above the most representative value for the stress in FEM solution is an average of the most spread values (figure 4.6):  $\sigma_{x,fem}mean = \frac{4.20 \cdot 10^5 \text{ Pa} + 3.90 \cdot 10^5 \text{ Pa} + 4.05 \cdot 10^5 \text{ Pa}}{3} = 4.05 \cdot 10^5 \text{ Pa}$  and the associated relative error is  $\epsilon\% = \frac{4.05-4.19}{4.05} \cdot 100 = -3.05\%$ . The *Nastran* mean value is thought to be lower than the tool one for the same reasons as before.

## 4.1.2 Semi-monocoque spacecraft configuration

**Semi-monocoque micro-satellite: bending moment** The FEM simulation of both cylindrical and prism satellites loaded with a bending moment initially showed that the tool was not able to calculate the realistic response of the structure, giving wrong values in the stress and deformations. Agreeing with the thin walled beam theory, the bending moment load in a reinforced structure is supported mainly by the longitudinal stringers. FEM models instead consider also the skin contribution to stiffness; for instance its stress values are lower than the tool ones. This fact led to the need to change the thickness of the shell in *Nastran* models so that the skin contribution was negligible. The new simulations showed that the tool results are right and that the idealized structure theory has been well put into practice, but that it is not realistic and has limits. The maximum normal stress values have been taken as example. For the cylindrical satellite they are (figure 4.7):

$$\begin{aligned} \sigma_{y,fem}max(with - skin) &= 3.07 \cdot 10^5 \text{ Pa} \\ \sigma_{y,fem}max(no - skin) &= 1.45 \cdot 10^6 \text{ Pa} \\ \sigma_{y,tool}max &= 1.40 \cdot 10^6 \text{ Pa} \end{aligned} \quad (4.8)$$

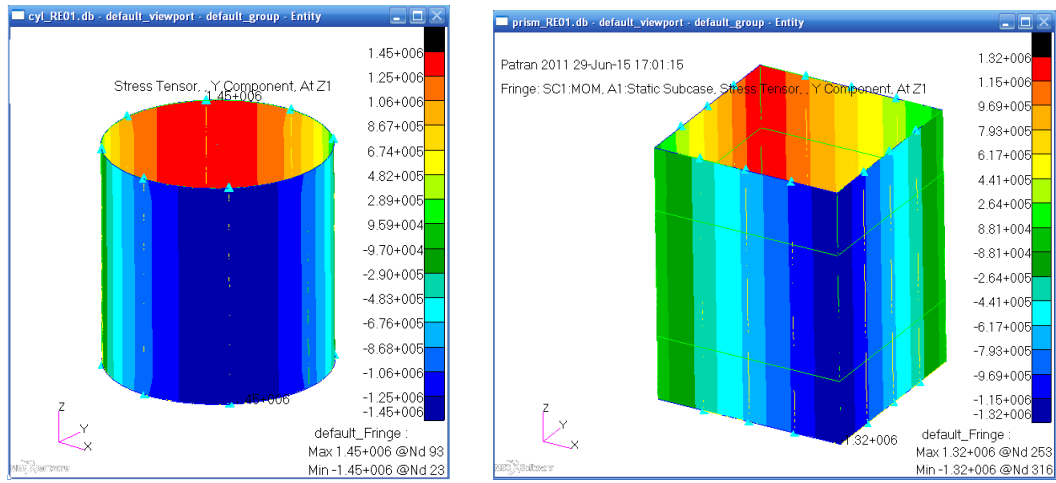
the first data (that is the most realistic one) is four times lower than the tool one. The error is not acceptable and the comparison can not be made. Instead

the second and the third do agree for the reasons explained above and the error is  $\epsilon\% = \frac{1.45-1.40}{1.45} \cdot 100 = 3.44\%$  and the order of magnitude is the same.

The same happened with the prism shaped satellite. The analogous results are (figure 4.7):

$$\begin{aligned}\sigma_{y,femmax}(with - skin) &= 5.52 \cdot 10^5 \text{ Pa} \\ \sigma_{y,femmax}(no - skin) &= 1.32 \cdot 10^6 \text{ Pa} \\ \sigma_{y,toolmax} &= 1.21 \cdot 10^6 \text{ Pa}\end{aligned}\tag{4.9}$$

and the error is  $\epsilon\% = \frac{1.31-1.21}{1.31} \cdot 100 = 7.63\%$ .



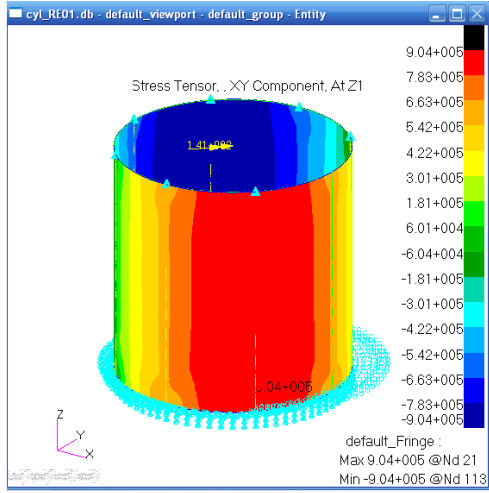
(a)  $\sigma_y$  stress component fringe due to bending moment in cylinder reinforced satellite.

(b)  $\sigma_y$  stress component fringe due to bending moment in prism reinforced satellite.

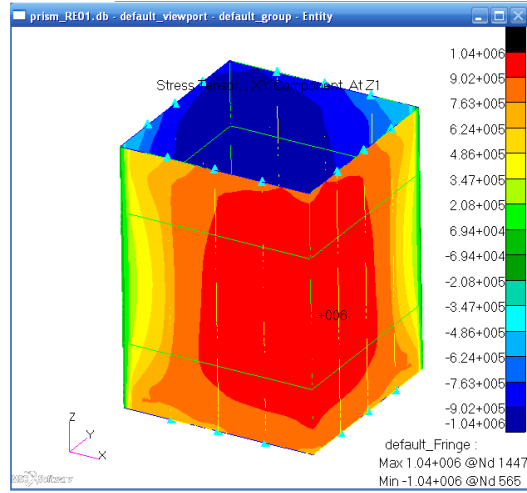
Figure 4.7: Bending moment loaded semi-monocoque structures; Left fringe  $[-1.45 \cdot 10^6; 1.45 \cdot 10^6] \text{ Pa}$ , right fringe  $[-1.32 \cdot 10^6; 1.32 \cdot 10^6] \text{ Pa}$

**Semi-monocoque micro-satellite: shear force** The presence of the stringer in the structure loaded with a shear force changes its behaviour and the stress values and distribution. The theory explained in section 3 shows that a simplified way to consider the reinforcement is to let them absorb part of the shear force giving discontinuity in the shear stress. Between two stringers there is a constant value of stress. This is an approximation caused by the structure idealization, but it is worth considering the results below visible in figure 4.8 and in the related data:

$$\tau_{xy,femmax} = 9.04 \cdot 10^5 \text{ Pa} \quad \tau_{xy,toolmax} = 8.54 \cdot 10^5 \text{ Pa} \tag{4.10}$$



(a)  $\tau_{xy}$  stress component fringe due to shear force in reinforced cylinder satellite.



(b)  $\tau_{xy}$  stress component fringe due to shear force in reinforced prism satellite.

Figure 4.8: Shear force loaded semi-monocoque structures; Left fringe  $[-9.04 \cdot 10^6; 9.04 \cdot 10^6]$  Pa, right fringe  $[-1.04 \cdot 10^6; 1.04 \cdot 10^6]$  Pa

The relative error is  $\epsilon\% = \frac{9.04-8.54}{9.04} \cdot 100 = 5.53\%$ , that is a good approximation given the idealized structure hypothesis. The maximum values of the shear stress related here are just an example of the accuracy of the calculation. Other comparisons can be made between the general distribution of the shear stress obtained through the tool and the *Nastran* results (see figures 4.9 and 4.8). The tool stress distribution around the skin perimeter of the satellites is considered to be constant along the  $z$  longitudinal axis.

The same hypothesis are valid for the square based prism satellite used in these examples. The results of the tool agree with the FEM ones, even for the distribution around the square perimeter. As usual the maximum values are given here, but the reader can compare also the general distribution through the screen shots in figure 4.8.

$$\tau_{xy,fem,max} = 1.04 \cdot 10^6 \text{ Pa} \quad \tau_{xy,tool,max} = 9.09 \cdot 10^5 \text{ Pa} \quad (4.11)$$

so the error is  $\epsilon\% = \frac{10.4-9.09}{10.4} \cdot 100 = 12.59\%$ . This time the error is more relevant. The reason is the idealization made and in part from the higher complexity degree of the geometry. Anyway the tool just have to be used for preliminary design, so the error is acceptable.

**Semi-monocoque micro-satellite: torque moment** The results given by the tools for the torque loaded structure do not consider the presence of the longitudinal reinforcements. According with the thin shell beam theory, the

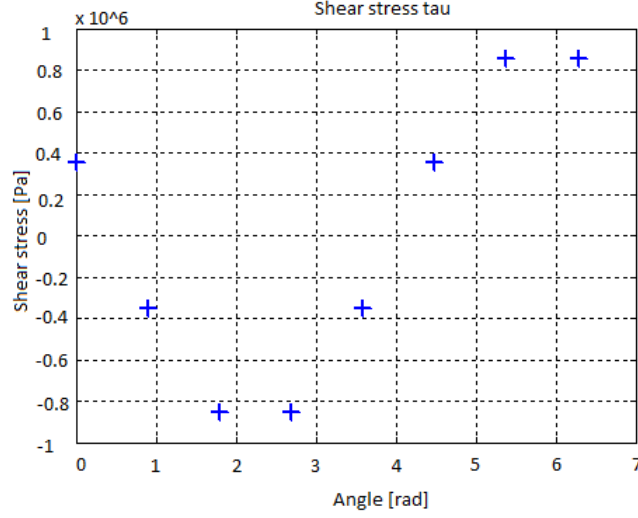


Figure 4.9:  $\tau_{xy}$  stress component distribution in the reinforcements along the perimeter of the cylinder structure due to shear load.

skin of the structure absorbs the load giving structural integrity. This is a strong hypothesis, but the results show that it does not compromise the tool veracity of the tool calculations. The tool value for the  $\tau$  stress is constant all over the skin (according with the theory), while the FEM one is the highest in the structure. From figure 4.11 can be seen that this value is representative for the whole structure, as there is very low change in the coloured fringe in most part of it. This means that the real mean value is lower and that it is not constant everywhere, but the highest one is more significant for design purposes. The cylinder and prism results are given below. The cylinder satellite maximum values are:

$$\tau_{xy,fem}max = 1.28 \cdot 10^6 \text{ Pa} \quad \tau_{xy,tool}max = 1.27 \cdot 10^6 \text{ Pa} \quad (4.12)$$

the error is negligible. Note that the presence of the reinforcement almost does not affect the stress distribution, expect for the top and base ends. This fact confirms the idealized structure hypothesis validity.

The prism satellite results are:

$$\tau_{xy,fem}max = 2.77 \cdot 10^6 \text{ Pa} \quad \tau_{xy,tool}max = 2.78 \cdot 10^6 \text{ Pa} \quad (4.13)$$

the error is negligible even for the square based satellite.

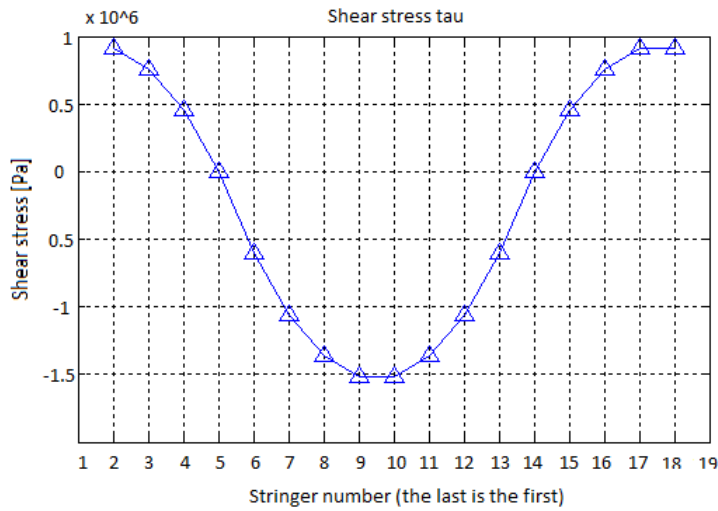
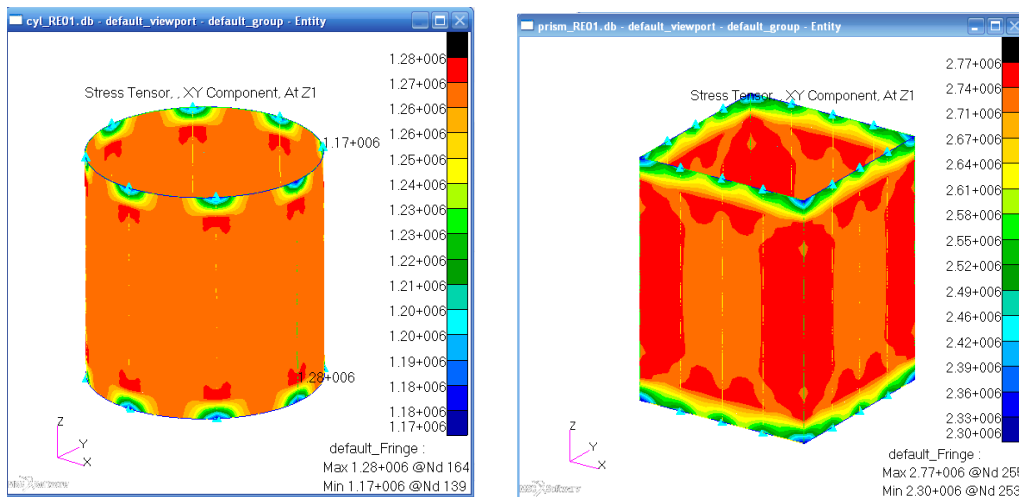


Figure 4.10:  $\tau_{xy}$  distribution given by the tool (shear load, prism structure).



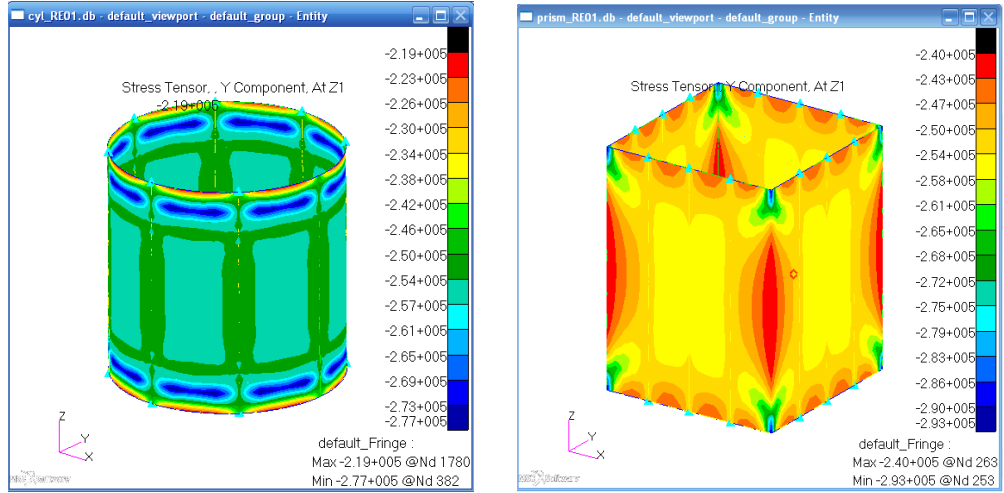
(a)  $\tau_{xy}$  stress distribution of the cylinder reinforced structure loaded with a torque moment.

(b)  $\tau_{xy}$  stress distribution of the prism reinforced structure loaded with a torque moment.

Figure 4.11: Torque moment loaded semi-monocoque structures; Left fringe  $[1.17 \cdot 10^6; 1.28 \cdot 10^6]$  Pa, right fringe  $[2.30 \cdot 10^6; 2.77 \cdot 10^6]$  Pa

**Semi-monocoque micro-satellite: axial force (compression)** In this case the distribution of the normal stress in the longitudinal axis direction is the most important set of value for the design. Figure 4.12 shows the  $\sigma_z$  component of the stress tensor in the prism structure.

The stress is subject to little changes near the edges where the stress value is higher especially in the corners ( $2.93 \cdot 10^5$  Pa), but its value is almost constant in the major part of the structure, so the mid section is representative and the related result has been taken in the comparison:



(a)  $\sigma_y$  stress distribution of the cylinder reinforced structure due to axial compressive load.

(b)  $\sigma_y$  stress distribution of the prism reinforced structure due to axial compressive load.

Figure 4.12: Axial (compressive) force loaded semi-monocoque structures; Left fringe  $[-2.77 \cdot 10^5; -2.19 \cdot 10^5]$  Pa, right fringe  $[-2.93 \cdot 10^5; -2.40 \cdot 10^5]$  Pa

$$\sigma_{y,femmean} = 2.48 \cdot 10^5 \text{ Pa} \quad \sigma_{y,tool} = 2.51 \cdot 10^5 \text{ Pa} \quad (4.14)$$

and  $\epsilon\% = \frac{2.48-2.51}{2.48} \cdot 100 = 1.20\%$ . The mean value has been calculated as the average among the most spread stress results in the section at half of the height. The tool and FEM results are almost equal thanks to the absence of restricting hypothesis in the axial loading of thin walled beams. In fact, the stress just depends on the total cross sectional area and the force. There is no difference (if the buckling does not occur) in skin and stringer roles.

Analogous considerations can be made for the cylindrical shaped satellite, for which the stress most representative values are:

$$\sigma_{y,femmean} = 2.52 \cdot 10^5 \text{ Pa} \quad \sigma_{y,tool} = 2.54 \cdot 10^5 \text{ Pa} \quad (4.15)$$

although the highest normal stress value in the structure is  $\sigma_{y,femmax} = 2.77 \cdot 10^5 \text{ Pa}$  as can be seen in figure 4.12

In both the types of structure the coloured fringe in the screen-shots shows a certain effect of the reinforcement presence. In fact, the stress is lower along the superposition of the stringer and the skin. This is the desired effect of the stringers that have a purpose in supporting axial loads, while they are almost useless in torque loaded structure.

## 4.2 Advanced dynamic analysis results example

### 4.2.1 Preconditions to the dynamic analyses results

The tool sub-part that performs dynamic calculations uses the lumped mass approach to simulate the behaviour of the structure. The idealization of the structure is the following: the tool takes the values of all the lumped masses added on the shelves by the user (that can be one, two or three and practically represent the degree of freedom), sums the portion of structure between two shelves and uses the results as concentrated mass. The stiffness are built with the data from the Young modulus, the length and area parameters of the thin walled beam between two degrees of freedom (for details see section ??). This is the fastest way to idealize a structure and it is certainly useful for rapid estimations, but it is susceptible to some disadvantages:

- i) The concentrated masses can not fully represent the behaviour of the distributed mass: there is loss of information of density, mass eccentricity, sloshing, real geometry. This affects the results tending to give for instance wrong values of acceleration or internal forces;
- ii) Only one degree of freedom at the time can be computed for each mass in order to maintain the tool script complexity low. The three-dimensions of the structure is lost. Assigning more than one degree of freedom (e.g. two translations or a translation and a rotation) would lead toward a FEM approach. This is not the original purpose of this preliminary design tool, although it could be the direction for the tool improvement;
- iii) Dynamic forces can only be applied directly to the degrees of freedom or through the base limiting the possible range of loads that exist for a satellite (e.g. other application points, distributed load, non-solid load path).

For these reasons the following results concerning the modal and random loaded analyses disagree with the FEM results. They still can be used to understand the order of magnitude of the physical quantities, but further analyses, or a different calculation method, are strictly necessary. As it has already been said this tool is meant to be an instrument for preliminary design, therefore the further analyses would be executed in any case, using stronger instruments. The option to change the calculus approach could be a natural continuation and improvement of this work.

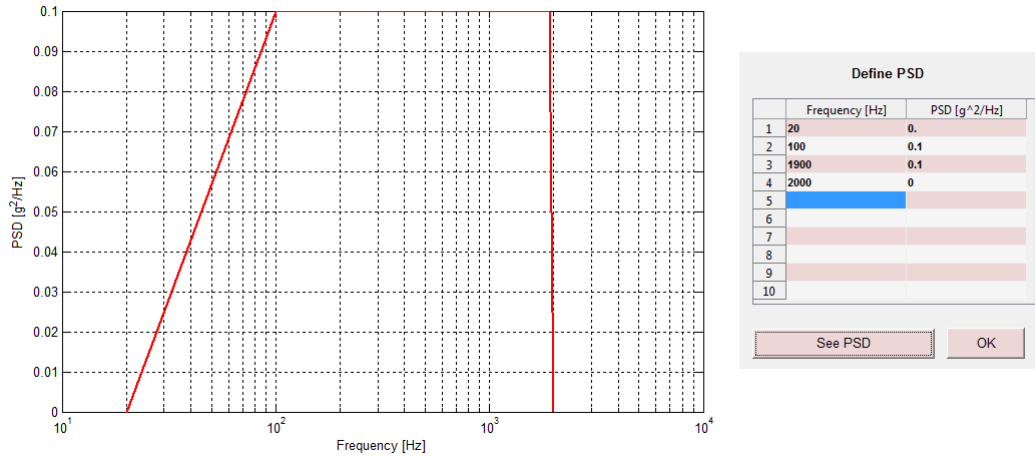


Figure 4.13: Power Spectral Density function used in the random analysis example.

## 4.2.2 Random analysis and normal modes

Random analyses have been performed as examples onto the cylinder mono-coque and prism semi-mono-coque structures. The relative outputs are related below. The Power Spectral Density (PSD) function used has a simple flat profile equal to  $0.1 \frac{g^2}{Hz}$ , from 100 Hz to 1900 Hz. The same PSD has been assigned as input to the structure tool and to the *Nastran* models. Figure 4.13 illustrates the frequency function as it can be displayed using the GUI interface in a semi-logarithmic plot and its user defined input table. The random acceleration stimulate the base of the structure transmitting its effect to the satellite trough the launcher interface. In *Nastran* models it has been applied directly to the base nodes of the mesh avoiding the realization of the interface support. Therefore in *Matlab*© tool the equivalent stiffness of the support has been chosen much higher than the stiffness of the first degree of freedom, in order to let its contribution disappear in the stiffness series formula  $\frac{1}{k_{eq}} = \frac{1}{k_1} + \frac{1}{k_2}$ . The calculations performed by the tool are explained in latter part of section ??.

*Nastran* random analyses results for the cylinder (non-reinforced) satellite are:

$$a_{rms,1} = 16.9g \quad a_{rms,2} = 28.3g \quad (4.16)$$

where the first mass (30 kg) is placed on the first shelf (dof) and the second mass (15 kg) on the second shelf. These values have to be compared with the tool results related below:

$$a_{rms,1} = 30.6g \quad a_{rms,2} = 52.2g \quad (4.17)$$

Expected values are almost half the estimated ones. This is a direct con-

sequence of the approximation made for the dynamic model (see the section intro). The prism shaped satellite results are:

*Nastran's*

$$a_{rms,1} = 19.1 \quad a_{rms,2} = 32.1g \quad (4.18)$$

Tool's

$$a_{rms,1} = 27.6g \quad a_{rms,2} = 53.8g \quad (4.19)$$

These comparisons show the limits of the concentrated mass dynamic model. The tool has been tested with pre-idealized structures and gave the expected results, therefore there is no error in the script and the outputs are numerically correct. Therefore the errors data must be caused by idealization process: the model that considers only one degree of freedom for each one of the nodes (the masses can make only an axial translation) is much more rigid than an hypothetical multiple degrees of freedom (MDOF) system. As a consequence the natural frequencies are much higher. For instance this can be seen comparing the FEM derived outputs with the tool ones. For the monocoque cylinder with two lumped masses described in this section the first natural frequencies are:

$$f_{n,1}(FEM) = 274 \quad Hz \quad f_{n,1}(tool) = 879 \quad Hz \quad (4.20)$$

The first value comes from a normal modes analysis performed on the cylinder model in figure 4.1, that is a pretty realistic model: it is a three-dimensional model with more than an hundred elements and six degree of freedom per node. Its results are expected to be quite accurate. The second value is obtained from a two node mono-dimensional model. That is a system analogous to the one in figure 3.16 made of two lumped masses and two springs. Its mass only have the axial translation degree of freedom. As explained above its accuracy was expected to be low. In the limited potentiality of its hypothesis it is the fastest way to calculate the natural frequencies.

The values extrapolated from the tool have little meaning, but they are numerically correct: in fact, another FEM model has been made trying to recreate the same limits: a mono-dimensional beam with circular section and lumped masses has been created and used in a normal modes analysis in *Nastran*. The first frequency obtained is  $f_{n,1}(1D-FEM) = 1051$  Hz, that is 16% higher than the tool one. Also another *Matlab*® model<sup>5</sup> with a higher number of nodes (but same lumped masses, cross section area, material and dimensions) shows that a more correct value for the 1 – D system is  $f_{n,1}(1D - Matlab) = 913$  Hz, which is just 3% higher than 879 Hz. A further set of calculations have confirmed the accelerations values obtained through the tool. They have been performed by adapting the tool script to the 1 – D model (see appendix). The

---

<sup>5</sup>The script is enclosed in appendix.

output range agrees with the two dof values:

$$a_{rms} \in [13; 53] \quad g \quad (4.21)$$

All the nodes accelerations belong to this interval. The root mean square acceleration corresponding to the mass nodes are:

$$a_{rms, mass1}(Matlab) = 28.5 \quad g \quad a_{rms, mass2}(Matlab) = 51.4 \quad g \quad (4.22)$$

that agree with the values obtained through the tool: results 4.19

This dissertation can partially explain the incongruity in the root mean square accelerations values. In fact, the possibility for the structure to vibrate in all the translational and rotational directions would spread the energy among the degrees of freedom, making the value of the accelerations in the longitudinal direction lower. Moreover also the the higher values of the frequencies denote that the loaded system is much more rigid than expected.

The tool could be modified in order to have a better FEM like feature: the structure idealization would be made using a higher number of nodes and rising the number of degree of freedom for each them. It could be done maintaining the mono-dimensional model or developing a three-dimensional model.

The first way would be a first easier step in which the mechanical matrices could be quite easily built, maintaining the script simplicity. It would mean to consider not only the axial stiffness, but also the bending, torquing and lateral ones, leading to a more realistic model.

The latter approach would be shifted towards a pure finite element approach and could take a lot of work, depending on the the new tool degree of versatility. It would mean to mesh the structure deriving the stiffness matrix of a three-dimensional model. It would be possible to consider the real position of the concentrated masses not only in the axial direction. Such work could be the second step of the improvement.



# Chapter 5

## Conclusions

In this thesis a calculus tool for preliminary design of small satellites structural subsystem has been described. The tool has been built programming a wide network of scripts (written in *Matlab*© language) and making them capable to perform the calculations; then, they all have been connected together to form a logically organized and handy instrument, through the Graphical User Interface (GUI) potentialities. Further, it and has been made to function next to other analogous tools in a Concurrent Design Facility (CDF) of the UPM's Ignacio De Riva department in Madrid. The main objective was to improve the capabilities of the existing *Excel* tool in order to have a more complex, versatile, complete instrument for the preliminary characterization of a satellite structure. To understand the work done an introductory explanation has been made. It dealt with

- The presentation of the concurrent engineering concept which has represented the leading point of view and the reference idea in the tool project. During the simulated design sessions with the other students in the CDF, it has been essential to understand the limits and errors that affected the approach to the use of the facility and the software itself.
- An overview on the structure subsystem of a satellite: its main characteristics, functions and purposes, weak points and its function environment. Starting from the environment and the loads to which a spacecraft is generally exposed, a brief digression on all the characteristics that the structure must provide has been made. It dealt with the structure strength, stiffness, stability, safety, mass distribution and reliability.
- The explanation of what a CDF is, how it works and its potentialities by a space mission design point of view. In particular, the UPM facility has been presented. One of the main objectives of this work has been to express through the tool the design characteristic of being preliminary and being part of a concurrent engineering environment. For this reason

it has been necessary to clearly understand the dynamics among the CDF users and their active role in the facility.

This document is just part of the work done. In fact, the real work has been to write the *Matlab*© code that properly performed the calculations. The whole tool has about thirty scripts with hundreds of code lines and ten *Simulink* files. A significant part of the tool realization has been occupied by giving it a meaningful and handy organization. This latter issue is part of the concurrent design point of view, too. The core of the script is full of calculus which base their validity on analytical theories of structures. The main one are the thin walled beam theory for static problems and the normal modes analysis for dynamic ones. Other secondary theories like solid and vibration mechanic or signal control have been used. Some ideas about what to insert in the tool came from the books and articles, others came from discussion with the Spanish correlator; but most of the times the ideas came out debating among the student in the CDF, while working to their own subsystem tool. This type of interaction has turn out to be very precious, as it could unveil directly the most important needs of the new tools set.

It is important to understand that this work has not produced any pristine result from a research perspective, neither it has not proved the capabilities of any new analysis method. Instead, this tool is the result itself. Better said: the most important and notable result is to have built this instrument following the will to create a new instrument for Universidad Politecnica de Madrid (UPM). This calculus tool and its interface are part (together with the other subsystem tools) of a project that pursued the original objective to develop such facility in a didactic environment. Moreover, in its future, it could become a midrange instrument between very inaccurate and low handy methods (such as *Excel* or raw FEM software) and too expensive and not usable-friendly softwares (e.g. *Nastran* and analogous). The software is improvable and it does not presume to be conclusive. For instance, through changes to the dynamic analysis modelling approach or by modifying the tool, making it more complex, adding modules, configurations, analysis types (e.g. thermal-mechanic) or modifying its interface making it handier. Certainly, one of the immediate future changes could deal with the dynamic tool part as suggested in section 4.2.

# Appendix A

## Matlab additional scripts

### Script for MDOF results comparison

```
%% Variables declaration
m1 =30 % mass 1
m2 = 15 % mass 2
h1 = .1 % heights
h2 = .3
A = 0.002*0.5*pi %cross sectional area
htot = 0.5 % total height

%% meshing
nodes = 100
dh1 = htot/(nodes-1)
dh = ones(nodes,1)*dh1
dk = 71000.e+6*A./dh1
dm = dh*A*2800
% Mass matrix
for i = 1:length(dm)-1
    if abs(dh1*i-h1)<=dh/2
        dm(i) = dm(i)+m1;
    elseif abs(dh1*i-h2)<=dh/2
        dm(i) = dm(i)+m2;
    end
end
M = diag(dm);
% Stiffness matrix
K = zeros(nodes);
for i = 1:nodes-1
    K(i,i) = 2*dk;
    K(i+1,i) = -dk;
    K(i,i+1) = -dk;
end
K(nodes,nodes) = dk;
```

```

%%%%%%%%%%%%%%%%%%%%%%%%%%%%%%%%%%%%%%%%%%%%%%%%%%%%%%%%%%%%%%%%%%%%%%%%%% eigenvalue problem: normal modes analysis %%%%%%%%%%%%%%%%%%%%%%%%%%%%%%%%%%%%%%%%%%%%%%%%%%%%%%%%%%%%%%%%%%%%%%%%%%%
[PHI,lambda] = eig(K,M);
oms = abs(sqrt(diag(lambda)));
%% frequency outputs
freq = oms/(2*pi);
f1 = min(freq);
%%%%%%%%%%%%%%%%%%%%%%%%%%%%%%%%%%%%%%%%%%%%%%%%%%%%%%%%%%%%%%%%%%%%%%%%%% root mean square accelerations %%%%%%%%%%%%%%%%%%%%%%%%%%%%%%%%%%%%%%%%%%%%%%%%%%%%%%%%%%%%%%%%%%%%%%%%%%%
gM = PHI'*M*PHI
for l = 1:size(gM,1)
    zeta_n(l) = 0.05;
    num_FFq(l,:) = [1];
    den_FFq(l,:) = (2*pi)^2*[1/(2*pi)^2 2*zeta_n(l)*oms(l)/(2*pi)^2 (oms(l)/(2*pi))^2];
    H(l) = tf(num_FFq(l,:),den_FFq(l,:))
end
m = diag(gM);
Wuu_f = 0.1; % PSD: scalar = function of frequency (function of f_vec)
f_vec = linspace(100,1900,200); %independent variable: frequency
ndf = length(f_vec);
T = ones(size(gM,1),1); %rigid body vector
Hm = zeros(nodes,nodes,ndf);
for i =1:ndf
    %%% accelerations
    j = sqrt(-1);
    s(i) = 2*pi*j*f_vec(i);
    for l = 1:nodes
        Hm(l,1,i) = [evalfr(H(l),s(i))/m(l)]; % (1x1x ndf)
    end
    Hzu_f(:, :, i) = (2*pi*f_vec(i))^2*PHI*(Hm(:, :, i)*PHI'*M*T);
    Hzupp_f(:, :, i) = Hzu_f(:, :, i)+T;
    Wxx_f(:, :, i) = (Hzupp_f(:, :, i)*(Hzupp_f(:, :, i))')*Wuu_f;
end
for i = 1:size(gM,1)
    Meff(i) = (PHI(:,i)')*M*T/sqrt(m(i))^2;
end
Exx = trapz(f_vec,Wxx_f,3);
a_rms = sqrt(diag(Exx)); %root mean square accelerations

```

# Appendix B

## Acronyms

**ABET** Accreditation Board for Engineering and Technology

**ADCS** Attitude Determination and Control Subsystem

**ASI** *Agenzia Spaziale Italiana* (Italian Space Agency)

**CDF** Concurrent Design Facility

**CE** concurrent engineering

**CESAR** Common European Space Robot Controller

**CG** centre of gravity

**CSA** cross sectional area

**ESA** European Space Agency

**ESTEC** European Space Research and Technology Centre

**FS** Factor of Safety

**FEM** finite element method

**GUI** Graphical User Interface

**IDR** Ignacio De Riva

**MDOF** multiple degrees of freedom

**MoS** Margin of Safety

**PSD** Power Spectral Density

**SCDT** Student Concurrent Design Tool

**SDOF** single degree of freedom

**SI** International System of Units

**TC** thermal subsystem

**TF** transfer function

**UPM** Universidad Politecnica de Madrid

# Bibliography

- [1] ABET engineering accreditation commission *Criteria for Accrediting Engineering Program*, document, 2012 ABET;
- [2] Bandecchi M., Melton B., Ongaro F. *Concurrent Engineering Applied to Space Mission Assessment and Design*, ESA bulletin, ESA Directorate for Technical and Operational Support, ESTEC 1999;
- [3] Bertrand Harold E., Pennell James P., Slusarczuk Marko M. G., Winner Robert I. *The Role of Concurrent Engineering in Weapons System Acquisition*, report R-338, Institute for Defense Analyses 1991;
- [4] A. Calvi *Spacecraft Loads Analysis*, presentation, ESA;
- [5] CEI Montegancedo campus *Description of the activities of the CDF project*, report, UPM;
- [6] Dupac M., Marghitu D.B., *Advanced Dynamics: Analytical and Numerical Calculations with Matlab*, book, 2012, Springer Science and Business Media;
- [7] Francesconi A. *Impianti e sistemi aerospaziali*, lessons and presentations, Padova;
- [8] Fulcher Clay W. G., Reese Garth M., Segalman Daniel J. *An Efficient Method for Calculating RMS von Mises Stress in a Random Vibration Environment*, paper, Sandia National Laboratories 1998;
- [9] Gómez-Calero Carlos, Herin Benôit, López de Echazarreta Carlos, Zornoza Eduardo, *Student Concurrent Design Tool (SCDT): User Manual*, document, 15-07-2011, European Space Astronomy Centre;
- [10] Gómez-Calero Carlos, Herin Benôit, López de Echazarreta Carlos, Zornoza Eduardo *Student Concurrent Design Tool (SCDT): Structure Subsystem User Manual*, document, 15-07-2011, European Space Astronomy Centre;
- [11] Larson Wiley J., Wertz James R. *Space Mission Analysis and Design*, book, Space Technology Library;

- [12] Malcolm Macdonald, Viorel Badescu *The International Handbook of Space Technology*, book, Springer;
- [13] Megson T.H.G *Aircraft Structures for engineering students*,book, Butterworth-Heinemann;
- [14] Mission Design Division Staff *Small Spacecraft Technology State of the Art*, paper, 2014 NASA;
- [15] Mulville Daniel R. *Load Analysis of Spacecraft and Payloads*, paper, 1996 NASA;
- [16] Rico Germán, Torralbo Ignacio *Concurrent Design Application*, presentation, 2014 Madrid;
- [17] Sarafin T.P. *Spacecraft Structures and Mechanisms*, book, Kluwer, The Space Technology Library 1995;
- [18] Ullman David G. *The Mechanical Design Process*, book , McGraw-Hill series in mechanical engineering ;
- [19] Wijker Jaap *Mechanical Vibrations in Spacecraft Design*, book, 2004 Springer
- [20] Wijker Jaap *Random Vibrations in Spacecraft Structures Design*, book, 2009 Springer;
- [21] Wijker Jacob Job *Spacecraft Structures*, book, 2008 Springer;
- [22] ESA web page <http://www.esa.int/CDF>;
- [23] Ignacio De Riva department web page <http://www.idr.upm.es>;
- [24] MathWorks, Inc. web site <http://it.mathworks.com/help>.

# Acknowledgments

I want to thank Professor Zaccariotto Mirco for his help and his precious suggestions, but mostly for being able to relax my anxiety during last weeks. I want to thank Professor Franchini Sebastìan who helped me during the realization of this work and made my Erasmus experience possible.

I want to thank my friends Pietro, Sara, Alessandro, Stefano, Alison, Marco, Giulia, Marco and Massimo who color my life every day, my Erasmus friends and my house-mates whom I'm very happy to have met. Thanks to my parkour friends for the great experiences and to Matteo for the thesis review. Thanks to Lucia who is always important to me.

Finally I want to thank my great family, but specially my parents who made me grow a lot during these last years, thrusting and treating me as an adult.